DTIC FILE COPY

SECURITY CLASSIFICATION OF THIS PAGE

1

REPORT DOCUMENTATION PAGE

Form Approved OMB No. 0704-0188

1a. REPORT SECURITY CLASSIFICATION: UNCLASSIFIED	1b. RESTRICTIVE MARKINGS: NONE
2a. SECURITY CLASSIFICATION AUTHORITY	3. DISTRIBUTION/AVAILABILITY OF REPORT: APPROVED FOR PUBLIC RELEASE; DISTRIBUTION UNLIMITED.
AD-A217 458	5. MONITORING ORGANIZATION REPORT NUMBER(S): AFIT/CI/CIA-88-195
6a. NAME OF PERFORMING ORGANIZATION: AFIT STUDENT AT PURDUE UNIVERSITY / 6b. OFFICE SYMBOL (If applicable)	7a. NAME OF MONITORING ORGANIZATION: AFIT/CIA
6c. ADDRESS (City, State, and ZIP Code)	7b. ADDRESS (City, State, and ZIP Code): Wright-Patterson AFB OH 45433-6583
8a. NAME OF FUNDING/SPONSORING ORGANIZATION / 8b. OFFICE SYMBOL (If applicable)	9. PROCUREMENT INSTRUMENT IDENTIFICATION NUMBER
8c. ADDRESS (City, State, and ZIP Code)	10. SOURCE OF FUNDING NUMBERS: PROGRAM ELEMENT NO. / PROJECT NO. / TASK NO. / WORK UNIT ACCESSION NO.

11. TITLE (Include Security Classification) (UNCLASSIFIED)

ANALYTICAL TECHNIQUES FOR TRACKING FILTER IMPLEMENTATION

12. PERSONAL AUTHOR(S)
DANIEL GLEASON

13a. TYPE OF REPORT	13b. TIME COVERED	14. DATE OF REPORT (Year, Month, Day)	15. PAGE COUNT
THESIS/~~DISSERTATION~~	FROM _____ TO _____	1988	201

16. SUPPLEMENTARY NOTATION
APPROVED FOR PUBLIC RELEASE IAW AFR 190-1
ERNEST A. HAYGOOD, 1st Lt, USAF
Executive Officer, Civilian Institution Programs

17. COSATI CODES			18. SUBJECT TERMS (Continue on reverse if necessary and identify by block number)
FIELD	GROUP	SUB-GROUP	

19. ABSTRACT (Continue on reverse if necessary and identify by block number)

90 02 01 034

20. DISTRIBUTION/AVAILABILITY OF ABSTRACT: ☒ UNCLASSIFIED/UNLIMITED ☐ SAME AS RPT. ☐ DTIC USERS	21. ABSTRACT SECURITY CLASSIFICATION: UNCLASSIFIED
22a. NAME OF RESPONSIBLE INDIVIDUAL: ERNEST A. HAYGOOD, 1st Lt, USAF	22b. TELEPHONE (Include Area Code): (513) 255-2259 / 22c. OFFICE SYMBOL: AFIT/CI

DD Form 1473, JUN 86 — Previous editions are obsolete. — SECURITY CLASSIFICATION OF THIS PAGE

AFIT/CI "OVERPRINT"

ANALYTICAL TECHNIQUES

FOR TRACKING FILTER IMPLEMENTATION

A Thesis

Submitted to the Faculty

of

Purdue University

by

Daniel Gleason

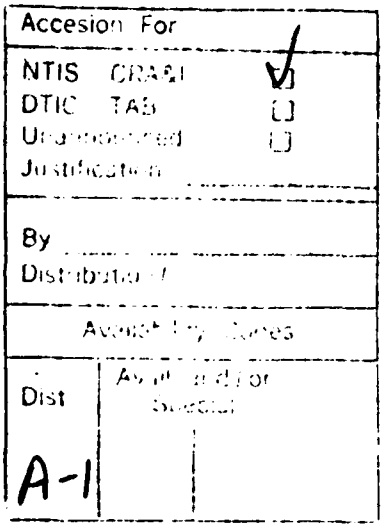

In Partial Fulfillment of the

Requirements for the Degree

of

Doctor of Philosophy

December 1988

Dedicated to
RMG

For her love and her smiles
For her laughter and her friendship

"Emerald eyes are a mystery ..."

ACKNOWLEDGMENTS

I would like to thank my major professor, Dr. Dominick Andrisani. His technical guidance, direction, support and friendship over these past years has been essential in the completion of this dissertation.

I also acknowledge the assistance of Professors David Schmidt, Arthur Frazho, and Rahmat Shoureshi for serving on my advisory committee.

The sacrifices and hard work placed in the achievement of a Ph.D. would be totally meaningless were it not for the love of my family. For this I am forever indebted to my wife, Regina, and my daughters, Rachael and Jessica for their never failing love and support.

TABLE OF CONTENTS

Page

LIST OF TABLES

LIST OF FIGURES

ABSTRACT

Gleason, Daniel. Ph.D., Purdue University, December 1988. Analytical Techniques For Tracking Filter Implementation. Major Professor: Dominick Andrisani.

The objective of this study is the development and verification of nonlinear and linear analysis techniques for aircraft tracking filter implementation.

The aircraft tracking problem has two distinct requirements. The first requirement is to accurately estimate the position of the aircraft at a present point in time. The second requirement is to predict the position of the aircraft at a given future time. Presently implemented tracking filters suffer from estimation and prediction accuracy degradation from two causes. The first cause is the lack of measurement information concerning the aircraft acceleration state. The second cause of error is attributable to a modeling insufficiency since, typically, the tracking filter is provided with no information concerning the system inputs.

This study addresses these two fundamental shortcomings to currently employed tracking filters. First, a nonlinear analysis is presented. In this analysis, a tracking filter that incorporates aircraft orientation in both the system model and measurements is compared to a tracker that uses only standard radar measurements. The addition of the orientation information enhances the tracking filter performance because, in general, aircraft orientation is strongly correlated with the acceleration of the aircraft. Improved position estimation and prediction is demonstrated with the tracking filter that incorporates orientation information.

The second fundamental cause of tracking filter errors (i. e. unknown system inputs) is investigated using linear analysis techniques. First, an analysis technique is developed using frequency and time domain methodologies for determining tracking filter gains for a system with unknown exogenous inputs. An analysis technique is also developed to determine the difference in tracking filter error covariance histories using variable structure models. This leads to a means for calculating process noise levels to achieve error covariance equivalent models. In addition, a three state, constant gain discrete tracking filter is investigated to determine filter gain behavior as a function of

process and measurement noise levels, and measurement sampling times. A limiting analysis is presented to determine the asymptotic behavior of the filter gains.

CHAPTER 1
INTRODUCTION

Target tracking and trajectory estimation has received a great deal of attention over the past number of years. The continuing and ongoing research effort being performed by both military and civilian agencies provides an indication of the importance of this topic, and the need to improve and extend presently implemented methodologies.

1.1 Problem Definition

The aircraft tracking problem has two distinct requirements. The first requirement is to accurately determine the inertial position of the aircraft at a present point in time. The second requirement is to predict the inertial position of the aircraft at a given future time. Knowledge of the future position is needed for civilian aircraft collision avoidance systems. Military anti-aircraft systems need predicted future positions in order to calculate projectile lead angles. Obviously, the accuracy achieved in predicting the future position is dependent upon the accuracy achieved in estimating the present position, velocity, and acceleration. If the estimation of these present kinematic values is poor, it is unlikely that estimates of future position will be satisfactory.

Difficulties arise in aircraft tracking due to two problem areas. First, the aircraft flight regime can vary from steady level nonmaneuvering flight to very unsteady highly maneuvering flight. Inherently, trackers that perform well against nonmaneuvering aircraft perform poorly against maneuvering aircraft and vice-versa. It is difficult to design trackers that perform well against both maneuvering and

nonmaneuvering aircraft. Second, trackers are provided with radar measurements (typically range, azimuth and elevation), but are provided with no information concerning vehicle velocity, acceleration, or pilot input. Without this information, the ability to estimate present and future aircraft position is severly degraded.

To overcome the problems described above, this research will examine a number of approaches and techniques to minimize these problems. Both nonlinear and linear analysis techniques will be explored.

The use of nonlinear techniques is necessitated by the fact that tracking a six degree of freedom maneuvering aircraft is a highly nonlinear problem. The nonlinearities are introduced in two ways. First, radar measurements are generally presented in spherical coordinates, while the differential equations governing the aircraft motion use a body-fixed cartesian coordinate system. Also, when orientation information is used, nonlinear direction cosine matrices are needed to transform force vector relationships between inertial and body coordinate systems. The introduction of these nonlinearities make it difficult to apply many standard engineering analysis techniques. Therefore a linearization of the problem is performed, and linear analysis techniques are developed and applied in order to make meaningful conclusions concerning tracker performance. The approach taken herein is to examine the complete nonlinear tracking problem, and then to use linear models to develop general methodologies to gain insight into the nonlinear problem development.

1.2 General Research Areas and Objectives

The research examines what improvements may be accrued if standard radar measurements are augmented with aircraft orientation (i.e. pitch, roll, and yaw) measurements. The concept behind this assumes that the pilot maneuvers the aircraft by orienting the aircraft to generate appropriate aerodynamic forces. There exists a strong

correlation between aircraft orientation and aircraft aerodynamic forces and thereby aircraft acceleration. For example, if the pilot wants to execute a climbing or diving maneuver, he pitchs the aircraft up or down as needed. When performing a turn, the aircraft is banked so that aerodynamic forces are oriented to produce the turning trajectory. Obtaining information about the pitch angle and/or bank angle will enhance tracker estimation, and in particular prediction performance.

This work does not investigate how the tracker obtains the orientation information. It assumes that the measurements are available from an on-board aircraft transponder as might be the case in a commercial aircraft. The development of surveillance radar mode S systems allows for the transmission of several airborne measurements to ground stations [Lefas; 1984]. Another possibility is to determine the aircraft orientation angles using advanced sensors on the tracker.

The nonlinear analysis requires numerous computational simulations to achieve satisfactory results for all filters. This work generated a number of questions concerning the optimization of the tracker designs. These questions dealt with tracker accuracy and robustness, Kalman filter tuning, and methods to optimize filter performance with incomplete tracker models. Addressing these questions with nonlinear Kalman filters is extremely difficult, since tracker performance is based on the particular aircraft trajectory that is selected. Therefore, follow on research is performed on linear models to gain insight into tracker robustness and filter tuning.

The linear aspects of this research explores four areas that are used to gain insight into the nonlinear problem. First, a simplified linear model that includes orientation information is developed. Many simple aircraft trackers are founded on treating the aircraft as constant velocity or constant acceleration point-mass vehicle. The tracker is provided with only noise corrupted position measurements. The tracker has no information concerning the pilot inputs or vehicle attitude. This lack of information

severly restricts the accuracy that is achievable in estimating the current aircraft position or predicting its future location. In the research presented here, the point-mass models are then modified to include aircraft orientation information, and noise corrupted aircraft orientation measurements. Again, the aircraft inputs are not provided to the tracker; however, since pilot inputs are initiated to change the aircraft orientation, a substantial improvement is seen in estimating and predicting the aircraft's position. In addition, the performance of the linear models with orientation information are found to be far less sensitive to whether the aircraft is in steady state level flight or in a highly maneuvering regime.

The second linear research area investigates a means for designing observers for systems with unknown exogenous inputs. In general, system observers are used to estimate state time histories for systems with an incomplete set of state measurements and unknown initial conditions. The design of the observer under these conditions is predicated on having a known model of the system and complete access to the system exogenous inputs. Under these circumstances, the performance of the system observer is well known and documented [Luenberger, 1971]. Adequate observer performance requires that system inputs be made available to the observer, and this is not the case for tracking maneuvering aircraft. However, performance improvements can be made by augmenting a control input model to the observer and selecting the observer gains to minimize error time histories. Observer performance is demonstrated for this methodology. The methodology is developed for a general linear dynamic system, and is not restricted to only the aircraft tracking problem. The methodology is developed for both continuous and discrete systems, and can be applied to any linear system with unknown exogenous inputs. An alternative application is the area of fault detection and isolation for failed/degraded aircraft control affectors [Gleason and Andrisani; 1986].

The third linear research area examines an error covariance analysis technique for variable order tracking filters. In general, an error covariance time history analysis for variable order filters is performed by exercising both models separately, and then differencing the individual error covariance histories. A more efficient method is to take advantage of the structural similarities between the models. By using appropriate matrix partitioning and differencing the Ricatti matrix differential or difference equations that govern the error covariances, a single equation can be obtained that describes the difference in the error covariance histories between a higher order and reduced order model. In addition, the resulting single matrix equation can be used in the development of error covariance equivalent models. Through the judicious selection of process noise levels, it is possible to achieve equivalent state error covariances for matching states between higher order and reduced order models. This leads to improved reduced order models with increased savings in computational resources. Also, tuning the process noise levels to account for reduced state dimensionality provides a quantitative measure of the effects of structural model modifications. The ability to achieve error covariance equivalent models also leads to a means for fairly evaluating tracker models of differing orders. A frequency domain technique for carrying out a variable order tracking filter analysis is provided by Andrisani [1985].

The fourth research area investigates steady state Kalman filter gains for discrete tracking filters. This is undertaken to develop insight into filter gain behavior as a function of process noise and measurement noise. The results demonstrate the application of a symbolic manipulation software package for solving complex engineering problems.

1.3 Report Organization

Chapter 2 provides the technical background and foundational analysis techniques used herein. A descriptive literature survey is presented. This is followed by the technical development for Kalman filter applications. First, the equations describing the linear Kalman filter are presented. Then the nonlinear or extended Kalman filter (EKF) equations are presented.

Chapter 3 discusses the nonlinear Kalman filters that are used in tracking maneuvering aircraft. Initially the radar-only tracker is discussed. For the radar-only tracker, a six state and nine state model are used to track a fighter aircraft performing a 5-g coordinated turn. Then aircraft orientation information is added to the system model and the system measurements, producing a twelve state and fifteen state tracking filters. Again these tracking filters are used to estimate and predict aircraft inertial position for an aircraft performing a 5-g coordinated turn. These results are then compared to the earlier results obtained by the six and nine state trackers. A number of sensitivity studies are undertaken to determine the criticality of a number of the nonlinear tracking filter parameters.

Chapter 4 describes the implementation of a linear Kalman filter for systems with and without orientation information. A 3-state ($\alpha - \beta - \gamma$), and 4-state($\alpha - \delta$) filters are analyzed.

Chapter 5 develops the observer augmentation technique that is used to enhance observer performance when unknown exogenous inputs exist. The technique is derived for both continuous and discrete systems. An application is demonstrated with both a continuous and discrete 3-state $\alpha - \beta - \gamma$ tracking filter.

Chapter 6 presents the error covariance analysis technique that is used in obtaining error covariance equivalent models for higher order and reduced order systems. Both continuous and discrete derivations are presented. A continuous closed

form application is presented for a 3-state $\alpha - \beta - \gamma$ tracking filter. The discrete case is verified with a closed form solution to the 2-state $\alpha - \beta$ tracking filter, and a numerical analysis of a 3-state $\alpha - \beta - \gamma$ tracking filter.

Chapter 7 presents the results of steady state gain analysis for the discrete $\alpha - \beta - \gamma$ tracking filter.

Chapter 8 summarizes conclusions, major contributions, and suggests recommendations for future research efforts.

CHAPTER 2
TECHNICAL BACKGROUND

2.1 Literature Survey

The problem of state estimation of maneuvering vehicles and its associated analytical complexities has engendered a substantial body of research literature. Chang and Tabaczynski [1984] present an excellent survey paper that discusses design problems and solutions for the target tracking problem. The paper addresses design tradeoffs, performance evaluations, and current issues. This chapter outlines pertinent approaches and key results taken in the past. The chapter outline is keyed on the major chapter areas that follow.

2.1.1 Nonlinear Tracking Filters

The introduction of nonlinearities to the tracking problem is brought about through the selection of coordinate systems for the system dynamics and sensor measurements. The natural coordinate system for the systems dynamics is a cartesian coordinate system. However, since the sensor measurements are generally radar measurements of range, azimuth, and elevation, the natural coordinate system for these measurements is a polar coordinate system. The designer must then decide whether to implement the tracking filter with linear system dynamics and nonlinear measurements, or with nonlinear system dynamics and linear measurements. The linear dynamics and nonlinear measurements results from using a state vector based on a cartesian coordinate system, while the nonlinear system dynamics and linear measurements result from selecting a state vector based on a polar coordinate systems. Brammer [1983] and Blackman [1986] outline the advantages and disadvantages to either

approach. Examples of nonlinear target models are presented by Lefas [1984], and Bullock and Sangsuk-Iam [1984]. In general, a state vector based on cartesian coordinates has an intuitive appeal [Chang and Tabaczynski; 1983] and therefore linear system dynamics are selected, and the nonlinear measurements are implemented with an nonlinear or extended Kalman filter.

Nonlinearities are also encountered when orientation information is incorporated into the system dynamics and sensor measurements. Kendrick et. al. [1981] note that previous research on tracking estimators suffer from one major flaw. Maneuver estimators that have only position measurements, experience significant delays before adjusting to unexpected target maneuvers. The authors point out that filter response time would be much faster if measurements of acceleration could be obtained. In order to circumvent the limitation of position only measurement filters, they incorporate orientation measurements. Having these additional measurements takes advantage of the high correlation between aircraft orientation and the direction of target acceleration. This coupling is characterized by the following relationships.

1. The velocity of the aircraft is nearly along the longitudinal axis, with the offset being angle of attack and sideslip.

2. Dominant acceleration is nearly normal to the velocity vector and nearly normal to the wings.

3. Positive lift is more likely than negative lift due both to pilot physiological factors and structural loading design.

4. Acceleration in the velocity direction (drag and thrust) are generally smaller in magnitude and of shorter duration than normal accelerations (lift).

5 Angle of attack is nearly proportional to the magnitude of the normal acceleration, and inversely proportional to the square of the speed.

The above relationships show the significant coupling between orientation and acceleration.

In the work of Kendrick, the nonnormal acceleration (lateral and tangential) components are modeled as a first order Gauss-Markov process with

$$\dot{a}(t) = -\frac{1}{\tau} a(t) + w(t) \tag{2.1-1}$$

The normal acceleration is modeled as an asymmetrically distributed, time correlated, random process with hard limits on acceleration magnitudes. The normal acceleration is given by

$$a_N = \alpha + \beta e^{\gamma \varepsilon} \tag{2.1-2}$$

where α, β, γ are constant for a particular type of aircraft and ε is derived from a colored noise process. This yields an asymmetric probability density function which can be shaped to provide a more realistic model of piloted aircraft maneuvering capability.

The tracker then consists of two simultaneous filters. The first filter estimates kinematic parameters of target position, velocity, and acceleration. The second filter estimates target orientation. Both filters are coupled in order to maximize estimation of target position and orientation.

The use of attitude measurements was extended by Andrisani et. al. [1986b, 1985a, 1985c, 1985d]. The achievement of improved current and future position estimates was achieved by estimating aerodynamic force magnitudes and direction. Details and results of this approach are presented in chapter 3 herein.

2.1.2 Linear Tracking Filters

In order to gain insight into tracking filter performance, the vehicle being modeled is often assumed to be a point-mass whose velocity or acceleration is constant in one of three orthogonal directions. The vehicle dynamics are presented in cartesian coordinates, and sensor measurements of position are assumed to be available in each of the three orthogonal directions. With this formulation the filter performance is decoupled in the three orthogonal directions, and therefore analyzed individually in one of the directions.

The earliest models chosen for describing aircraft motion were classified as $\alpha - \beta$ trackers. These models assumed that the aircraft was flying a constant velocity flight path trajectory. Deviations from the constant velocity trajectory are modeled as gaussian white noise. $\alpha - \beta$ trackers are sometimes referred to as the random walk velocity (RWV) or "white acceleration" models [Fitzgerald; 1981]. The state vector is formulated as

$$\bar{x} = \left[x, \dot{x}, y, \dot{y}, z, \dot{z} \right]^T \tag{2.1-3a}$$

$$= \left[x_1, x_2, \ldots, x_6 \right]^T \tag{2.1-3b}$$

where (x,y,z) are coordinates of a Cartesian coordinate system. The notation $\dot{x}(t)$ indicates time differentiation (i.e. dx/dt). The three degree of freedom continuous equations of motion are

$$\dot{x}_i = x_{i+1} \qquad i = 1,3,5 \tag{2.1-4a}$$

$$\dot{x}_{i+1} = w_i \tag{2.1-4b}$$

where w_i is a process noise used to account for modeling errors. The continuous state space formulation including measurements dynamics in one of the three orthogonal directions is then

$$\begin{bmatrix} \dot{x}(t) \\ \ddot{x}(t) \end{bmatrix} = \begin{bmatrix} 0 & 1 \\ 0 & 0 \end{bmatrix} \begin{bmatrix} x(t) \\ \dot{x}(t) \end{bmatrix} + \begin{bmatrix} 0 \\ w_v \end{bmatrix} \quad ; \; w_v \tilde{} N(0,q_v) \tag{2.1-5}$$

$$z = \begin{bmatrix} 1 & 0 \end{bmatrix} \begin{bmatrix} x(t) \\ \dot{x}(t) \end{bmatrix} + v_v \quad ; \; v_v \tilde{} N(0,r) \tag{2.1-6}$$

where w_v and v_v are zero-mean uncorrelated Gaussian noise sources with noise intensity of q_v and r, respectively.

An extension of the $\alpha-\beta$ tracker is the $\alpha-\beta-\gamma$ tracker. This tracker assumes the aircraft is flying with constant acceleration. Deviations from this trajectory are modeled as gaussian white noise. $\alpha-\beta-\gamma$ filters are sometimes referred to as random walk acceleration (RWA) or "white jerk" models [Fitzgerald; 1981]. The state vector is formulated as

$$\bar{x} = \left[x, \dot{x}, \ddot{x}, y, \dot{y}, \ddot{y}, z, \dot{z}, \ddot{z} \right]^T \tag{2.1-7a}$$

$$= \left[x_1, x_2, \ldots, x_9 \right]^T \tag{2.1-7b}$$

where again, (x, y, z) are coordinates in a cartesian coordinate system. The three degree of freedom continuous equations of motion are

$$\dot{x}_i = x_{i+1} \tag{2.1-8a}$$

$$\dot{x}_{i+1} = x_{i+2} \quad i=1,4,7 \tag{2.1-8b}$$

$$\dot{x}_{i+2} = w_i \tag{2.1-8c}$$

The continuous state space formulation including measurements dynamics in one of the three orthogonal directions is then

$$\begin{bmatrix} \dot{x}(t) \\ \ddot{x}(t) \\ \dddot{x}(t) \end{bmatrix} = \begin{bmatrix} 0 & 1 & 0 \\ 0 & 0 & 1 \\ 0 & 0 & 0 \end{bmatrix} \begin{bmatrix} x(t) \\ \dot{x}(t) \\ \ddot{x}(t) \end{bmatrix} + \begin{bmatrix} 0 \\ 0 \\ w_a \end{bmatrix} \quad ; \; w_a \tilde{} N(0,q_a) \tag{2.1-9a}$$

$$z = \begin{bmatrix} 1 & 0 & 0 \end{bmatrix} \begin{bmatrix} x(t) \\ \dot{x}(t) \\ \ddot{x}(t) \end{bmatrix} + v_a \quad ; \; v_a \tilde{} N(0,r) \tag{2.1-9b}$$

where w_a and v_a are zero-mean uncorrelated gaussian noise sources of intensity q_a and r respectively.

The period 1970 through the present shows a proliferation of papers dealing with the problem of tracking maneuvering targets. One of the first papers of this period was a paper by Singer [1970] who developed a correlated noise model that is used extensively in many papers that followed. Singer reasoned that modeling the pilot's input as white noise was a poor representation of reality. Instead he proposed modeling the pilot's input as correlated function of time. Singer's continuous time model is

$$\begin{bmatrix} \dot{x}(t) \\ \ddot{x}(t) \\ \dddot{x}(t) \end{bmatrix} = \begin{bmatrix} 0 & 1 & 0 \\ 0 & 0 & 1 \\ 0 & 0 & -1/\tau_m \end{bmatrix} \begin{bmatrix} x(t) \\ \dot{x}(t) \\ \ddot{x}(t) \end{bmatrix} + \begin{bmatrix} 0 \\ 0 \\ 1 \end{bmatrix} w(t) \tag{2.1-10}$$

The correlation function for this colored acceleration is shown in Figure 2-1, where

$$r(\tau) = E\{\bar{x}(t)\bar{x}(t+\tau)\} = \sigma_m^2 \exp(-\tau/\tau_m) \tag{2.1-11}$$

where E $\{\cdot\}$ denotes the expectation operator.

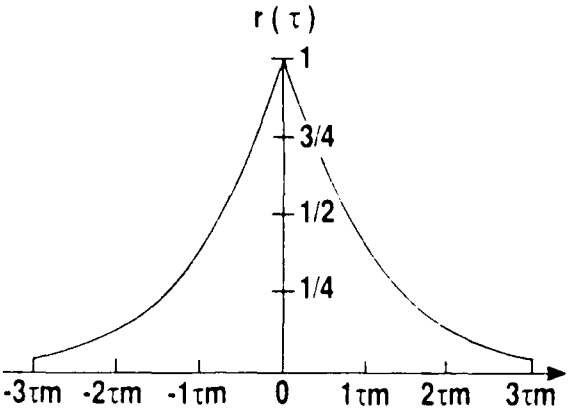

Figure 2-1 Correlation Function for Target Acceleration

Two parameters are critical in this formulation. The first is the correlation time constant, τ_m. Singer provides the following guidelines for the selection of τ_m :

1. Lazy turns give rise to correlated accelerations for up to one minute (i.e. τ_m = sixty seconds)

2. Evasive maneuvers provide correlated acceleration inputs between ten and thirty seconds

3. Atmospheric turbulence provides correlated acceleration inputs for one or two seconds.

The second critical descriptive parameter is σ_m^2 , the variance of the target acceleration. For a target acceleration model, Singer uses the probability distribution function shown in Figure 2-2.

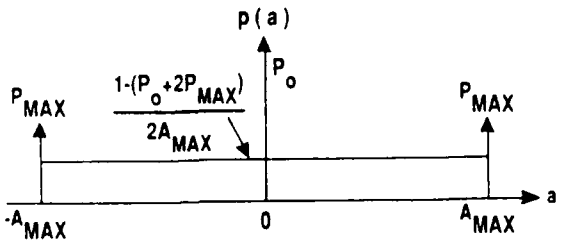

Figure 2-2 Target Acceleration Probability Density

This distribution is a modified uniform probability distribution based on the following considerations:

1. The maximum target acceleration is $\pm A_{max}$ and has an associated probability P_{max}

2. The target has zero acceleration with probability P_o.

3. The target will accelerate between the limits $-A_{max}$ and $+A_{max}$ according to a uniform probability distribution with probability

$$p(a) = \frac{1 - (P_o + 2P_{max})}{2A_{max}} \tag{2.1-12}$$

The variance (σ_m^2) of this model is

$$\sigma_m^2 = \frac{A_{max}^2}{3}(1 + 4P_{max} - P_o) \tag{2.1-13}$$

Singer states that this model has been used in tracking simulations and has been shown to provide a satisfactory representation of the targets instantaneous maneuver characteristics.

Since many measurement sensors sample target position with a constant data rate T, it is necessary to formulate the discrete counterparts to the continuous $\alpha - \beta$ and $\alpha - \beta - \gamma$ tracking filters. If the continuous system dynamics are given as

$$\dot{x}(t) = Fx(t) + Gu(t) \tag{2.1-14}$$

then the discrete system dynamics may be represented as [Kwakernaak and Sivan; 1972]

$$x(k+1) = \Phi x(k) + \Gamma u(k) \tag{2.1-15}$$

where

$$\Phi = e^{FT}$$

and

$$\Gamma = (\int_0^T e^{A\tau} d\tau) B$$

where it is assumed that the sampling time is held constant and the input u(t) is held constant over the sampling period T.

Applying this discretization procedure to the RWV and RWA models of Fitzgerald or the exponentially correlated acceleration model of Singer's with a very short sampling period and large correlation time constant results in the discrete $\alpha - \beta$ and $\alpha - \beta - \gamma$ tracking models. The discrete state space formulation of these models is given by

$\alpha - \beta$ Trackers

$$p(k+1) = p(k) + Tv(k) + \frac{T^2}{2} w_a(k) \tag{2.1-16a}$$

$$v(k+1) = v(k) + Tw_a(k) \tag{2.1-16b}$$

$\alpha - \beta - \gamma$ Trackers

$$p(k+1) = p(k) + Tv(k) + \frac{T^2}{2} a(k) + \frac{T^3}{6} w_j(k) \tag{2.1-17a}$$

$$v(k+1) = v(k) + Ta(k) + \frac{T^2}{2} w_j(k) \tag{2.1-17b}$$

$$a(k+1) = a(k) + Tw_j(k) \tag{2.1-17c}$$

where T = discrete time between increments k and k+1; p(k), v(k), and a(k) represent position, velocity, and acceleration, respectively. The terms w_v, w_a, and w_j are discrete zero-mean uncorrelated Gaussian noise sequences used to account for modeling uncertainties in velocity, acceleration and jerk (acceleration derivative) respectively.

The discrete matrices governing the discrete system dynamics are then given as

$\alpha - \beta$ Tracker

$$\Phi = \begin{bmatrix} 1 & T \\ 0 & 1 \end{bmatrix} \quad \Gamma = \begin{bmatrix} T^2/2 \\ T \end{bmatrix}$$

$$\alpha - \beta - \gamma \text{ Tracker}$$

$$\Phi = \begin{bmatrix} 1 & T & T^2/2 \\ 0 & 1 & T \\ 0 & 0 & 1 \end{bmatrix} \quad \Gamma = \begin{bmatrix} T^3/6 \\ T^2/2 \\ T \end{bmatrix}$$

For the $\alpha - \beta - \gamma$ tracking dynamics, it is assumed that the input to the system represents the time derivative of acceleration. If the system input is in fact a system acceleration, then Γ must be modified to

$$\Gamma = \begin{bmatrix} T^2/2 \\ T \\ 1 \end{bmatrix}$$

It should be noted that the fundamental structure for the $\alpha - \beta$ and $\alpha - \beta - \gamma$ results in upper triangular matrices for the continuous F matrices and the discrete Φ matrices. This fact is exploited in the error covariance analysis that will be investigated. This upper triangular form results from the phase variable nature of this problem and also due to the fact that the true system input is unknown. The lack of knowledge of the system inputs severly degrades the performance capabilities of the filter. A means for overcoming this performance degradation is also investigated using orientation information and input estimation techniques.

These trackers are supplemented with measurements of vehicle position and possibly vehicle velocity that are corrupted by a discrete zero-mean white noise sequence. This information is then used in a standard discrete Kalman filter to estimate vehicle trajectories.

Singer's work analyses the discrete $\alpha - \beta - \gamma$ tracker and then provides a technique for estimating tracking performance using the following design parameters:

1. T, sampling time
2. τ_m, maneuver correlation time
3. σ_m^2, maneuvering variance
4. σ_r^2, measurement variance

Plots of normalized error covariance values versus sampling period are presented for a variety of design parameter combinations.

Singer's model is generic in nature and is simple to implement. For this reason, it has received a great deal of attention in the literature. However, Singer points out some shortcomings of the model. The tracking performance of this filter will often be below that obtained by simple filters, such as a least squares filter, when tracking targets that move at a constant velocity. The correlated noise filter must keep the gain vector relatively large in order to follow maneuvers as soon as they occur. Consequently, although performance against maneuvers is good, performance against nonmaneuvers is degraded from that of simple filters. The designer must select τ_m and σ_m^2 in advance, which presents a problem. Filter performance is relatively insensitive to τ_m, particularly as the sampling period T decreases. Unfortunately, the filter performance is sensitive to the selection of σ_m^2, and the designer must select this value a priori with the hope of maintaining adequate filter performance for maneuvering and nonmaneuvering targets.

A follow on paper by Singer and Behnke [1971] presents a comparison of five real time tracking filters based on tracking accuracy and computer requirements. The five filters are:

1. Kalman filter
2. Simplified Kalman filter
3. $\alpha - \beta$ filter
4. Weiner filter
5. Two point extrapolator

The authors conclude that in many practical systems, the constant gain Weiner filter provides tracking accuracy equivalent to that of the more sophisticated Kalman filter, at one third the computational cost. The authors qualify this statement by noting that if high accuracy is required and if the length of the transient period of the filter approaches that of the tracking interval, the simplified Kalman filter becomes attractive for implementation.

Spingarn and Weidman [1972] took the approach of using a linear regression filter for tracking maneuvering targets. The approach is basically a linear least squares estimation problem using both an expanding memory filter, and a truncated or fading memory filter. The authors conclude that the filtering should be performed in cartesian coordinates in order to avoid large dynamic errors associated with a line of sight (polar) coordinate formulation. They also conclude that the fading memory filter outperforms the expanding memory filter for maneuvering targets.

Noting the tradeoff of tracking maneuvering versus nonmaneuvering targets, extensive work was done to see if this shortcoming could be circumvented. The general approach taken to resolve this shortcoming was to develop an adaptive filter that incorporated some type of decision making mechanism to determine if the aircraft was in a maneuvering or nonmaneuvering mode. Appropriate adaptive tracking modifications are then performed.

McAulay and Denlinger [1973] combine an optimum maneuver detector with Singer's generalized tracking model. The maneuver detector is based upon whether the filter residuals are zero mean for the nonmaneuvering case, or biased for the maneuvering case. The detection of a maneuver is equivalent to the detection of a deterministic signal of unknown amplitude and unknown time of arrival, corrupted by white gaussian noise. The maneuver discriminant is then based upon a generalized likelihood ratio test.

The authors outline an optimal bias detector based on a bank of M square-law-detection filters, where M determines how many past sample periods will be tested for bias detection. Noting the computational effort associated with this optimal bias detector, the authors go on to present a suboptimal bias detector. The suboptimal detector uses a simplified detection statistic denoted as the exponential bias detector. This detector requires, a priori, the selection of appropriate detection thresholds and memory periods to get reasonable maneuver detection/false-detection performance.

Thorpe [1973] introduces a binary random variable in the target state equations to account for maneuvering target motion. The tracker uses a maneuver detector to determine if the binary random variable is to take on the value of 1 (maneuver) or 0 (nonmaneuver). The value of the binary random variable determines if a forcing function should be present or not. The maneuver detector is a likelihood ratio test based on measurement residual characteristics.

Gholson and Moose [1977] outline two adaptive state estimation techniques. Both estimates incorporate a semi-Markov modeling process for the target model. A semi-Markov process is a probabilistic system that randomly selects its acceleration input command vector according to the transition probability matrix of a Markov process. A semi-Markov process differs from a Markov process in that the duration time in one state prior to switching to another state is itself a random variable. The model

for the maneuvering target (using the authors notation) is

$$x(k+1) = \Phi x(k) + \Gamma(w(k) + u(k)) \qquad (2.1\text{-}18)$$

where x(k) represents the state vector and w(k) and u(k) are stochastic and deterministic inputs respectively. Note that this model includes a deterministic input u(k), whose value is based on a semi-Markov model. In this way large scale target maneuvers are modeled as a stochastic process whose mean value switches randomly among a finite set of predetermined values. A limitation to this method is the requirement for a large number of preselected mean values in order to ensure convergence of the estimation process.

A later approach by Moose et. al. [1979] takes this model one step further by incorporating Singer's correlated acceleration model. The inclusion of this time correlated, randomly switching forcing function is more representative of real world target maneuvers.

Ricker and Williams [1978] take an approach that is similar to Gholson et. al. [1977,1979] where they develop an adaptive filter by augmenting the tracking filter with additional filters for input estimation purposes. The method treats the residuals as having a multivariate gaussian density and through the use of Bayesian decision rule develops the probabilities of occurrence associated with a prescribed set of discrete maneuvers. The paper states that an error analysis determines that a set of five possible inputs is sufficient for accurate tracking.

Two studies by Clark [1976, 1977] explore means to overcome the estimation accuracy versus responsiveness to maneuvering targets tradeoff problem. Clark's solution was the development of a dual bandwidth adaptation filter with residual feedback maneuver detection. This work clearly demonstrates the need to tune the filter to achieve a filter bandwidth that will yield the smoothest unbiased estimates. Using a discrete $\alpha - \beta - \gamma$ filter, examples of acceleration estimates are presented. These

examples clearly demonstrate that a low bandwidth filter provides very good estimates for a nonmaneuvering target; but given the onset of an acceleration input, filter performance is severly compromised due to the poor transient response of the filter. If the bandwidth of the filter is increased, then filter performance for nonmaneuvering vehicles is degraded due to increased noise corruption of the estimate; but the transient response is enhanced when maneuvers are encountered. Clark's method is then to statistically analyze the filter residuals to determine when a maneuver occurs. If no maneuver is detected the process noise covariance is set at a low value yielding a low bandwidth filter with it's accompanying advantages. Upon the detection of a maneuver, the process noise is increased to widen the bandwidth, and to achieve a satisfactory response.

Bar-Shalom and Birmiwal [1982] use a variable dimension filter approach. A low order model is used when the target is not maneuvering. The state transition matrix is augmented with additional states upon a maneuver detection. The system reverts to the lower order model when the filter deems that the maneuver has ended. The maneuver detector employed is similar in nature to McAulay and Denlinger's [1973], although two different test statistics are used in the switching process.

Berg [1983] describes a tracking algorithm that was implemented in a General Dynamic's radar tracker and tested against a variety of fixed wing aircraft targets. Berg tests the tracking algorithm against an aircraft performing a coordinated turn where

1. Mean target lift acceleration is constant.

2. Mean target thrust (i.e. thrust minus drag) is constant

3. Mean target roll rate is zero.

Berg modifies Singer's correlated acceleration by including an additional term $\bar{a}$, which is computed as a function of the most recent estimates of target velocity and

acceleration. This term represents the mean target jerk. The acceleration model is

$$\dot{a}(t) = -\frac{1}{\tau} a(t) + \frac{1}{\tau} w(t) + \bar{a} \qquad (2.1\text{-}19)$$

The process noise intensity Q and the measurement noise intensity R are computed adaptively as a function of the most recent estimates of the state. Simulation results demonstrated the fact that for expected target trajectories and engagement ranges, the incremental transformation of the estimation covariance matrices, between measurement updates, played a negligible role in the determination of the filter gains. Since Q and R were slowly varying functions of time (relative to the measurement update rate), then the steady state filter gains could be closely approximated by steady state gain values computed strictly as a function of Q and R for each channel. In order to meet imposed fire control computer memory and execution time constraints, the choice of filter gains were based on steady state results for given levels of Q and R.

Given the inherent limitations on tracking filters that use only measurements of position, Kendrick as stated previously, incorporated measurements of attitude based on the premise that attitude is strongly correlated with vehicle acceleration. Unfortunately, the six degree of freedom equations of motion associated with this approach are highly nonlinear. Andrisani [1985a, 1987] examines simplified linear models that utilize orientation measurements to enhance filter estimates and predictions.

Andrisani [1985a] first examined fixed wing aircraft models that incorporated pitch attitude information and its relationship to aircraft vertical velocity and acceleration. A frequency domain error analysis was performed between $\alpha - \beta$, $\alpha - \beta - \gamma$, and filters using orientation information. This analysis shows that attitude information dramatically improved estimates of the aircraft's position, velocity, and acceleration.

A later study by Andrisani [1987], examines the performance of helicopter tracking filters that incorporate attitude and rotor angle measurement. Trajectory simulations demonstrated a substantial improvement in estimating future helicopter position when using attitude and rotor angle measurements as compared to standard $\alpha - \beta$ trackers.

2.1.3 Input Estimation

In general, efficient estimation schemes require complete knowledge about system dynamics, inputs, disturbances, and initial conditions. Incomplete information with respect to any of these factors will generally result in degraded estimates of state time histories. This section reviews the problems and suggested solutions to estimating state time histories when incomplete input information is available. The tracking problem is a prime example of trying to estimate position, velocity and acceleration of a vehicle without the benefit of knowing the system inputs. Another example is the case of an aircraft performing maneuvers with degraded or failed control affectors. Under these circumstances a fault detection and isolation (FDI) procedure is needed to identify the location and magnitude of the degraded/failed control affector. A single input-single output (SISO) FDI met methodology is presented by Gleason and Andrisani [1987b]. A multiple input-multiple output methodology is presented by Mayhew and Gleason [1988].

Chan et. al. [1979] develop a tracking scheme that estimates the acceleration inputs from the residuals, and uses the input estimates to update the Kalman filter. At each measurement, the scheme produces an estimate of the maneuvering input vector whose norm is then checked against a threshold level. When there is a detection, the filter is updated by the estimate of the input vector. The aim of updating the filter output is simply to remove the filter bias caused by the target deviating from the assumed

constant velocity, straight line motion.

A later paper by Chan et. al. [1982] develops a computationally simpler implementation of the input estimation concept. The resulting filter is suboptimal, but the authors state that the computational savings make this a superior tracker as compared with their earlier work.

Bogler [1987] extends the work of Chan et al. [1981], by developing recursive relationships for the Chan formulation. This methodology is verified using a one dimensional Kalman filter.

An alternative approach to input estimation is to augment the tracker with a model of the system inputs, and then to select the tracker gains to minimize the errors between the true state and predicted state. This approach is examined in chapter 5 using a generalized approach to observer design for systems with unknown exogenous inputs. The continuous and discrete results parallel the techniques developed for designing robust control schemes. This methodology is commonly referred to as Linear Quadratic Gaussian/Loop Transfer Recovery (LQG/LTR). The original continuous work was performed by Doyle [1979] who demonstrated the technique of picking observer gains to recover stability margins (i.e. gain and phase margins) for systems that are implemented with observers. Maybeck [1982] presents the technique for discrete time systems.

2.1.4 Error Covariance Analysis

As stated previously, the model selection procedure for tracking filters is based on the underlying assumptions concerning the vehicle motion. These assumptions deal with whether the vehicle is moving with a constant velocity or constant acceleration in one of three orthogonal directions. The selected model is then used with measurements of vehicle position in a state estimation filter to estimate the vehicle trajectory. The

resulting error covariance for the state estimator is then determined by the model structure, along with the selected process noise and measurement noise intensity levels. The process noise is added to the system model to account for modeling deficiencies due to model structure or unknown inputs. Therefore the selection of the process noise levels is key design factor. An obvious evaluation figure of merit is the error covariance that results from a selected level of process noise.

Hutchinson et. al. [1985] investigate the selection of a process noise level that yields a minimum variance reduced order (MVRO) estimator. Their approach uses linear transformation techniques in conjunction with the matrix minimization principles.

Mavromatis et. al. [1987] develop a procedure for the numerical optimization of tracking filters. This method is used select optimum process noise levels to account for unknown input levels. The results include tracker tuning parameters and tracker gains as a function of the severity of the motion of the aircraft.

Gleason and Andrisani [1987a, 1986] examine an error covariance analysis technique for models of differing orders. This technique exploits the upper triangular structure of tracking filters to develop a Ricatti equation solution for the error covariance difference that between higher order and reduced order models. This result is used to determine process noise levels to achieve a reduced order model that has an equivalent error covariance history to that of a higher order model. The results are presented for continuous and discrete systems, and is formulated for generalized system dynamics that can be modeled with an upper triangular system dynamics matrices. Although the objectives and methodologies are different from those of Hutchinson et. al., the results are identical for systems of similar structure.

2.1.5 Constant Gain Analysis For Discrete Tracking Filters

To reduce computational requirements, filters are often implemented using a constant gain Kalman filter [Berg; 1983]. For this reason extensive work has been done to find closed form solution to the steady state continuous and discrete Ricatti equation used in determining Kalman filter gains.

Fitzgerald [1981, 1980] provides closed form solutions for the error covariance and Kalman gains of continuous trackers with exponentially correlated velocity (ECV) and acceleration (ECA) inputs. By allowing the correlation time constant to approach infinity, a limiting analysis yields closed form solutions for the random walk velocity (RWV), and the random walk acceleration (RWA) cases.

Ekstrand [1985] provides closed form solutions for continuous $\alpha - \beta$ filters that have both position and velocity measurements.

A number of analyses have been performed on discrete steady state tracking filters. Friedland [1973, 1975] provided closed form solutions for error covariance and estimator gains for $\alpha - \beta$ trackers with position only measurements. Yu and Meyer [1985] provide steady state closed form solutions for $\alpha - \beta$ trackers with no process noise and position only measurements. Ekstrand [1983] analyzed steady state $\alpha - \beta$ trackers that include velocity measurements in addition to position measurements. Kalata [1984] examined α, $\alpha - \beta$, and $\alpha - \beta - \gamma$ trackers with position only measurements. Kalata identifies a tracking index which is a function of the design parameters. He shows that the gain solutions are functions of this tracking parameter and provides a graphical solution for position gains. Ramachandra [1987] has also investigated steady state filters for position, velocity and acceleration estimates. Chapter 7 herein also investigates closed form solutions to three state tracking filter. Like Ramachandra, the solution necessitates solving a quartic equation. This is done using a symbolic manipulation program entitled MACSYMA. Ramachandra's work is extended by

performing a limit analysis, and presenting three dimensional representations of the tracker gains as a function of the process noise and measurement noise covariances.

2.2 Kalman Filters

The Kalman filter [Kalman; 1960] is the predominant analytical tool used in modern day trajectory estimation. Some of the many advantages of the Kalman filter, when properly applied, are:

1. The output of the linear Kalman filter provide optimal (meaning unbiased, minimum variance) estimates of the state vector.

2. Kalman filters utilize state space representations which are ideally suited to the modern analytical and computational environment. For the problem of trajectory prediction, this is exceptionally useful, as it provides the flexibility of analyzing and comparing simplistic one-degree of freedom trackers to the more complete six-degree of freedom models.

3. Kalman filters have inherent diagnostic capabilities via residual or innovations analysis to determine it's efficacy in state estimation.

These are just of few of the advantages of the Kalman filter. The widespread use and attention given to the Kalman filter is a testimony to its usefulness as an engineering tool. However, like all mathematical techniques, its usefulness is model and assumption dependent. If the real world application differs significantly from the proposed mathematical model and assumptions, then problems are bound to arise. This is inherently true in the estimation and prediction of aircraft trajectories, since complete model information is generally unavailable.

As stated earlier, if the aircraft is following a steady, level constant velocity flight path, then the estimator can use, in a very straightforward manner, a low order linear Kalman filter. However, if the aircraft is maneuvering to any significant degree,

the application of the Kalman filter is no longer a straightforward procedure. In this case, the equations of motion become highly nonlinear, and an extended Kalman filter would be used. Unfortunately, many of the optimal properties of the linear Kalman filter are not retained with the extended Kalman filter. The qualities of the estimates become trajectory dependent, and the gain and the covariance never achieve steady state values and therefore cannot be precomputed. However, the performance of extended Kalman filters has been good in a number of practical applications [Gelb; 1974]. Preliminary results of this effort also reveal good performance by the extended Kalman filter.

This chapter describes the equations used in a linear Kalman filter (LKF), and the extended Kalman filter (EKF). Both the continuous and discrete filters are presented for the LKF. The measurements used in the aircraft tracking problem are given at discrete time intervals, and therefore the discrete LKF is generally used. However, the observer augmentation technique of Chapter 5, and the error covariance technique of Chapter 6 are presented for both the continuous and discrete LKF. For this reason both continuous and discrete developments are presented in this chapter. The Kalman filter developments in this chapter are based on those found in Gelb [1974].

2.2.1 Linear Kalman Filters

2.2.1.1 Continuous Linear Kalman Filters

The state and measurement model for the continuous Kalman filter are

$$\dot{x}(t) = Fx(t) + Gw(t), \quad x(0) = x_0 \tag{2.2-1}$$

$$z(t) = Hx(t) + v(t) \tag{2.2-2}$$

where $x(t) \in R^n$ is the system state vector, $z(t) \in R^l$ is the system measurement vector. The terms $w(t) \in R^m$ and $v(t) \in R^l$ represent process noise and measurement

noise respectively. The matrices F, G, and H are dimensioned to ensure compatibility. The optimality of the LKF is based on knowing the statistics for the initial conditions, process noise, and measurement noise. These are assumed to be (Note : E $\{\cdot\}$ denotes the expectation operator.)

Initial Condition Statistics

$$E\{x(0)\} = \hat{x}_0 \tag{2.2-3a}$$

$$E\{[x(0) - \hat{x}_0][x(0) - \hat{x}_0]^T\} = P_0 \tag{2.2-3b}$$

Process Noise Statistics

$$E\{w(t)\} = 0 \tag{2.2-4a}$$

$$E\{w(t)w(\tau)^T\} = Q\,\delta(t - \tau) \tag{2.2-4b}$$

Measurement Noise Statistics

$$E\{v(t)\} = 0 \tag{2.2-5a}$$

$$E\{v(t)v(\tau)^T\} = R\,\delta(t - \tau) \tag{2.2-5b}$$

where $\delta(t - \tau)$ is the Dirac delta function defined as

$$\delta(t - \tau) = \begin{cases} \infty & \tau = t \\ 0 & \tau \neq t \end{cases} \tag{2.2-6a}$$

$$\lim_{\varepsilon \to 0} \int_{t-\varepsilon}^{t+\varepsilon} \delta(t - \tau)d\tau = 1 \tag{2.2-6b}$$

and Q and R are the spectral density matrices for the process noise and measurement noise, respectively. The spectral density matrix R is assumed to be positive definite.

Additional assumption concerning correlations between the noise sources and initial conditions are enumerated as follows

1. $E[w(t)\,v(\tau)^T] = 0$, for all t, $\tau \geq 0$

2. $E[x(0)\,w(t)^T] = 0$, for all t, ≥ 0

3. $E[x(0)\,v(t)^T] = 0$, for all t, ≥ 0

The Kalman filter equations are given as

State Estimate

$$\dot{\hat{x}}(t) = F\hat{x}(t) + K(t)[z(t) - H\hat{x}(t)], \quad \hat{x}(0) = \hat{x}_0 \tag{2.2-7}$$

Error Covariance Propagation

$$\dot{P}(t) = FP(t) + P(t)F^T + GQG^T - K(t)RK(t)^T, \quad P(0)=P_o \tag{2.2-8}$$

where P is the error covariance matrix defined as

$$P(t) = E\{[x(t)-\hat{x}(t)][x(t)-\hat{x}(t)]^T\} \tag{2.2-9}$$

Kalman Gain

$$K(t) = P(t)H^T R^{-1} \tag{2.2-10}$$

The continuous LKF has an inherent diagnostic capability based on the statistical properties of the residuals or innovations which are defined as

$$r(t) = z(t) - H\hat{x}(t) \tag{2.2-11}$$

If the LKF is performing in an optimal manner (i.e. providing unbiased, minimum variance estimates), then it can be shown that the residuals have the following statistical properties [Kailath; 1968].

Optimal LKF Residual Statistics

$$E\{r(t)\} = 0 \tag{2.2-12a}$$

$$E\{r(t)r(\tau)^T\} = R\,\delta(t-\tau) \tag{2.2-12b}$$

The residuals can be analyzed statistically to determine if the above statistics are satisfied. If the residuals have the above statistics, then the continuous LKF is performing optimally.

2.2.1.2 Discrete Linear Kalman Filters

The state and measurement models for the discrete LKF are

$$x(k+1) = \Phi x(x) + \Gamma w(k) \tag{2.2-13}$$

$$z(k) = Hx(k) + v(k) \tag{2.2-14}$$

where $x(k) \varepsilon R^n$ is the discrete system state vector, $z(k) \varepsilon R^l$ is the discrete system measurement vector. The terms $w(k) \varepsilon R^m$ and $v(k) \varepsilon R^l$ represent process noise and measurement noise sequences respectively. The matrices Φ, Γ, and H are dimensioned to ensure compatibility. The optimality of the LKF is based on knowing the statistics for the initial conditions, process noise, and measurement noise. These are assumed to be

Initial Condition Statistics

$$E\{x(0)\} = \hat{x}_0 \tag{2.2-15a}$$

$$E\{[x(0) - \hat{x}_0][x(0) - \hat{x}_0]^T]\} = P_0 \tag{2.2-15b}$$

Process Noise Statistics

$$E\{w(k)\} = 0 \tag{2.2-16a}$$

$$E\{w(i)w(j)^T\} = Q\,\delta_{ij} \tag{2.2-16b}$$

Measurement Noise Statistics

$$E\{v(k)\} = 0 \tag{2.2-17a}$$

$$E\{v(i)v(j)^T\} = R\,\delta_{ij} \tag{2.2-17b}$$

where δ_{ij} is the Kronecker delta defined as

$$\delta_{ij} = \begin{cases} 1 & i = j \\ 0 & i \neq j \end{cases} \tag{2.2-18}$$

and Q and R are the covariance matrices for the process noise and measurement noise, respectively. The assumption of no correlation between process noise and measurement noise is made (i.e. $E\{w(i)v(j)^T\} = 0$, for all i,j ≥ 0.

The discrete Kalman filter equations are separated into two sets of equations designated as the prediction equations and the filtered equations. The definitions for the state estimates and their associated covariances are as follows

Predicted Estimate

$$\bar{x}(k) = E\{x(k) \mid z(j),\ j = 1,2,\ldots,k-1\} \tag{2.2-19}$$

Predicted Error Covariance

$$M(k) = E\{[x(k) - \bar{x}(k)][x(k) - \bar{x}(k)]^T\} \tag{2.2-20}$$

Filtered Estimate

$$\hat{x}(k) = E\{x(k) \mid z(j),\ j = 1,2,\ldots,k\} \tag{2.2-21}$$

Filtered Error Covariance

$$P(k) = E\{[x(k) - \hat{x}(k)][x(k) - \hat{x}(k)]^T\} \tag{2.2-22}$$

The predicted and filtered equations are

Predicted Equations

$$\bar{x}(k+1) = \Phi\hat{x}(k) \tag{2.2-23}$$

$$M(k+1) = \Phi P(k)\Phi^T + \Gamma Q \Gamma^T \tag{2.2-24}$$

Filtered Equations

$$\hat{x}(k+1) = \bar{x}(k+1) + K(k+1)[z(k+1) - H\bar{x}(k+1)] \tag{2.2-25}$$

$$K(k+1) = M(k+1)H^T[HM(k+1)H^T + R]^{-1} \tag{2.2-26}$$

$$P(k+1) = [I - K(k+1)H]M(k+1) \tag{2.2-27}$$

where K(k+1) = Kalman filter gain at time k+1.

The discrete LKF also has an inherent diagnostic capability based on the statistical properties of the residuals or innovations which are defined as

$$r(k) = z(k) - H\bar{x}(k) \tag{2.2-28}$$

If the LKF is performing in an optimal manner (i.e. providing unbiased, minimum variance estimates), then it can be shown that the residuals have the following statistical properties.

Optimal LKF Residual Statistics

$$E\{r(k)\} = 0 \tag{2.2-29a}$$

$$E\{r(i)r(j)^T\} = R_r\delta(t-\tau) \tag{2.2-29b}$$

where

$$R_r = HMH^T + R \tag{2.2-30}$$

The residuals can be analyzed statistically to determine if the above statistics are satisfied. If the residuals have the above statistics, then the discrete LKF is performing optimally.

2.2.2 Nonlinear Kalman Filters

If the model of the aircraft dynamics is nonlinear, then a nonlinear or extended Kalman filter (EKF) must be used to estimate current and future positions of the aircraft. Since the measurements are provided at discrete points in time, a continuous-discrete or hybrid EKF is formulated. A standard approach is used in developing the EKF equations [Gelb; 1974].

The system and measurement models are given by

$$\dot{x}(t) = f(x(t),t) + w(t), \quad x(0) = x_0 \tag{2.2-31}$$

$$z(k) = h(x(t_k,k)) + v(k) \tag{2.2-32}$$

where $x(t) \in R^n$ is the continuous system state vector, $z(k) \in R^l$ is the discrete system measurement vector. The terms $w(t) \in R^m$ and $v(k) \in R^l$ represent process noise and measurement noise respectively. The terms f(x(t),t) and h(x(t_k, k)) are time-varying vector functions consisting of the nonlinear relationships describing the state propagation and measurements. The statistical characteristics for the above stochastic system are

Initial Condition Statistics

$$E\{x(0)\} = \hat{x}_0 \tag{2.2-33a}$$

$$E\{[x(0) - \hat{x}_0][x(0) - \hat{x}_0]^T\} = P_0 \tag{2.2-33b}$$

Process Noise Statistics

$$E\{w(t)\} = 0 \tag{2.2-34a}$$

$$E\{w(t)w(\tau)^T\} = Q\,\delta(t - \tau) \tag{2.2-34b}$$

Measurement Noise Statistics

$$E\{v(k)\} = 0 \tag{2.2-35a}$$

$$E\{v(i)v(j)^T\} = R\,\delta_{ij} \tag{2.2-35b}$$

The EKF is implemented under the assumption that the process noise is uncorrelated with the measurement noise (i.e. E $\{w(t)v(k)^T\} = 0$ for all k and all t.)

The implementation of the EKF requires the linearization of the nonlinear equations of f(x(t),t) and h(x(t_k, k)). This is achieved using a Taylor series expansion of these relationships and neglecting higher order terms. Using the notation developed

in the LKF section of this chapter, the following definitions will be used.

$$F(\hat{x}(t),t) = \frac{\partial f(x(t),t)}{\partial x(t)}\Big|_{x(t)=\hat{x}(t)} \tag{2.2-36}$$

$$H(\bar{x}(k),k) = \frac{\partial h(x(t_k),k)}{\partial x(t_k)}\Big|_{x(t_k)=\bar{x}(k)} \tag{2.2-37}$$

The following conditions are assumed to hold for the initial conditions and cross correlation between the process and measurement noise

$$\hat{x}(0) = E[x(0)] \tag{2.2-38a}$$

$$P(t=0) = E[(x(0)-\hat{x}(0))(x(0)-\hat{x}(0))^T] = P_o \tag{2.2-38b}$$

$$E[x(0)\,w(t)^T] = 0 \quad \text{for } all\ t \geq 0 \tag{2.2-38c}$$

$$E[x(0)\,v(k)^T] = 0 \quad \text{for } all\ k = 0,1,2,\ldots \tag{2.2-38d}$$

$$E[w(t)\,v(k)^T] = 0 \quad \text{for } all\ t,k \tag{2.2-38e}$$

The EKF is then given by

Predicted Equations ((k-1)T < t < kT)

$$\dot{\hat{x}}(t) = f(\hat{x}(t),t) \tag{2.2-39}$$

with initial condition $\hat{x}(k-1)$

$$\dot{P}(t) = F(\hat{x}(t),t)P(t) + P(t)F(\hat{x}(t),t)^T + Q \tag{2.2-40}$$

with initial condition P(k-1)

The matrix relationships represent n state equations and n^2 variance equations. For the nonlinear trackers of chapter 3, each equation is integrated forward in time using a fourth order Runge-Kutta integration routine to yield estimates $\bar{x}(k) = \hat{x}(t=kT)$ and M(k) = P(t=kT).

Filtered Equations ((k-1)T < t < kT)

$$\hat{x}(k) = \bar{x}(k) + K(k)[z(k) - h(\bar{x}(k),k)] \tag{2.2-41}$$

$$P(k) = [I - K(k)H(\bar{x}(k))]M(k) \tag{2.2-42}$$

$$K(k) = M(k)H(\bar{x}(k))^T [H(\bar{x}(k))M(k)H(\bar{x}(k))^T + R]^{-1} \tag{2.2-43}$$

In addition to the predicted equations, which are used at a specified time (k = t_k), the tracker must be able to predict what the future states of the aircraft will be. This is done using predictor equations, which are identical to the predicted equations, except that the predicted equations are integrated over one measurement time interval, while the predictor equations are integrated over N measurement time intervals. N is determined by how far into the future a prediction value is needed. A prediction time of one second was chosen for this study, therefore since the integration interval is one thirtieth of a second, then N = 30.

The above EKF equations are used to track the full six degree of freedom aircraft motions analyzed in chapter 3.

CHAPTER 3
NONLINEAR TRACKING FILTER ANALYSIS

3.1 Introduction

This chapter presents the technical formulation and results of four nonlinear trackers. The first two trackers are six and nine state models of trackers based on point-mass representations of a maneuvering aircraft. The tracker measurements are radar measurements of range, azimuth, and elevation and their associated rates. The last two trackers have twelve and fifteen states, and include orientation information in both the dynamics model of the aircraft, and in measurement sequences being provided to the tracker.

All four trackers are then exercised against a fixed wing aircraft performing a 5-g right turn. Performance figures of merit are calculated and presented for evaluation and comparisons of the trackers. A tuning study of the process noise is undertaken for the 5-g right turn maneuver. The results of the tuned filters are presented.

3.2 Nonlinear Tracking Filter Models

3.2.1 Tracking Filters With Radar Measurements

As was stated earlier, the design of tracking filter models requires a preliminary decision on coordinate selection for the system dynamics, and the system measurements. This analysis is based on using a cartesian coordinate system for the system dynamics and a polar coordinate system for the measurement dynamics. The state vector for the Kalman filter will be composed of the position, velocity, and acceleration of

the aircraft in one of three orthogonal directions of an earth-fixed coordinate system. Therefore, the resulting radar based measurements must be converted to the elements of the state vector which results in a nonlinear measurement matrix, which necessitates the use of an extended Kalman filter.

3.2.1.1 Six State Nonlinear Tracking Filter

The six state nonlinear tracking filter consists of a state vector of positions and velocities in three orthogonal directions. The state vector is

$$\bar{x} = \left[\dot{x}, \dot{y}, \dot{z}, x, y, z \right]^T \tag{3.2-1a}$$

$$= \left[x_1, x_2, \ldots, x_6 \right]^T \tag{3.2-1b}$$

where (x, y, z) are coordinates of a cartesian coordinate system. This selection of states corresponds to the random walk velocity of Fitzgerald [1981]. The equations of motion for this tracker are given in Table 3-1.

Table 3-1. Six State Tracking Equations

$$\dot{x} = \dot{x}$$

$$\dot{y} = \dot{y}$$

$$\dot{z} = \dot{z}$$

$$\ddot{x} = w_4$$

$$\ddot{y} = w_5$$

$$\ddot{z} = w_6$$

The terms $w_4, w_5,$ and w_6 are additive zero-mean, uncorrelated, gaussian noise terms.

The six state filter is provided with discrete radar measurements of range (R), azimuth (η), elevation (ζ), and their associate rates. A pictorial of the radar measurements is given in Figure 3-1. The equations relating the radar measurements to the selected state variables are given in Table 3-2. The v_i, i=4,9 terms are additive zero-mean, uncorrelated, gaussian noise terms.

Table 3-2 Radar Measurement Equations

$$R = [x^2 + y^2 + z^2]^{1/2} + v_4$$

$$\eta = \tan^{-1}(y/x) + v_5$$

$$\zeta = \tan^{-1}(-z/(x^2 + y^2)^{1/2}) + v_6$$

$$\dot{R} = (x\dot{x} + y\dot{y} + z\dot{z}) / (x^2 + y^2 + z^2)^{1/2} + v_7$$

$$\dot{\eta} = (x\dot{y} - y\dot{x}) / (x^2 + y^2) + v_8$$

$$\dot{\zeta} = [z(x\dot{x} + y\dot{y}) - \dot{z}(x^2 + y^2)] / [(x^2 + y^2 + z^2)(x^2 + y^2)^{1/2}] + v_9$$

3.2.1.2 Nine State Nonlinear Tracking Filter

The nine state nonlinear tracking filter consists of a state vector of position, velocity, and an exponentially correlated noise state in three orthogonal directions.

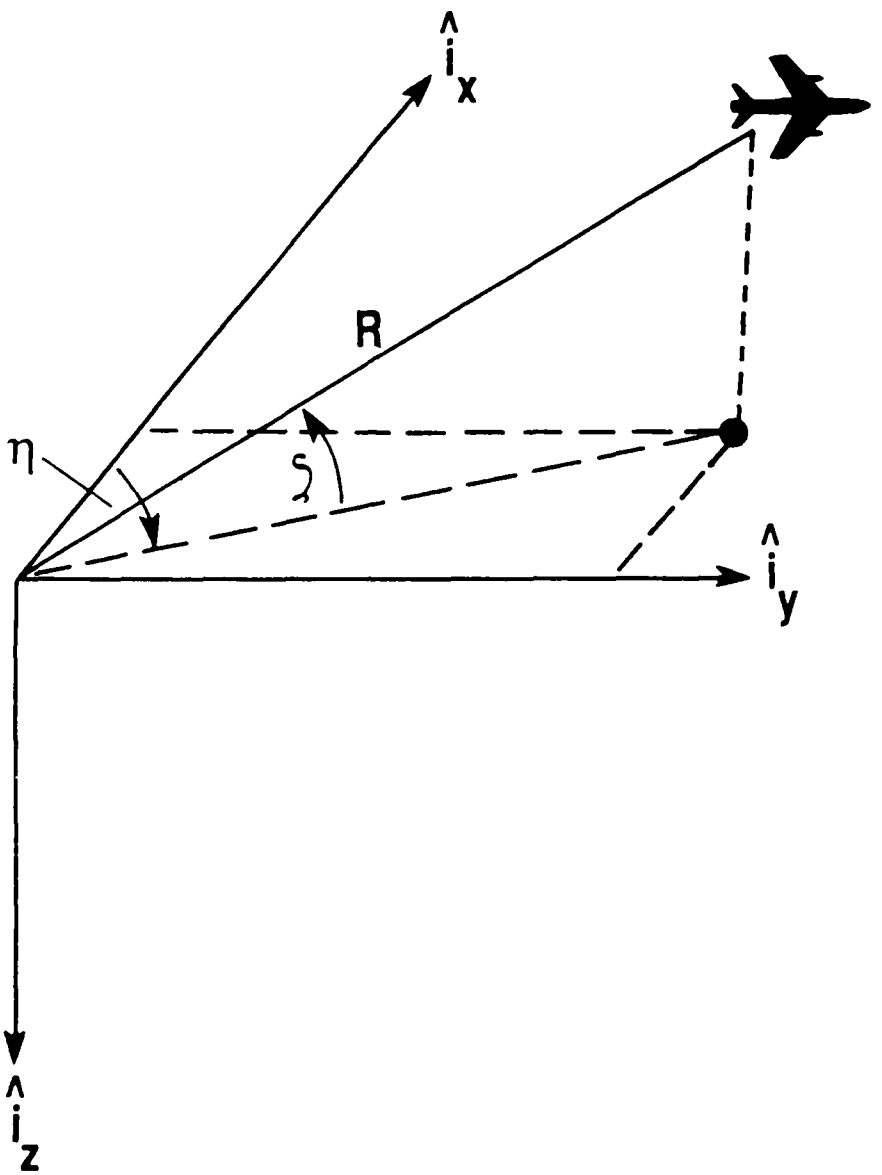

Figure 3-1 Radar Measurement Definitions

The exponentially correlated noise states are added to more accurately model aircraft inputs. The state vector is

$$\bar{x} = \left[\dot{x}, \dot{y}, \dot{z}, x, y, z, b_x, b_y, b_z \right]^T \tag{3.2-2a}$$

$$= \left[x_1, x_2, \ldots, x_9 \right]^T \tag{3.2-2b}$$

where again, (x, y, z) are coordinates in a cartesian coordinate system, with b_x, b_y, and b_z representing the correlated noise states. The equations of motion for the nine state tracker are given in Table 3-3.

Table 3-3. Nine State Tracking Equations

$$\dot{x} = \dot{x}$$

$$\dot{y} = \dot{y}$$

$$\dot{z} = \dot{z}$$

$$\ddot{x} = \kappa(b_x + w_4)$$

$$\ddot{y} = \kappa(b_y + w_5)$$

$$\ddot{z} = \kappa(b_z + w_6)$$

$$\dot{b_x} = (\frac{1}{\tau})b_x + w_7$$

$$\dot{b_y} = (\frac{1}{\tau})b_y + w_8$$

$$\dot{b_z} = (\frac{1}{\tau})b_z + w_9$$

The terms w_i, i=4,9 are additive white noise terms. The constant κ is included to account for scaling effects.

The nine state filter is provided with the identical discrete radar measurements as the six state filter. The relationships between the elements of the state vector and the radar variables are presented in Table 3-2.

3.2.2 Tracking Filters With Radar and Orientation Measurements.

3.2.2.1 Twelve State Nonlinear Tracking Filter

The twelve state tracker is based on including additional information concerning aircraft orientation. This orientation information is assumed to be the Euler angles that relate the orientation of an earth-fixed dextral coordinate system to an aircraft body-fixed dextral coordinate system. The orientation angles selected are the standard aircraft rotation angles of [Roskam; 1972]

1. θ -- Pitch angle
2. ϕ -- Roll angle
3. ψ -- Yaw angle

The inclusion of these rotational degrees of freedom introduces a certain degree of complication to the problem. In general, the rotational equations of motion are formulated in an axis system that is body fixed (i.e. remains stationary with respect to the aircraft). This is problematic since the most pertinent information to the tracker is the positional estimates of the aircraft in the tracker coordinate frame, which for this problem is considered an inertial frame. This problem is overcome by using appropriate coordinate transformations. The use of coordinate transformations allows for information developed in the body fixed frame to be used as needed in the inertial frame.

The coordinate systems used in this development are shown in Figure 3-2. Note that the body fixed ($\hat{b}_x - \hat{b}_y - \hat{b}_z$) coordinate system is both translating and rotating with respect to the inertial ($\hat{i}_x - \hat{i}_y - \hat{i}_z$) coordinate system. The body fixed coordinate system is an orthogonal right handed system described as follows.

1. The positive x-axis is defined as the line that runs from the aircraft center of gravity (c.g.) through the nose of the aircraft.

2. The positive y-axis is defined as the line perpendicular to the x-axis that runs from the aircraft c.g. through the right wing.

3. The positive z-axis is mutually perpendicular to the x and y axes and runs from the aircraft c.g. through the bottom of the aircraft.

The orientation angles are defined by three consecutive rotations (as shown in Figure 3-3) and carried out in the following order.

1. The inertial ($\hat{i}_x - \hat{i}_y - \hat{i}_z$) coordinate system is rotated about the $\hat{i}_z$ axis over an angle ψ. This yields the first intermediate coordinate system, $X_1 - Y_1 - Z_1$.

2. The $X_1 - Y_1 - Z_1$ system is rotated about the Y_1 axis over an angle θ. This provides the second intermediate coordinate system, $X_2 - Y_2 - Z_2$.

3. The $X_2 - Y_2 - Z_2$ system is rotated about the X_2 axis over an angle ϕ. This yields the body fixed coordinate system $\hat{b}_x - \hat{b}_y - \hat{b}_z$

Using the above coordinate systems and orientation angles, the angular velocity vector ($\bar{\omega}$) of the body fixed coordinate system with respect to the inertial coordinate system is defined as

$$\bar{\omega} = p\hat{b}_x + q\hat{b}_y + r\hat{b}_z \qquad (3.2\text{-}3)$$

where p is roll angular velocity, q is the pitch angular velocity and r is the yaw angular velocity.

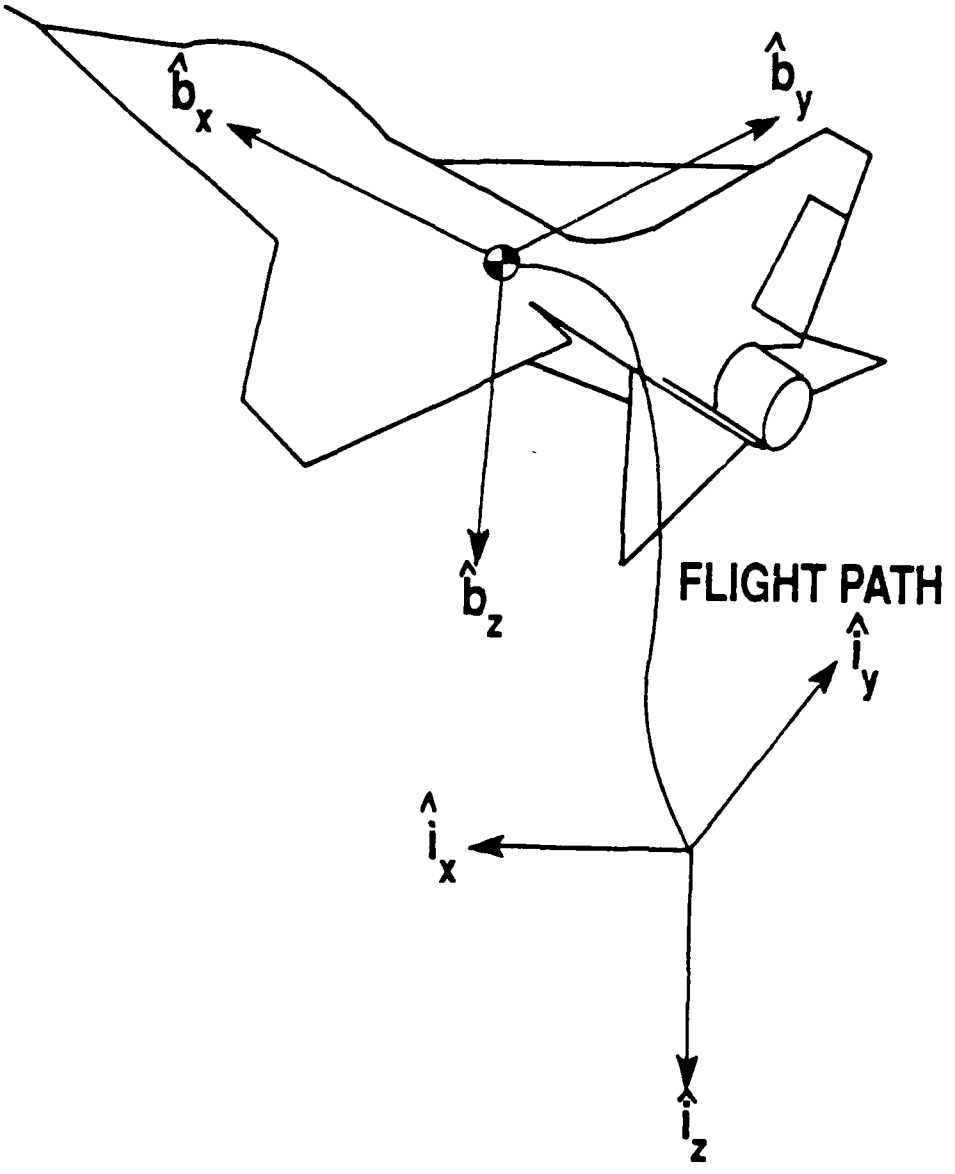

Figure 3-2 Inertial and Body-Fixed Coordinate Systems

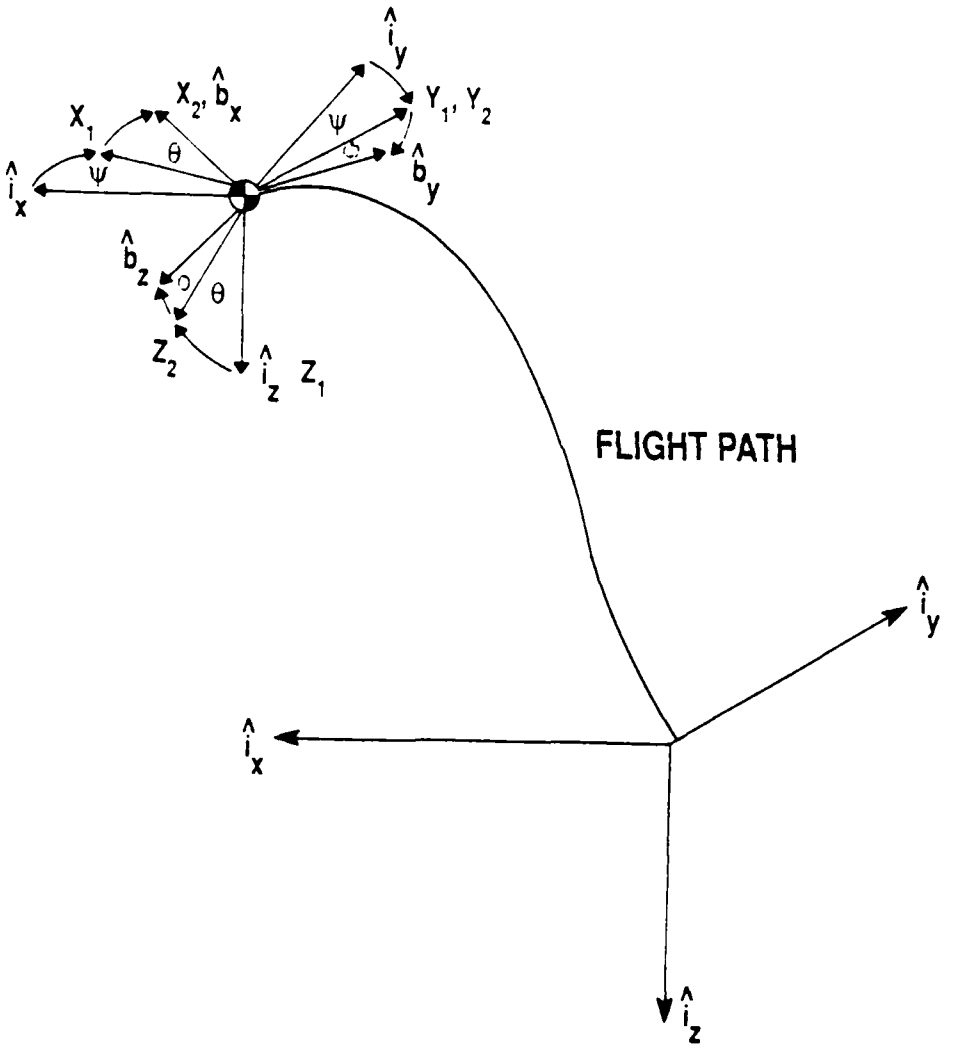

Figure 3-3 Euler Angle Rotations

The rotational equations of motion are developed using the following assumptions.

1. The aircraft has a plane of symmetry given by the x-z plane. Under this condition, the products of inertia I_{xy} and I_{yz} are zero.

2. The mass of the aircraft is constant.

3. The aircraft is a rigid body.

The angular rotation of the aircraft is then governed by the following equations [Roskam; 1972]

$$I_{xx}\dot{p} - I_{xz}\dot{r} - I_{xz}pq + (I_{zz} - I_{yy})rq = L \tag{3.2-4}$$

$$I_{yy}\dot{q} + (I_{xx} - I_{zz})pr + I_{xz}(p^2 - r^2) = M \tag{3.2-5}$$

$$I_{zz}\dot{r} - I_{xz}\dot{p} + (I_{yy} - I_{xx})pq + I_{xz}qr = N \tag{3.2-6}$$

$$\dot{\phi} = p + q\sin\phi\tan\theta + r\cos\phi\tan\theta \tag{3.2-7}$$

$$\dot{\theta} = q\cos\phi - r\sin\phi \tag{3.2-8}$$

$$\dot{\psi} = (q\sin\phi + r\cos\phi)/\cos\theta \tag{3.2-9}$$

where I_{xx}, I_{yy}, I_{zz}, and I_{xz} are moments and products of inertia, and L, M, N, are external moments.

The above kinematic equations contain tan θ terms which can present numerical problems for trajectories with large pitch angles. Under these conditions, the selection of quaternions or the selection of an alternative sequence of Euler angle rotations would correct this situation. Since the trajectories examined in this research will not have large pitch angles over the selected trajectories, the use of these Euler angles will not present a problem.

A set of generalized equations for the external moments is given by

$$L = k_1\beta + k_2 p + k_3 r + k_4\delta_a + k_5\delta_r \tag{3.2-10}$$

$$M = k_6 u + k_7\alpha + k_8 q + k_9\delta_e + k_{10} \tag{3.2-11}$$

$$N = k_{11}\beta + k_{12} p + k_{13} r + k_{14}\delta_a + k_{15}\delta_r \tag{3.2-12}$$

where α and β are angle of attack and sideslip angles respectively, and u is the component of vehicle speed along the x-axis. The constants k_i, i=1,15, would be composed of relevant aerodynamic and thrust stability derivatives. The terms δ_a, δ_r and δ_e are the aileron, rudder and elevator angles respectively.

Examining the above equations shows that certain elements of the equation are dominant in determining the motion of the aircraft. Specifically, pilots input of elevator, aileron or rudder is of major importance in determining aircraft motion. Since this input is unknown, it will be modeled as a stochastic process. In view of this, smaller terms can be ignored. The equations are simplified using the following assumptions.

1. $\beta \approx 0$
2. $k_3 = k_5 = k_6 = k_8 = k_{10} = k_{12} = k_{13} = k_{14} = 0$
3. $I_{xz} = 0$

The resulting rotational equations are

$$I_{xx}\dot{p} + (I_{zz} - I_{yy})rq = k_2 p + k_4\delta_a \tag{3.2-13}$$

$$I_{yy}\dot{q} + (I_{xx} - I_{zz})pr = k_7\alpha + k_9\delta_e \tag{3.2-14}$$

$$I_{zz}\dot{r} + (I_{yy} - I_{xx})pq = k_{15}\delta_r \tag{3.2-15}$$

$$\dot{\phi} = p + q\sin\phi\tan\theta + r\cos\phi\tan\theta \tag{3.2-16}$$

$$\dot{\theta} = q\cos\phi - r\sin\phi \tag{3.2-17}$$

$$\dot{\psi} = (q\sin\phi + r\cos\phi)/\cos\theta \tag{3.2-18}$$

As stated earlier, the aircraft tracker requires information concerning aircraft position in an inertial reference frame. This is unfortunate since the aircraft orientation information and therefore the force and moment information is developed in a body fixed reference frame. This necessitates the use of coordinate transformation matrices so that the force and moment information developed in a body fixed reference frame can be used in an inertial reference frame.

The inertial translation motion of the aircraft is modeled as

$$\dot{x} = \dot{x} \tag{3.2-19}$$

$$\dot{y} = \dot{y} \tag{3.2-20}$$

$$\dot{z} = \dot{z} \tag{3.2-21}$$

$$m\ddot{x} = F_x^i \tag{3.2-22}$$

$$m\ddot{y} = F_y^i \tag{3.2-23}$$

$$m\ddot{z} = F_z^i + mg \tag{3.2-24}$$

where the i superscript designates force components in the inertial coordinate direction, m is the mass of the aircraft, and g is the acceleration due to gravity acting in the

positive $\hat{i}_z$ direction.

The inertial components of the force vector are derived from aircraft orientation and velocity information as described in the following paragraphs.

The external forces acting on the aircraft and the aircraft velocity vector, $\bar{V}$, are shown in Figure 3-4. The following assumptions are made concerning the external forces.

1. The force resultant vector $\bar{F}$ due to aerodynamic and thrust forces is located in the aircraft plane of symmetry (x-z plane). This assumes that all aircraft turns are coordinated turns.

2. Thrust exactly cancels aerodynamic drag so neither one needs to be modeled.

3. The vehicle is flying in still air, and therefore the wind vector is in the opposite direction of the c.g. velocity vector.

The magnitude of the force vector is modeled as

$$F = 1/2\rho V^2 S C_{L_\alpha} \alpha \tag{3.2-25}$$

where

ρ = air density

V = airspeed, assumed to be the speed of the c.g.

S = wing area

C_{l_α} = lift curve slope

α = aircraft angle of attack

The force and velocity vectors can be represented in either the body fixed $(\hat{b}_x - \hat{b}_y - \hat{b}_z)$ or the inertial $(\hat{i}_x - \hat{i}_y - \hat{i}_z)$ reference frame as follows

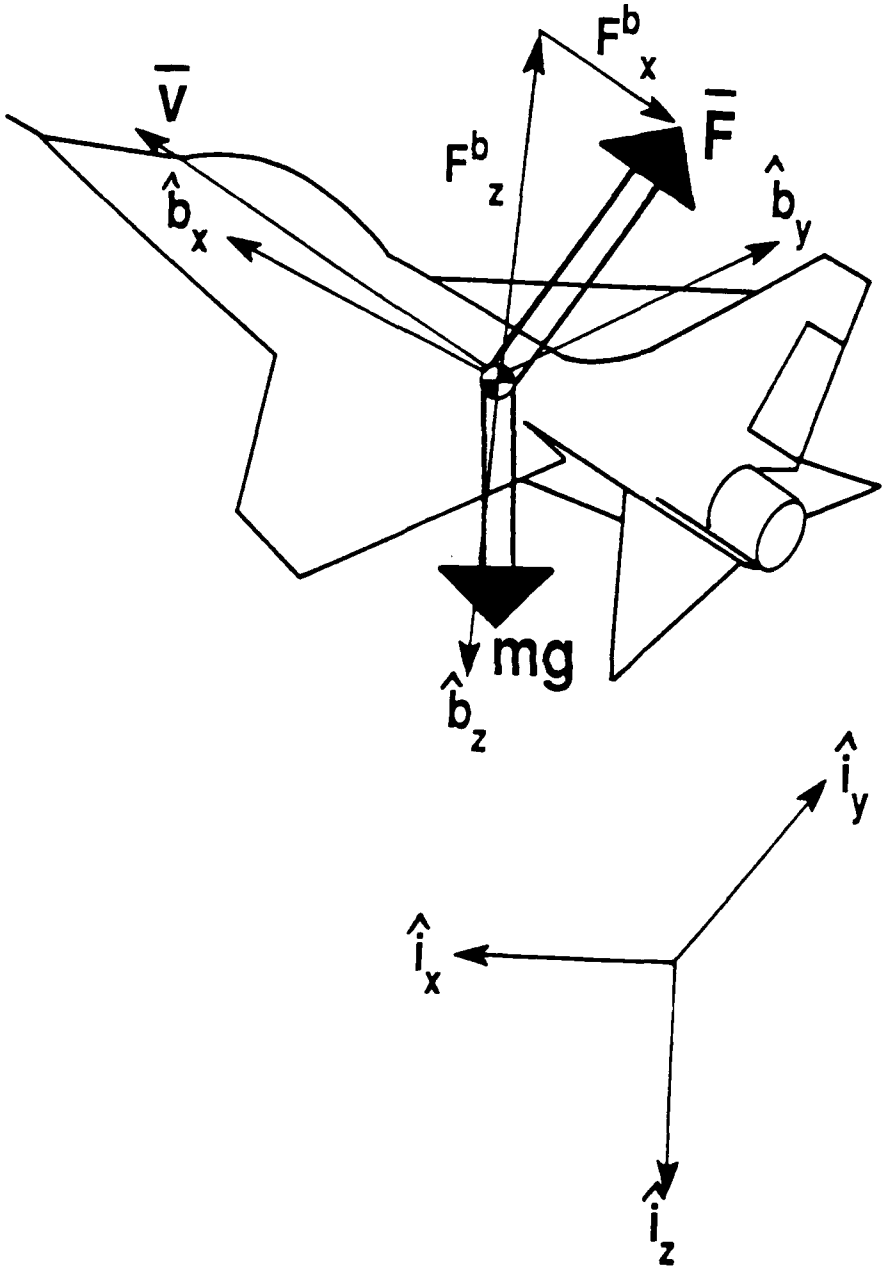

Figure 3-4 External Aircraft Forces

Inertial Representation

$$\bar{F} = F_x^i \, \hat{i}_x + F_y^i \, \hat{i}_y + F_z^i \, \hat{i}_z \tag{3.2-26}$$

$$\bar{V} = \dot{x} \, \hat{i}_x + \dot{y} \, \hat{i}_y + \dot{z} \, \hat{i}_z \tag{3.2-27}$$

Body Fixed Representation

$$\bar{F} = F_x^b \, \hat{b}_x + F_y^b \, \hat{b}_y + F_z^b \, \hat{b}_z \tag{3.2-28}$$

$$\bar{V} = u \, \hat{b}_x + v \, \hat{b}_y + w \, \hat{b}_z \tag{3.2.29}$$

To move freely between frames of reference, a coordinate transformation matrix consisting of direction cosines is needed. For the inertial and body fixed reference frames selected for this research, the following transformation matrices are used.

Body to Inertial $[T_i^b]$

$$[T_i^b] = \begin{bmatrix} \cos\psi\cos\theta & \cos\psi\sin\theta\sin\phi - \sin\psi\cos\phi & \cos\psi\sin\theta\cos\phi + \sin\psi\sin\phi \\ \sin\psi\cos\theta & \sin\psi\sin\theta\sin\phi + \cos\psi\cos\phi & \sin\psi\sin\theta\cos\phi - \cos\psi\sin\phi \\ -\sin\theta & \cos\theta\sin\phi & \cos\theta\cos\phi \end{bmatrix}$$

Inertial to Body Transformation $[T_b^i]$

$$[T_b^i] = \begin{bmatrix} \cos\psi\cos\theta & \sin\psi\cos\theta & -\sin\theta \\ \cos\psi\sin\theta\sin\phi - \sin\psi\cos\phi & \sin\psi\sin\theta\sin\phi + \cos\psi\cos\phi & \cos\theta\sin\phi \\ \cos\psi\sin\theta\cos\phi + \sin\psi\sin\phi & \sin\psi\sin\theta\cos\phi - \cos\psi\sin\phi & \cos\theta\cos\phi \end{bmatrix}$$

In order to calculate the direction of the force vector $\bar{F}$, we must transform inertial velocities to body fixed velocities.

This is performed using the inertial to body transformation $[T_b^i]$.

$$\begin{Bmatrix} u \\ v \\ w \end{Bmatrix} = [T_b^i] \begin{Bmatrix} \dot{x} \\ \dot{y} \\ \dot{z} \end{Bmatrix} \tag{3.2-30}$$

Figure 3-5 shows the relationship between the aircraft velocity vector, the components of the aircraft velocity vector and the body fixed axis system. The velocity components along the body fixed axes are then (with V = magnitude of $\bar{V}$)

$$u = V \cos\beta \cos\alpha \tag{3.2-31}$$

$$v = V \sin\beta \tag{3.2-32}$$

$$w = V \cos\beta \sin\alpha \tag{3.2-33}$$

The earlier assumption of $\beta = 0$ reduces these equations to

$$u = V \cos\alpha \tag{3.2-34}$$

$$v = 0 \tag{3.2-35}$$

$$w = V \sin\alpha \tag{3.2-36}$$

Rearranging the equation 3.2-36 gives

$$\alpha = \sin^{-1}(w/V) \tag{3.2-37}$$

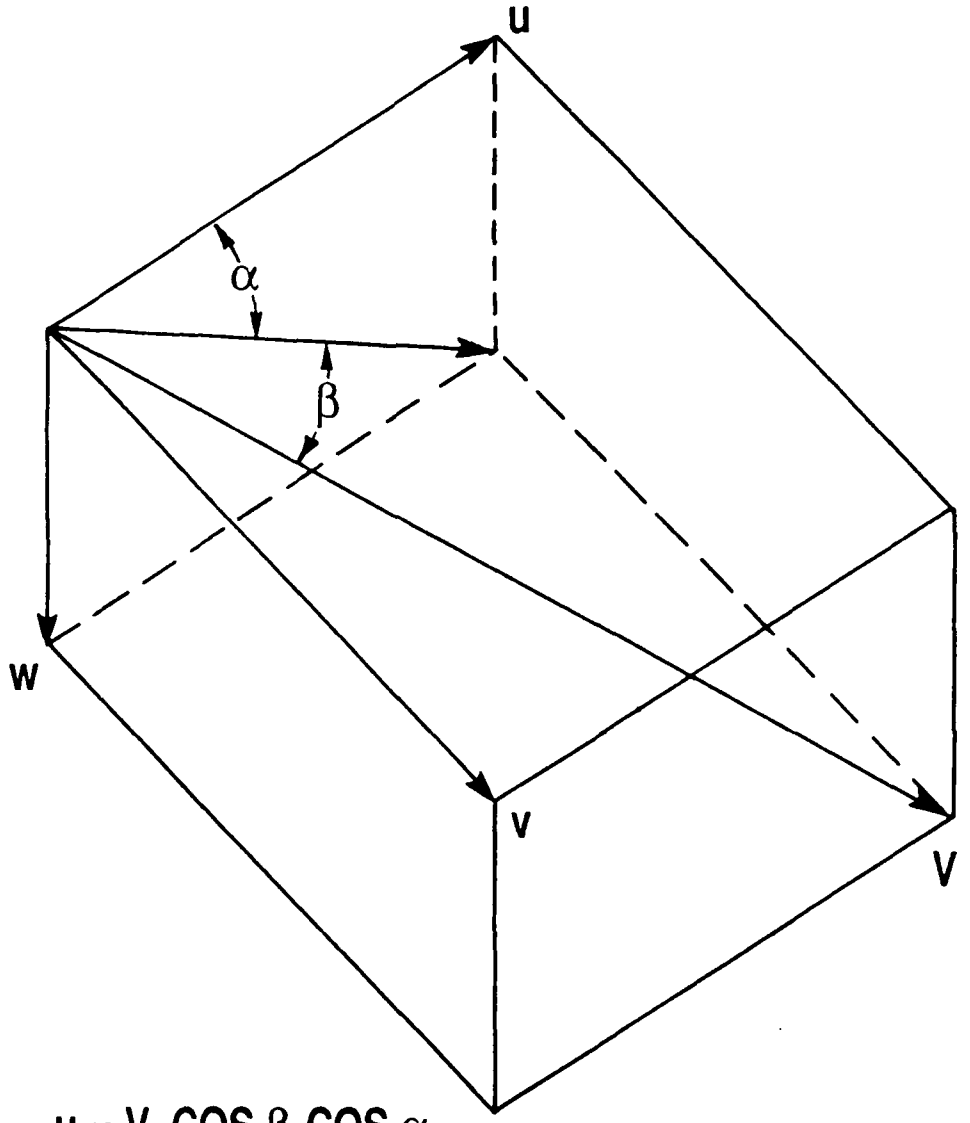

$u = V \cos\beta \cos\alpha$

$v = V \sin\beta$

$w = V \cos\beta \sin\alpha$

Figure 3-5 Angle of Attack and Sideslip Angles in Body-Fixed Axis System

Under the previous assumption that the force vector lies in the x-z plane, and is perpendicular to the velocity vector, the following relationships hold for the force vector components in the body fixed coordinates.

$$F_x^b = F \sin\alpha \tag{3.2-38}$$

$$F_y^b = 0 \tag{3.2-39}$$

$$F_z^b = -F \cos\alpha \tag{3.2-40}$$

The inertial components of the force vector are needed as inputs to the translational equations of motion. These are obtained by transforming the body fixed components to inertial components.

$$\begin{Bmatrix} F_x^i \\ F_y^i \\ F_z^i \end{Bmatrix} = [T_i^b] \begin{Bmatrix} F_x^b \\ F_y^b \\ F_z^b \end{Bmatrix} \tag{3.2-41}$$

In summary the procedural steps for determining the inertial components of the force vector are

1. Transform the inertial velocity components $(\dot{x}, \dot{y}, \dot{z})$ to body fixed velocity components (u, v, w).

2. Using body fixed velocity components, calculate the aircraft angle of attack (α).

3. Using α, calculate the body fixed components (F_x^b, F_y^b, F_z^b) of the force vector $(\bar{F})$.

4. Transform the body fixed components of the force velocity to inertial components (F_x^i, F_y^i, F_z^i) of the force vector.

These procedural steps are depicted pictorially in Figure 3-6. This figure clearly shows the interaction between the translational motion and the rotational motion that is exploited in this approach. This approach yields a coupled set of 12 nonlinear equations of motion which are summarized in Table 3-4.

The equations of Table 3-4 are then implemented with an extended Kalman filter. The state vector for the twelve state EKF is

$$\bar{x} = \left[p, q, r, \phi, \theta, \psi, \dot{x}, \dot{y}, \dot{z}, x, y, z \right]^T \tag{3.2-42a}$$

$$= \left[x_1, x_2, \ldots, x_{12} \right]^T \tag{3.2-42b}$$

The input elements of δ_a, δ_e, δ_r, are unknown, and therefore will be modeled as noise processes. The equations of motion for the twelve state tracker are presented in Table 3-5.

The twelve state tracking filter is provided with discrete radar measurements of range (R), azimuth (η), elevation (ζ), and measurements of the Euler angles ϕ, θ, and ψ. The radar and orientation measurement equations are shown in Table 3-6. The v_i, i=1,9 are additive zero-mean, uncorrelated, gaussian noise terms.

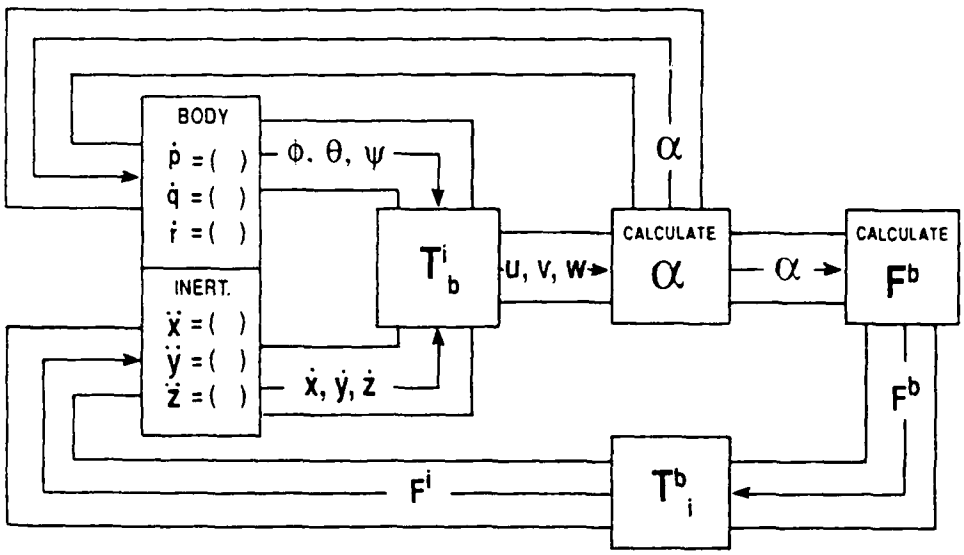

Figure 3-6 Inertial Force Component Calculation

Table 3-4 Aircraft Six Degree of Freedom Equations of Motion

$$I_{xx}\dot{p} + (I_{zz} - I_{yy})rq = k_2 p + k_4\delta_a$$

$$I_{yy}\dot{q} + (I_{xx} - I_{zz})pr = k_7\alpha + k_9\delta_e$$

$$I_{zz}\dot{r} + (I_{yy} - I_{xx})pq = k_{15}\delta_r$$

$$\dot{\phi} = p + q\sin\phi\tan\theta + r\cos\phi\tan\theta$$

$$\dot{\theta} = q\cos\phi - r\sin\phi$$

$$\dot{\psi} = (q\sin\phi + r\cos\phi)/\cos\theta$$

$$\dot{x} = \dot{x}$$

$$\dot{y} = \dot{y}$$

$$\dot{z} = \dot{z}$$

$$m\ddot{x} = F_x^i$$

$$= (\cos\psi\sin\alpha\cos\theta - \cos\psi\cos\alpha\cos\phi\sin\theta - \sin\psi\cos\alpha\sin\phi)\, F$$

$$m\ddot{y} = F_y^i$$

$$= (\sin\psi\sin\alpha\cos\theta - \sin\psi\cos\alpha\cos\phi\sin\theta + \cos\psi\cos\alpha\sin\phi)\, F$$

$$m\ddot{z} = F_z^i + mg$$

$$= (-\sin\alpha\sin\theta - \cos\alpha\cos\phi\cos\theta)\, F + mg$$

Table 3-5 Twelve State Tracking Equations

$$\dot{p} = \left(\frac{1}{I_{xx}}\right)\left\{(I_{yy} - I_{zz})rq + k_2 p + k_4 w_1\right\}$$

$$\dot{q} = \left(\frac{1}{I_{yy}}\right)\left\{(I_{zz} - I_{xx})pr + k_7\alpha + k_9 w_2\right\}$$

$$\dot{r} = \left(\frac{1}{I_{yy}}\right)\left\{(I_{xx} - I_{yy})pq + k_{15} w_3\right\}$$

$$\dot{\phi} = p + q\sin\phi\tan\theta + r\cos\phi\tan\theta$$

$$\dot{\theta} = q\cos\phi - r\sin\phi$$

$$\dot{\psi} = (q\sin\phi + r\cos\phi)/cos\,\theta$$

$$\dot{x} = \dot{x}$$

$$\dot{y} = \dot{y}$$

$$\dot{z} = \dot{z}$$

$$\ddot{x} = F_x^i/m$$

$$= (cos\,\psi\sin\alpha\cos\theta - \cos\psi\cos\alpha\cos\phi\sin\theta - \sin\psi\cos\alpha\sin\phi)\,F/m + \kappa w_4$$

$$\ddot{y} = F_y^i/m$$

$$= (sin\,\psi\sin\alpha\cos\theta - \sin\psi\cos\alpha\cos\phi\sin\theta + \cos\psi\cos\alpha\sin\phi)\,F/m + \kappa w_5$$

$$\ddot{z} = F_z^i/m + g$$

$$= (-\sin\alpha\sin\theta - \cos\alpha\cos\phi\cos\theta)\,F/m + g + \kappa w_6$$

Table 3-6 Radar and Orientation Measurement Equations

$$\phi_m = \phi + v_1$$

$$\theta_m = \theta + v_2$$

$$\psi_m = \psi + v_3$$

$$R = [x^2 + y^2 + z^2]^{1/2} + v_4$$

$$\eta = \tan^{-1}(y/x) + v_5$$

$$\zeta = \tan^{-1}(-z/(x^2 + y^2))^{1/2} + v_6$$

$$\dot{R} = (x\dot{x} + y\dot{y} + z\dot{z}) / (x^2 + y^2 + z^2)^{1/2} + v_7$$

$$\dot{\eta} = (x\dot{y} - y\dot{x}) / (x^2 + y^2) + v_8$$

$$\dot{\zeta} = [z(x\dot{x} + y\dot{y}) - \dot{z}(x^2 + y^2)] /$$

$$[(x^2 + y^2 + z^2)(x^2 + y^2)^{1/2}] + v_9$$

3.2.2.2 Fifteen State Nonlinear Tracking Filter

The fifteen state tracker consists of the twelve state tracker with the addition of three exponentially correlated noise states. The exponentially correlated states are added to account for the fact that aircraft input is a correlated function of time. The addition of the three correlated states leads to the following state vector

$$\bar{x} = \left[p, q, r, \phi, \theta, \psi, \dot{x}, \dot{y}, \dot{z}, x, y, z, b_x, b_y, b_z \right]^T \tag{3.2-43a}$$

$$= \left[x_1, x_2, \ldots, x_{15} \right]^T \tag{3.2-43b}$$

The equations of motion for the fifteen state tracker are presented in Table 3-7. The terms w_i,i=1,9 are additive zero-mean uncorrelated gaussian noise processes.

The radar and orientation measurement equations are unchanged from the twelve state filter.

The equations of motion shown in Tables 3-1, 3-3, 3-5, and 3-7 are combined with the measurement equations of Tables 3-2 and 3-6 as the basis for the four non-linear tracking filters. The performance characteristics of these tracking filters are now examined.

Table 3-7 Fifteen State Tracking Equations

$$\dot{p} = (\frac{1}{I_{xx}})\left\{ (I_{yy} - I_{zz})rq + k_2 p + k_4 w_1 \right\}$$

$$\dot{q} = (\frac{1}{I_{yy}})\left\{ (I_{zz} - I_{xx})pr + k_7 \alpha + k_9 w_2 \right\}$$

$$\dot{r} = (\frac{1}{I_{yy}})\left\{ (I_{xx} - I_{yy})pq + k_{15} w_3 \right\}$$

$$\dot{\phi} = p + q\sin\phi\tan\theta + r\cos\phi\tan\theta$$

$$\dot{\theta} = q\cos\phi - r\sin\phi$$

$$\dot{\psi} = (q\sin\phi + r\cos\phi)/cos\,\theta$$

$$\dot{x} = \dot{x}$$

$$\dot{y} = \dot{y}$$

$$\dot{z} = \dot{z}$$

$$\ddot{x} = F_x^i/m$$

$$= (cos\,\psi\sin\alpha\cos\theta - \cos\psi\cos\alpha\cos\phi\sin\theta - \sin\psi\cos\alpha\sin\phi)\, F/m + \kappa w_4$$

$$\ddot{y} = F_y^i/m$$

$$= (sin\,\psi\sin\alpha\cos\theta - \sin\psi\cos\alpha\cos\phi\sin\theta + \cos\psi\cos\alpha\sin\phi)\, F/m + \kappa w_5$$

$$\ddot{z} = F_z^i/m + g$$

$$= (-\sin\alpha\sin\theta - \cos\alpha\cos\phi\cos\theta)\, F/m + g + \kappa w_6$$

$$\dot{b}_x = (\frac{1}{\tau})b_x + w_7$$

$$\dot{b}_y = (\frac{1}{\tau})b_y + w_8$$

$$\dot{b}_z = (\frac{1}{\tau})b_z + w_9$$

3.3 Tracking Filter Comparisons

The four tracking filters are now exercised against an aircraft performing a variety of maneuvers.

The first maneuver investigated is a 5-g turn performed by an aircraft of the F-5 or T-38 class of fighter aircraft. The vehicle is initially traveling in an easterly direction (along the inertial $\hat{i_y}$ axis) at 440 ft/sec. The tracker is centered on the inertial coordinate system and begins tracking when the aircraft is at the following coordinates.

x = 3000 feet (north of tracker)

y = -1445 feet (west of tracker)

z = -1000 feet (above the tracker)

One and one half seconds into the trajectory, the aircraft begins a banked turn to the right. Three seconds later, a maximum bank angle of 78 degrees is achieved. The aircraft then begins to slowly reduce the bank angle so that the aircraft achieves a southerly heading. The aircraft undergoes a decrease in altitude of 780 feet and maintains an approximately steady 440 ft/sec velocity throughout the maneuver. The trajectory for this turn is shown in Figure 3-7.

Using a digital flight simulator program entitled FLTSIM [Jones; 1978], the nonlinear six degree of freedom differential equations of motion are integrated using a fourth order Runge-Kutta numerical integration routine.

The measurement sequence for a given trajectory is given by

a) Converting exact inertial positions and velocities to a corresponding measurement variable of range (R), range rate ($\dot{R}$), azimuth (η), azimuth rate ($\dot{\eta}$), elevation (ζ), and elevation rate ($\dot{\zeta}$). This is accomplished using the relationships of Table 3-2. A zero-mean, uncorrelated, gaussian noise sequence of

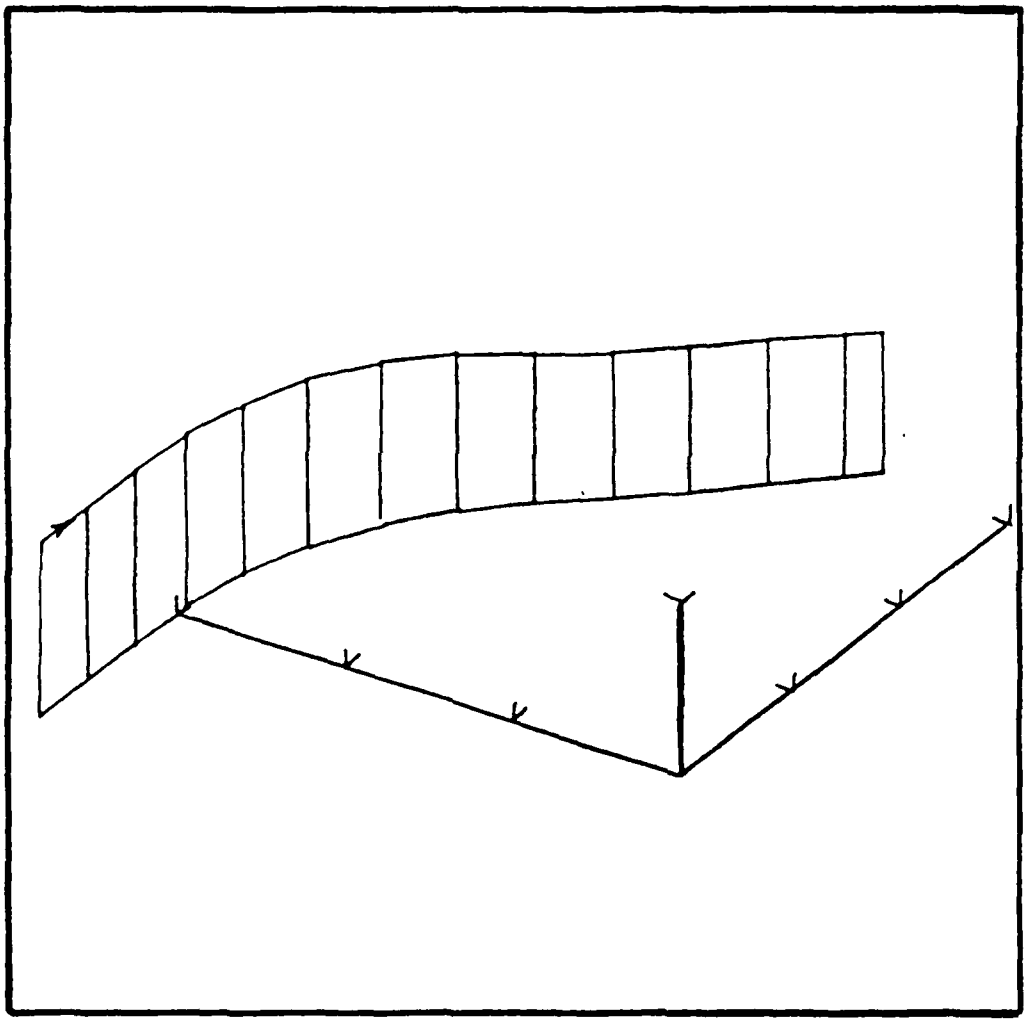

Figure 3-7 Right Turn Trajectory

approriate variance is added to each measurement.

b) The exact orientation angles are also corrupted by an additive zero-mean, uncorrelated, gaussian noise sequence to produce orientation measurements. The noise variances for the nine measurements are presented in Table 3-8.

Table 3-8 EKF Measurement Noise Statistics

$$v_1 \sim N(0,r_1) \quad r_1 = .7x\,10^{-4}(rad)^2$$

$$v_2 \sim N(0,r_2) \quad r_2 = .2x\,10^{-2}\,(rad)^2$$

$$v_3 \sim N(0,r_3) \quad r_3 = .2x\,10^{-2}\,(rad)^2$$

$$v_4 \sim N(0,r_4) \quad r_4 = .25x\,10^{4}\,(ft)^2$$

$$v_5 \sim N(0,r_5) \quad r_5 = .4x\,10^{-5}\,(rad)^2$$

$$v_6 \sim N(0,r_6) \quad r_6 = .4x\,10^{-5}\,(rad)^2$$

$$v_7 \sim N(0,r_7) \quad r_7 = .25x\,10^{4}\,(ft/sec)^2$$

$$v_8 \sim N(0,r_8) \quad r_8 = .16x\,10^{-4}\,(rad/sec)^2$$

$$v_9 \sim N(0,r_9) \quad r_9 = .16x\,10^{-4}\,(rad/sec)^2$$

The process noise statistics for the additive noises of Tables 3-1, 3-3, 3-5, and 3-7 are shown in Table 3-9.

Table 3-9 EKF Process Noise Statistics

$w_1 \sim N(0,q_1)\ \ q_1 = 4.0x\,10^{-6}\ (rad/sec^2)^2$

$w_2 \sim N(0,q_2)\ \ q_2 = 2.0x\,10^{-4}\ (rad/sec^2)^2$

$w_3 \sim N(0,q_3)\ \ q_3 = 6.0x\,10^{-6}\ (rad/sec^2)^2$

$w_4 \sim N(0,q_4)\ \ q_4 = 1.2x\,10^{-4}\ (ft/sec^2)^2$

$w_5 \sim N(0,q_5)\ \ q_5 = 1.2x\,10^{-4}\ (ft/sec^2)^2$

$w_6 \sim N(0,q_6)\ \ q_6 = 1.2x\,10^{-4}\ (ft/sec^2)^2$

$w_7 \sim N(0,q_7)\ \ q_7 = 1.0x\,10^{-3}\ (ft/sec^2)^2$

$w_8 \sim N(0,q_8)\ \ q_8 = 1.0x\,10^{-3}\ (ft/sec^2)^2$

$w_9 \sim N(0,q_9)\ \ q_9 = 1.0x\,10^{-3}\ (ft/sec^2)^2$

The four trackers are now analyzed to determine their ability to predict the aircraft position one second ahead into the future. The results of this analysis are now discussed and summarized in the following tables and figures.

Figures 3-8 through Figures 3-14 plot the one second ahead predicted values versus the true state values. In performing the one second ahead predictions, the algorithm assumes that angular velocities p, q and r are zero.

Figures 3-8 through 3-13 depict the 12-state and 15-state one second ahead predicted values for pitch, roll and yaw angles. Examination of these estimates shows that in general the orientation angle predictions lag the true values by one to two seconds. A significant proportion of this lag is due to the assumption of zero angular velocities Later in this chapter, the angular predictions are made under the assumptions of constant angular velocities and time varying angular velocities. Using these assumptions significantly reduces or completely eliminates the prediction lag.

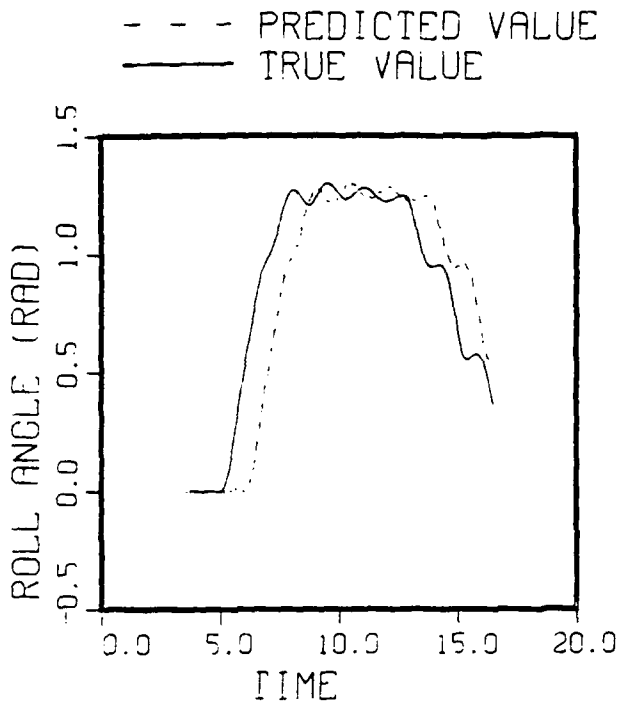

Figure 3-8 Predicted vs True Roll Angle (12-State Est.)

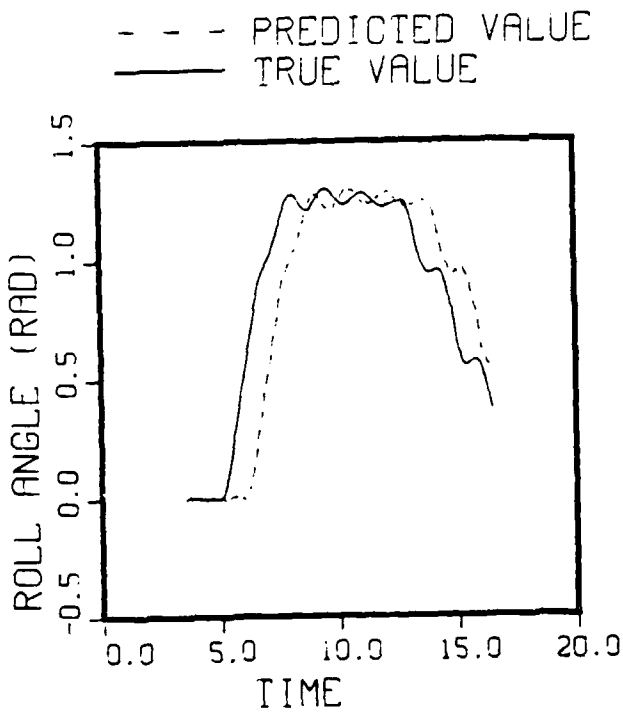

Figure 3-9 Predicted vs True Roll Angle (15-State Est.)

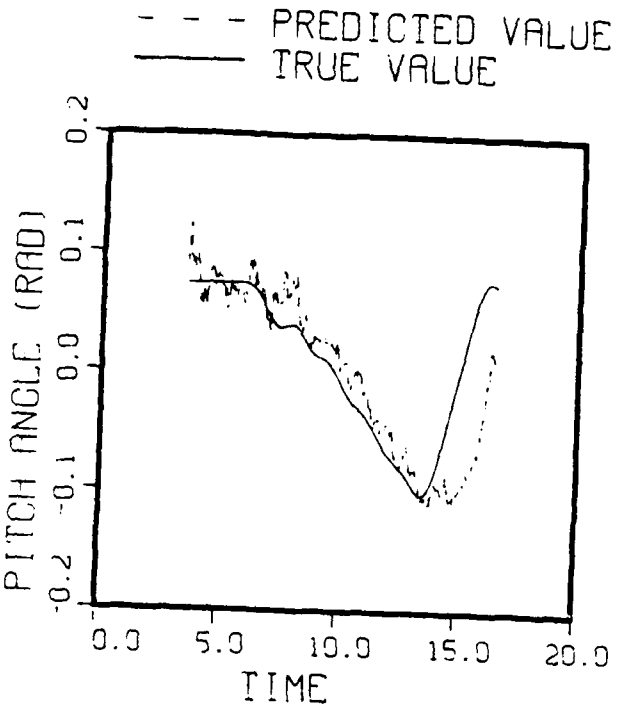

Figure 3-10 Predicted vs True Pitch Angle (12-State Est.)

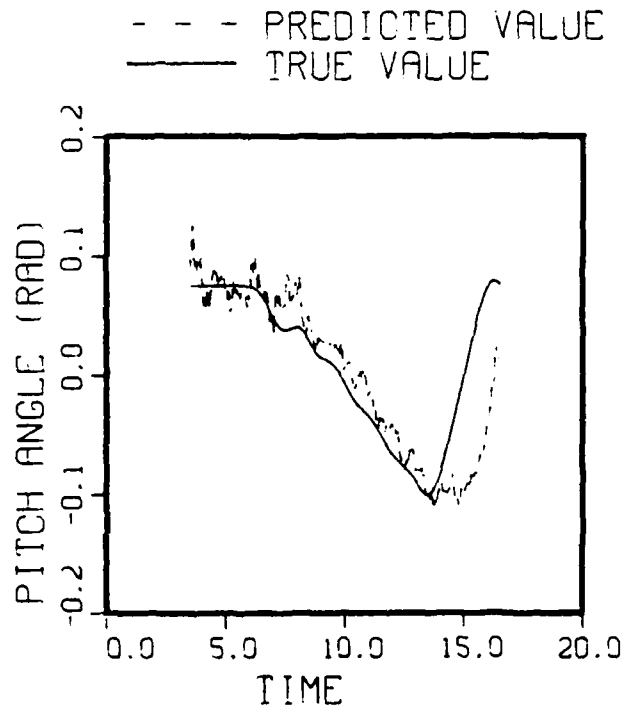

Figure 3-11 Predicted vs True Pitch Angle (15-State Est.)

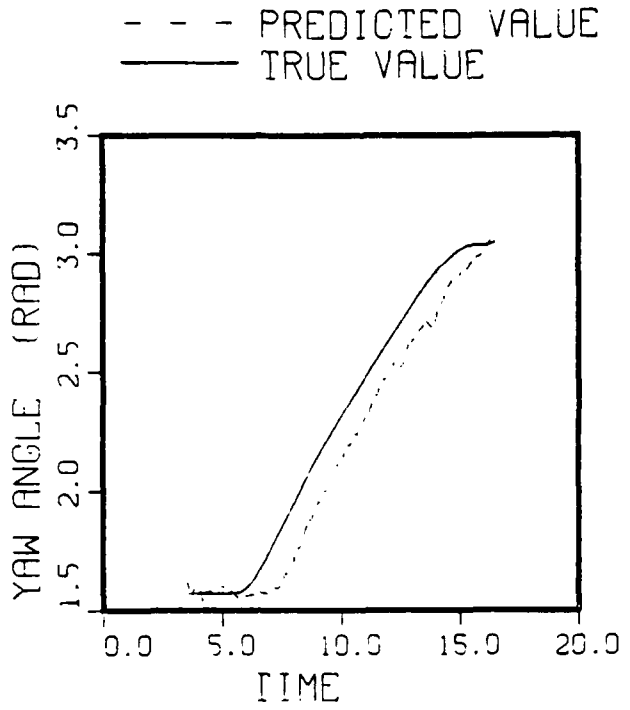

Figure 3-12 Predicted vs True Yaw Angle (12-State Est.)

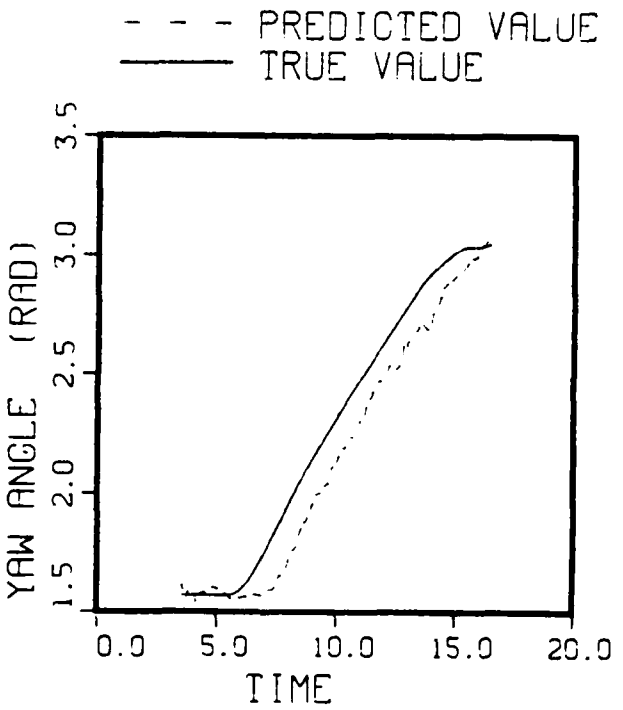

Figure 3-13 Predicted vs True Yaw Angle (15-State Est.)

The prediction angles for the 6-state and 9-state estimators are not shown since they provide no information to these estimators.

Figures 3-14 through 3-25 depict the one second ahead predicted values for x, y and z positions. In these figures, there are obvious differences in the quality of the predictions.

Figures 3-14 through 3-17 show the results for the x-position. It is apparent that the 6-state estimator is deficient from approximately 8 seconds to 14 seconds. Including the colored noise states (i.e. 9-state estimator) reduces the errors, although the errors are still significant in the 8 to 10 second time frame. The 12 and 15-state estimators outperform the 6 and 9-state estimators and are relatively comparable in prediction accuracy.

Figures 3-18 through 3-21 show the results for the y-position prediction. Figure 3-18 reveals an increasing degradation in estimation accuracy starting at 10 seconds. The 9, 12, and 15-state estimators maintain an accurate track of y-position throughout the trajectory.

The z-position prediction results are given in Figures 3-22 through 3-25. Again, the 6-state estimator turns in the worst performance. The 9 and 15-state estimators provide comparable predictions of z-position. The 12-state estimator appears to provide the best estimates of the z-position.

Figures 3-26 through 3-29 provide plots of miss distance versus time for the four estimators. The miss distance is defined as

$$\begin{aligned} miss\ distance = [&(x(k+30) - \hat{x}(k+30|k))^2 \\ &(y(k+30) - \hat{y}(k+30|k))^2 \\ &(z(k+30) - \hat{z}(k+30|k))^2]^{1/2} \end{aligned} \tag{3.3-1}$$

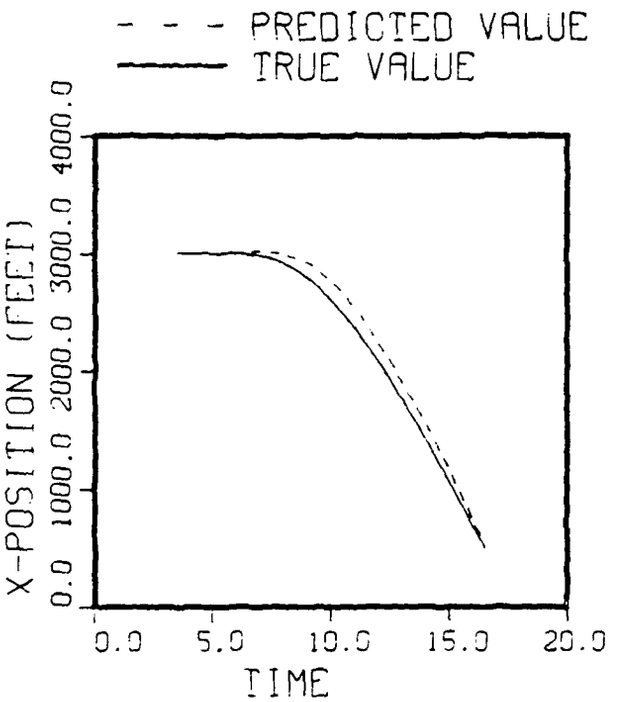

Figure 3-14 Predicted vs True X-Position (6-State Est.)

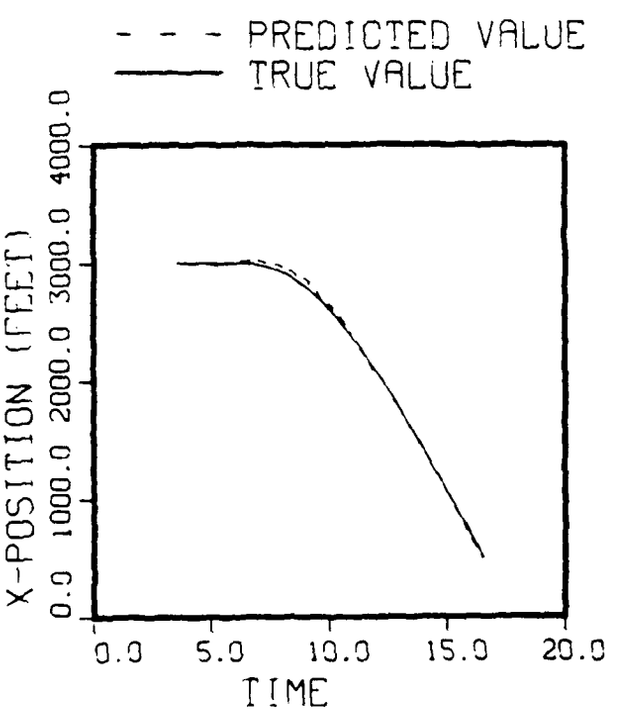

Figure 3-15 Predicted vs True X-Position (9-State Est.)

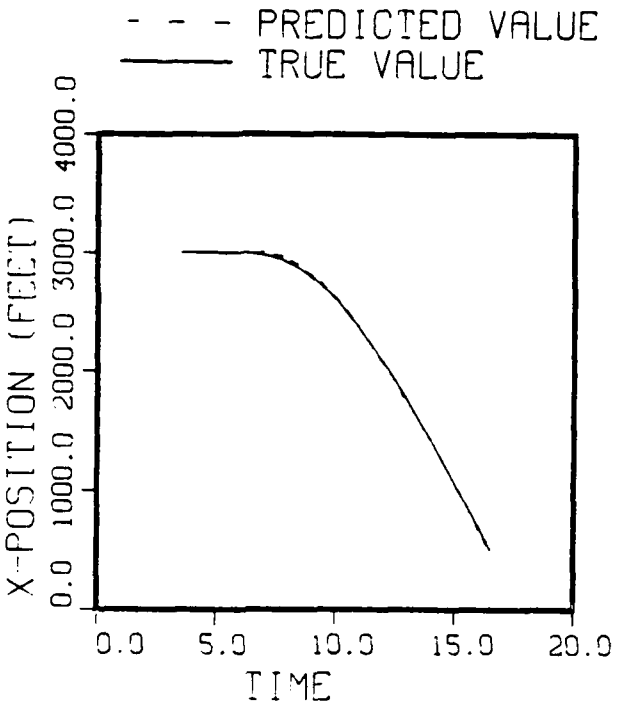

Figure 3-16 Predicted vs True X-Position (12-State Est.)

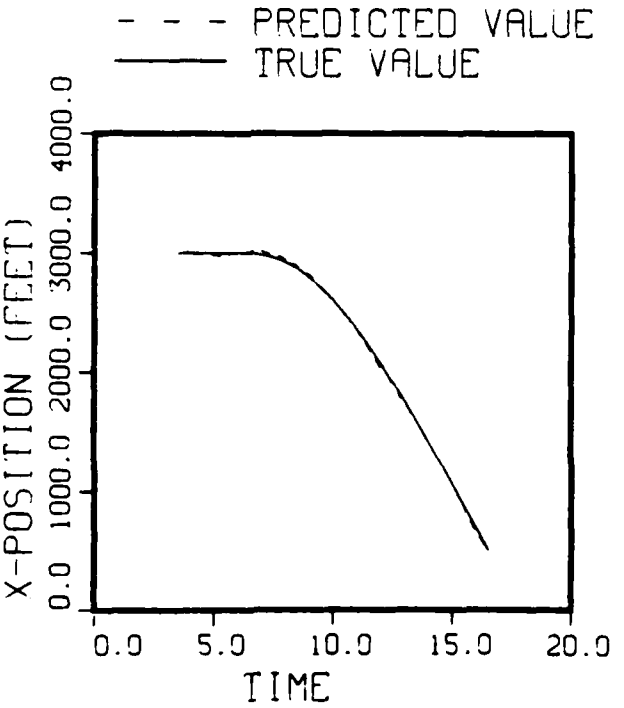

Figure 3-17 Predicted vs True X-Position (15-State Est.)

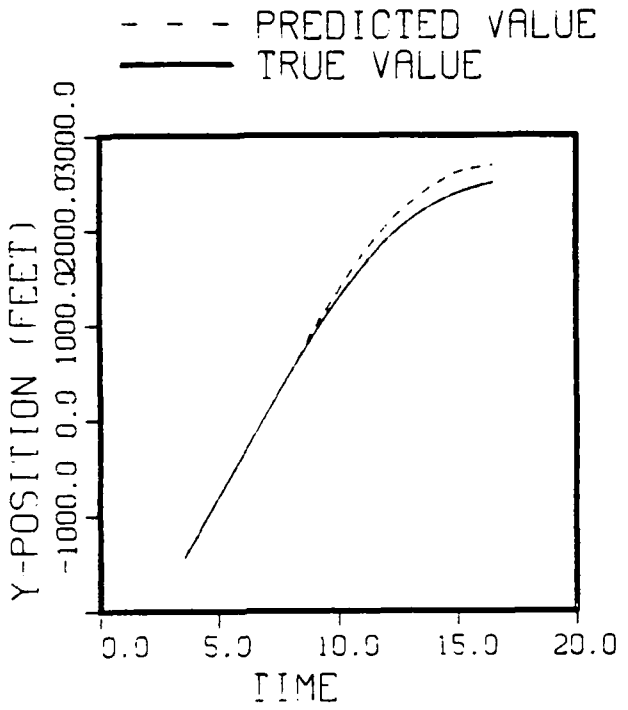

Figure 3-18 Predicted vs True Y-Position (6-State Est.)

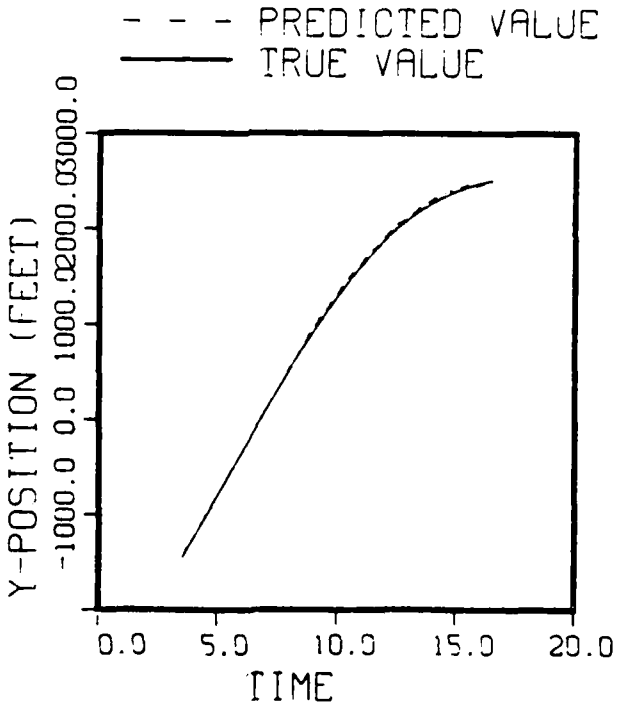

Figure 3-19 Predicted vs True Y-Position (9-State Est.)

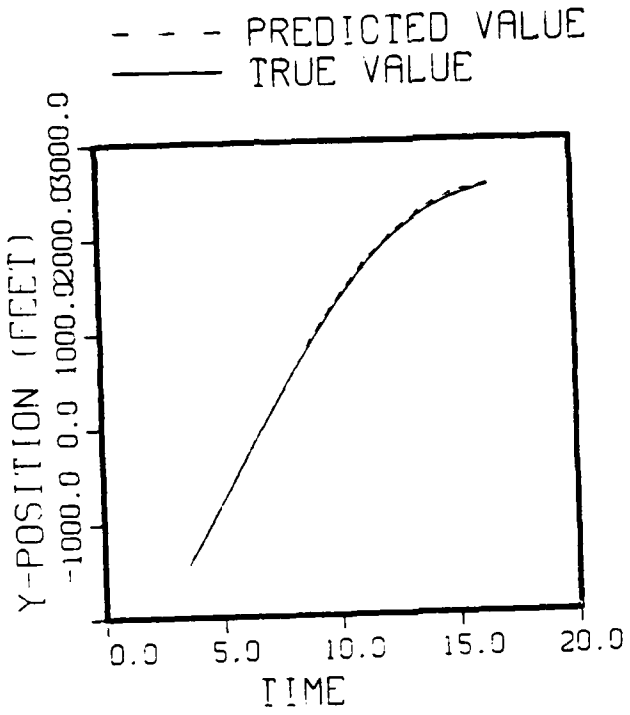

Figure 3-20 Predicted vs True Y-Position (12-State Est.)

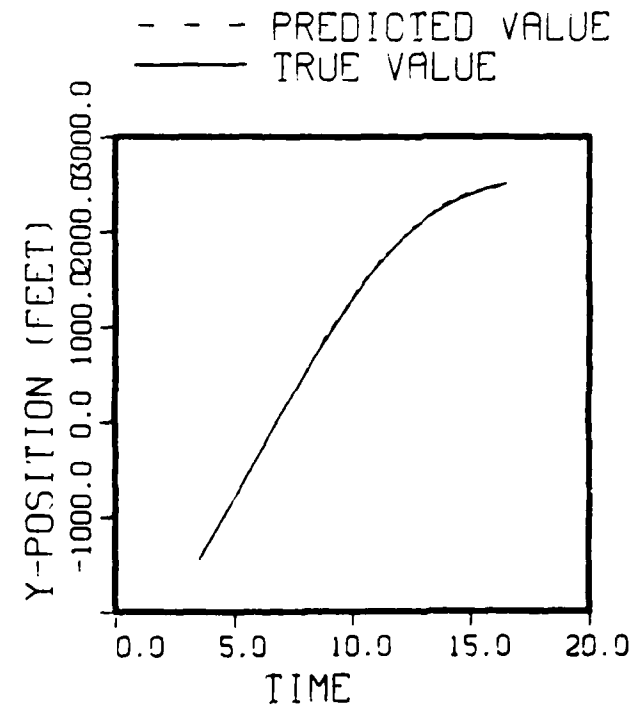

Figure 3-21 Predicted vs True Y-Position (15-State Est.)

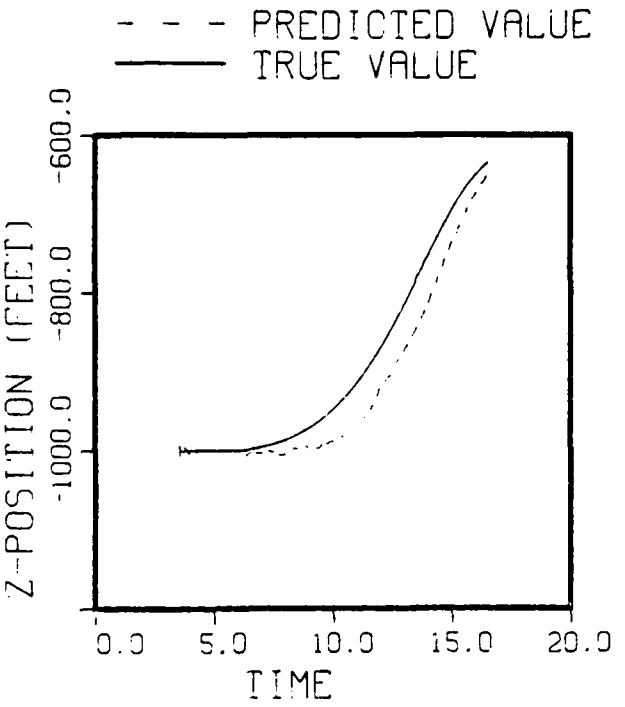

Figure 3-22 Predicted vs True Z-Position (6-State Est.)

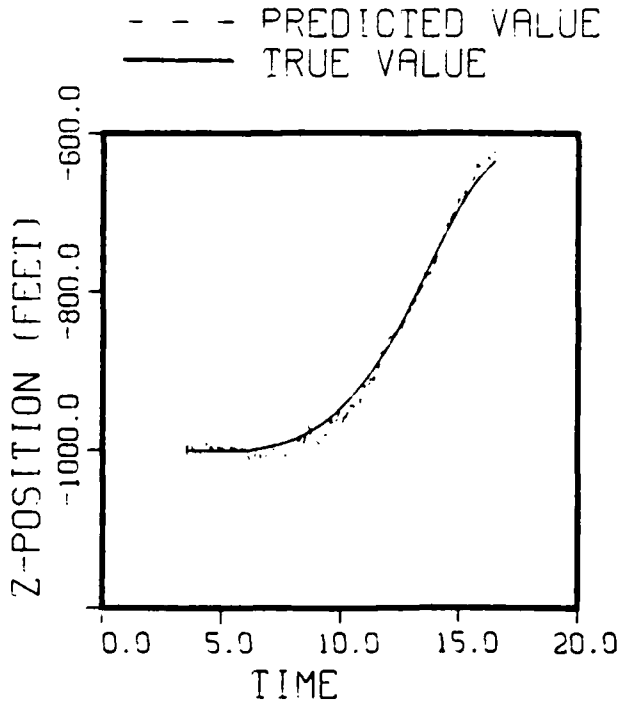

Figure 3-23 Predicted vs True Z-Position (9-State Est.)

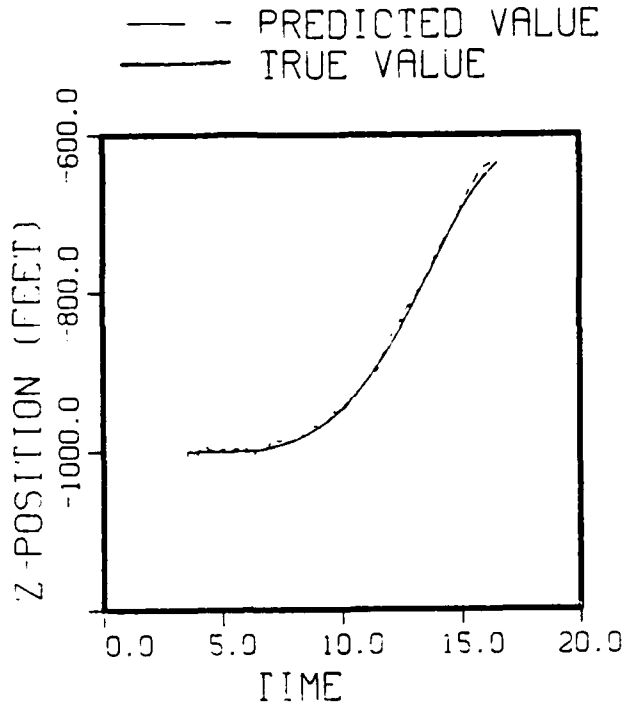

Figure 3-24 Predicted vs True Z-Position (12-State Est.)

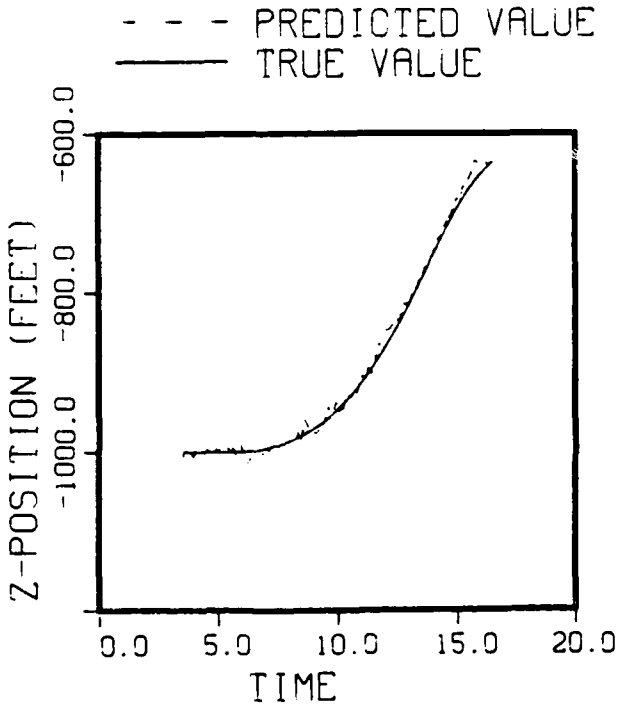

Figure 3-25 Predicted vs True Z-Position (15-State Est.)

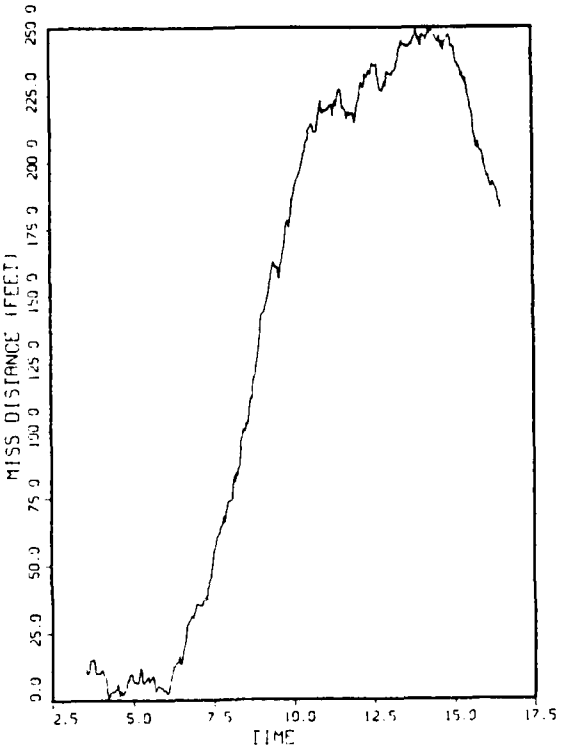

Figure 3-26 Miss Distance (6-State Est.)

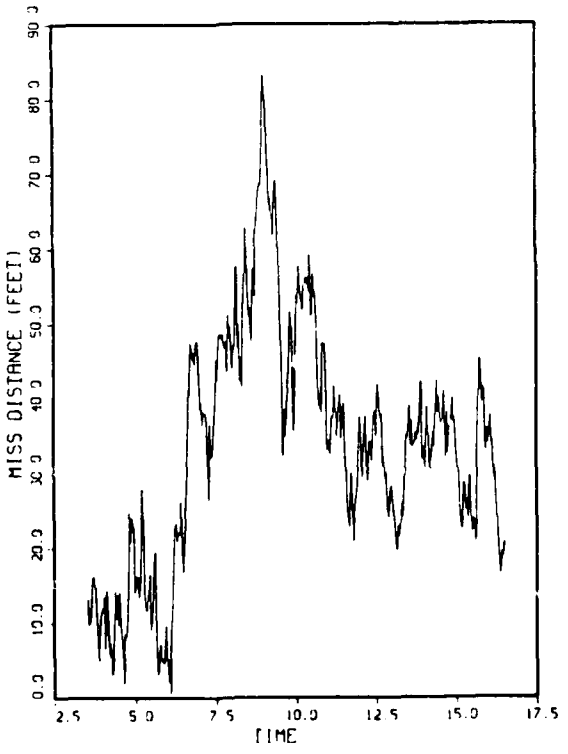

Figure 3-27 Miss Distance (9-State Est.)

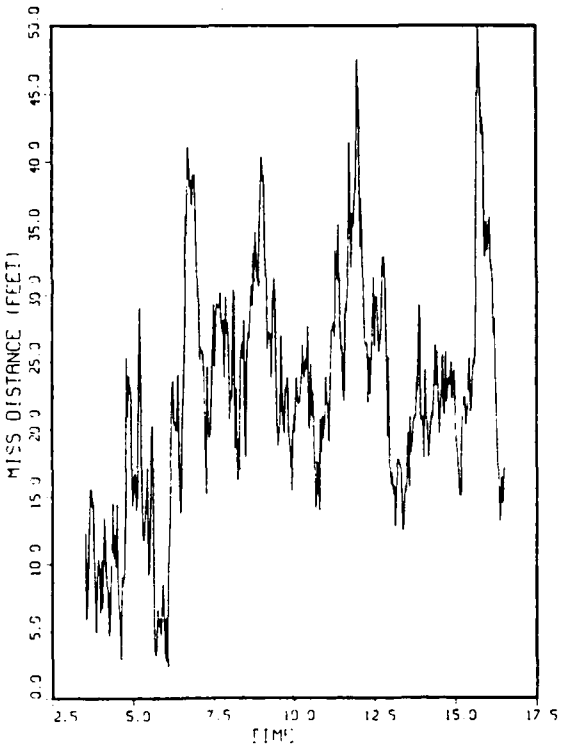

Figure 3-28 Miss Distance (12-State Est.)

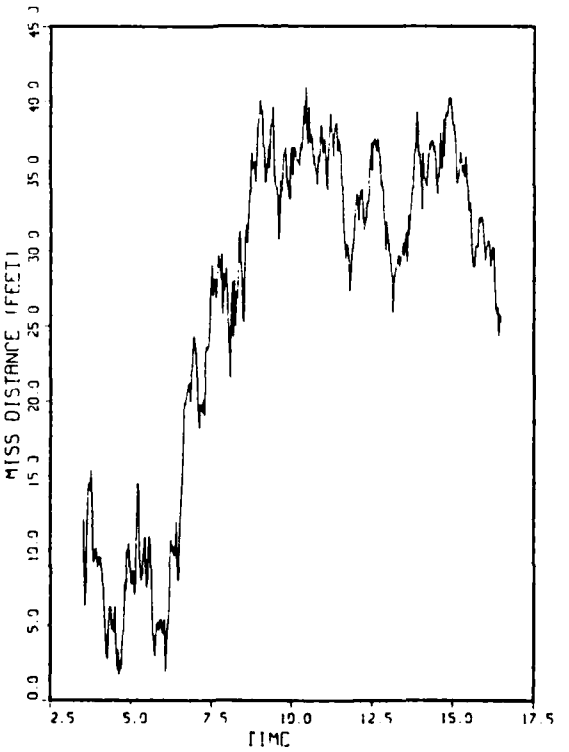

Figure 3-29 Miss Distance (15-State Est.)

where $\hat{x}(k+30|k)$ represents the the predicted estimate of x-position at t = (k+30)T given measurements to t = kT. For the sampling period of T = 1/30 second used in this analysis, this yields the one second ahead prediction.

As anticipated, the 6 and 9-state estimators performance is below the 12 and 15-state estimators. The 12-state estimator yields a lower maximum error than the 15-state error, but the 15-state estimator appears to have a lower average error value across the trajectory period.

In order to evaluate estimation performance across the complete trajectory period, an RMS error value was calculated for the x, y, z states and for the miss distance calculation. The results are given in Table 3-10.

Table 3-10 EKF RMS Prediction Errors

Estimator	x (ft)	y (ft)	z (ft)	miss distance (ft)
6-state	108.0	124.5	37.6	169.1
9-state	26.5	24.5	9.6	37.3
12-state	14.0	24.8	5.1	29.0
15-state	17.2	14.9	8.1	24.2

In general, the 15-state estimator gives the minimum RMS error for a majority of the states. The miss distance RMS error is the best overall indicator of tracking performance, and the minimum error is given by the 15-state estimator.

The results of Figures 3-8 through 3-29 and Table 3-10 were then used as baseline figures in a number of sensitivity analyses. These were used for comparison purposes in evaluating alternative tracker implementations. The alternative tracker

implementations investigated are:

1) Process Noise Tuning Analyses

2) Alternative Rotation Prediction Assumptions

3) Radar Rate Assumptions

4) Aircraft Dependent Stability Derivative Assumptions

In general, the selection or tuning of the process noise for an extended Kalman filter presents a difficult problem. Since the filter results are suboptimal from a mathematical vantage point, the achievement of the "best" suboptimal results depends upon trial and error techniques for selecting process noise levels. This tuning process is trajectory dependent, and therefore must be reaccomplished for every trajectory modification. Given the nature of the tracking problem, where the trajectory is unknown a-priori, the achievement of the best trajectory estimates is unlikely. However, a process noise tuning analysis can provide insight into relative process noise level selection and the sensitivity of the estimates to various process noise levels.

Starting with the baseline noise statistics of Table 3-8, the process noise levels were increased and decreased by orders of magnitude. The computer simulations were then rerun to determine the effects on RMS miss distances. The runs that produced the lowest RMS miss distances are presented in Table 3-11.

Table 3-11 Tuned Process Noise Levels

	6-State	9-State	12-State	15- State
q_1	----------	----------	4.0E-04	4.0E-06
q_2	----------	----------	2.0E-02	2.0E-04
q_3	----------	----------	6.0E-05	6.0E-07
q_4	1.2E-02	1.2E-04	1.2E-04	1.2E-04
q_5	1.2E-02	1.2E-04	1.2E-04	1.2E-04
q_6	1.2E-02	1.2E-04	1.2E-04	1.2E-04
q_7	----------	1.0E-02	----------	1.0E-04
q_8	----------	1.0E-02	----------	1.0E-04
q_9	----------	1.0E-02	----------	1.0E-04
miss distance	45	33	28	24

Although the results of Table 3-11 are not guaranteed to provide the minimum miss distance, it is felt that the process noise levels represent reasonable values to use in the follow-on analyses. In addition, two important conclusions can be drawn. First, the inclusion of orientation measurements results in a more robust estimator. In other words, the 12 and 15- state trackers were far less sensitive to selecting "correct" values for process noise. This is a significant conclusion, since the values for the process noise must be selected to account for unknown inputs and trajectories. A model that is less sensitive to this selection procedure is clearly superior to a model whose tracking performance depends strongly upon selecting correct values for process noise levels. The second conclusion is that the addition of the exponentially correlated noise sources enhances tracker performance. Examination of Tables 3-10 and 3-11 reveals the superior results obtained by the 9-state tracker and 15-state tracker over the 6-state tracker and 12-state tracker. Therefore, only the 9-state and 15-state trackers are used in the

following evaluations of the performance capabilities of trackers using standard radar measurements versus those augmented with orientation measurements.

An analysis of rotation predictions assumptions is also performed. In previously calculating the one second ahead predictions, it was assumed that the aircraft orientation angles remain unchanged over the prediction period. This was done by setting the derivative rotational equations to zero and thereby reducing the load of the estimators. To see what effect this assumption has on the estimation accuracy, additional runs were performed assuming constant and time varying angular rates. These additional runs were performed for the 15-state estimator. For each of the runs the RMS error values were computed and are presented in Table 3-12.

Table 3-12 EKF RMS Errors for Rotation Assumptions

Assumption	x (ft)	y (ft)	z (ft)	miss distance (ft)
Zero Rot.	15.3	17.2	6.7	24
Cnst Rot.	15.0	16.2	6.7	23
T.V. Rot.	14.4	20.3	8.7	26

Again there are no clear discriminatory differences between any of the three different approaches. The constant rotation rate for this maneuver gives the lowest RMS miss distance errors. The conclusion that can be drawn is that the assumptions made for the rotation rates are not critical. Future runs will be made with the assumption of zero rotation rates since this appears to give an acceptable prediction accuracy and reduced computational requirements.

The next analysis addresses the effect of the radar rate measurements of $\dot{R}$, $\dot{\eta}$, and $\dot{\zeta}$ on the tracking performance of the 9-state and 15-state trackers. This is accomplished since certain tracker implementations may not have these measurements. The

two trackers were rerun against the 5-g right turn; however this time the measurement noise variance corresponding to the range rate measurements were set to 1.0E06 in order to substantially reduce the EKF gains associated with these measurements. This has the effect of essentially ignoring the contributions of these measurements. The results of deemphasizing the radar rates is shown in Table 3-13. As can be seen, the radar rates are more critical to the 9-state tracker than to the 15-state tracker. This is not a surprising result since range rates provide velocity information, which is unavailable to the 9-state tracker.

Table 3-13 EKF RMS Errors for Radar Rate (RR) Assumptions

Estimator	x	y	z	miss distance
9-state				
with RR	24.4	18.9	11.0	32
without RR	76.8	75.3	27.3	11
15-state				
with RR	15.3	17.2	6.7	24
without RR	14.5	20.1	8.0	26

The final analysis investigates the sensitivity of the 15-state tracker performance to the aircraft dependent constants used in the equations of motion found in Table 3-7. This is achieved by setting the aircraft dependent constant for the angular rate equations to zero. This amounts to modeling the angular rates of roll, pitch, and yaw as white noise. The 9 and 15-state trackers were run against the 5-g right turn trajectory. The results of these runs are displayed in Figures 3-30 and 3-31. The line in Figure 3-30 represents the actual trajectory. The squares represent the one second predicted positions made by the 9-state tracker. The plus symbols represent the one second prediction made by the 15-state tracker. Figure 3-31 shows the top view of

Figure 3-30 starting from 2.5 seconds into the trajectory. This is the point where the aircraft initiates it's maneuver. The RMS miss distance for the 9-state tracker is 51.4 feet. The RMS miss distance for the 15-state tracker is 25 feet. This is over a 100 percent reduction in RMS error.

Additional maneuvers were also investigated. The maneuvers are:

1. 5-g S-turn.
2. 5-g Pull-up/Push-over.
3. 2-g Dive/Pull-up.
4. 5-g Right Turn with Rudder.

The results for these maneuvers can be found in the report Target Trackers for Maneuvering Aircraft by Andrisani et. al. [1985].

The work presented in this chapter resulted in a number of research questions which were difficult to address due to the nonlinear nature of the tracking problem. To investigate these questions, it was necessary to make certain assumptions that lead to linear models that can be analyzed with the extensive linear techniques that are available. These analyses are found in the next chapters.

3.4 Summary

This chapter presents the development and implementation of nonlinear tracking filters. A radar measurement only tracking filter is improved by incorporating orientation information. This allows for the estimation of both the magnitude and direction of the force system acting on the aircraft, which improves aircraft acceleration estimates. Knowledge of acceleration is used to improve estimates of present and future positions of the aircraft. Simulation of a manuevering fighter aircraft indicates that dramatic tracking improvements are achieved.

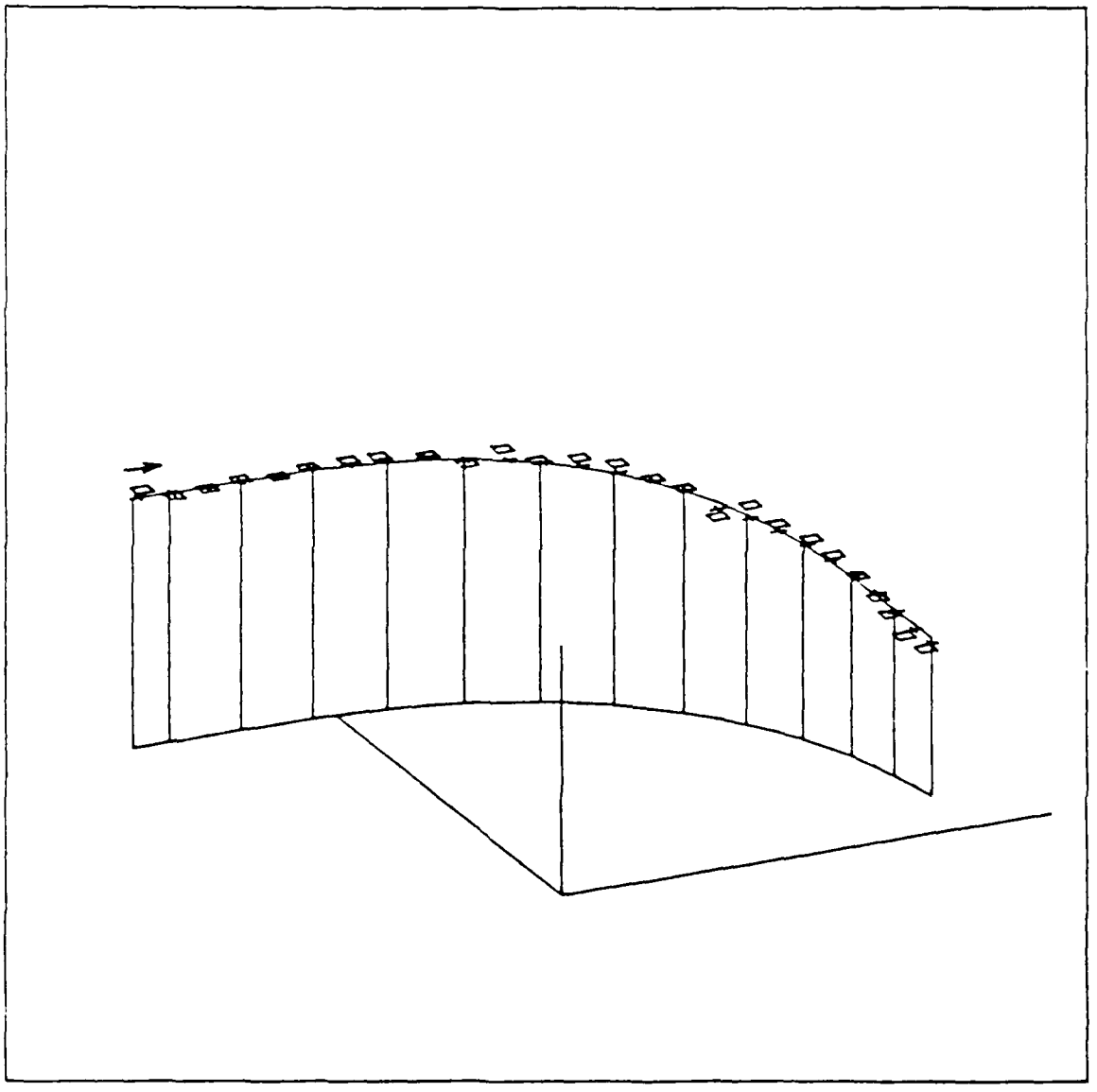

Figure 3-30 5-g Right Turn (9-state vs 15-state)

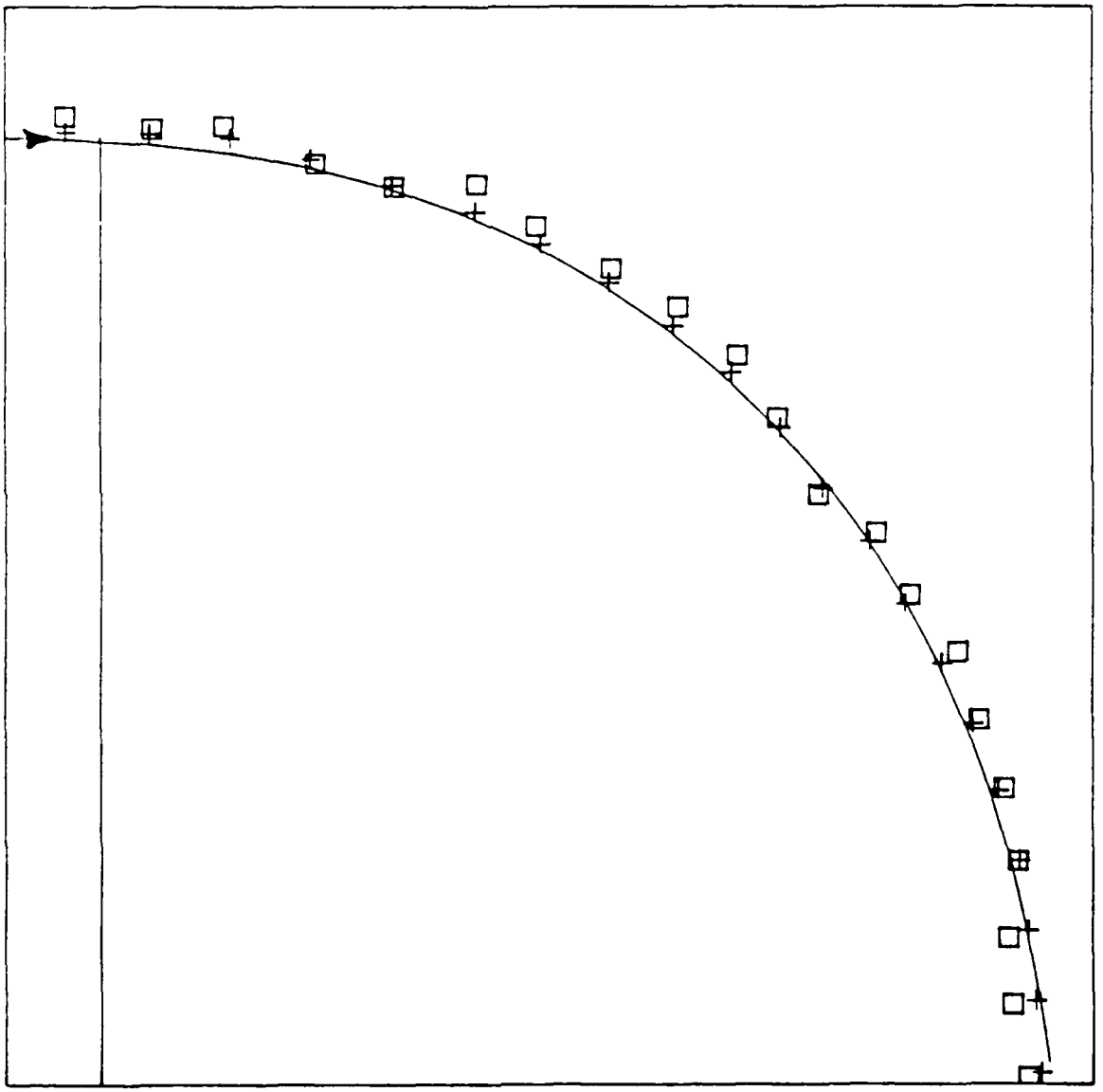

Figure 3-31 Top View 5-g Right Turn (9-state vs 15-state)

CHAPTER 4
LINEAR TRACKING FILTER ANALYSIS

The linear $\alpha - \beta - \gamma$ trackers discussed previously, uses a very simplistic approach to modeling aircraft trajectory motion. This approach models the aircraft as a point-mass, and uses derivative relationships between position, velocity and acceleration to estimate aircraft motion. The more extensive nonlinear models that include orientation information, take a more detailed approach to modeling the aircraft motion. Although this approach will, in general, provide a more accurate representation of aircraft motion, it provides little insight into which parameters and variables are critical in determining the aircraft trajectory. Many important and key concepts can be disguised by a 12th or 15th order system of nonlinear differential equations. This chapter therefore investigates the inclusion of orientation information with a linear model. The purpose being to find an improved model that extends the simplistic $\alpha - \beta - \gamma$ model, while retaining the advantages associated with a linear modeling process.

4.1 $\alpha - \beta - \gamma$ Tracking Filters

The first model analyzed is the three degree of freedom $\alpha - \beta - \gamma$ model. Rather than examining a nine state model which incorporates position (x) , velocity (v), and acceleration (a) in three directions (i.e. x-y-z), a simpler three state model which only uses position, velocity and acceleration in one direction is considered. Since the $\alpha - \beta - \gamma$ tracker treats each direction independently, no loss of generality occurs with this approach.

The true model, which generates true values of position, velocity and acceleration is given by

$$\begin{bmatrix} x(k+1) \\ v(k+1) \\ a(k+1) \end{bmatrix} = \begin{bmatrix} 1 & T & T^2/2 \\ 0 & 1 & T \\ 0 & 0 & 1 \end{bmatrix} \begin{bmatrix} x(k) \\ v(k) \\ a(k) \end{bmatrix} + \begin{bmatrix} T^3/6 \\ T^2/2 \\ T \end{bmatrix} u(k) \qquad (4.1\text{-}1a)$$

$$z(k) = [1\ 0\ 0] \begin{bmatrix} x(k) \\ v(k) \\ a(k) \end{bmatrix} + v(k) \qquad (4.1\text{-}1b)$$

Since the input is known, no process noise drives the true model. Also, only a single measurement of position (which is corrupted by a zero-mean, uncorrelated, gaussian noise) is used by the filter. The true input to the model results in a positive 16.05 ft/sec^2 (1/2 g) step acceleration starting at 5 seconds and lasting 5 seconds. Then a negative 16.05 ft/sec^2 acceleration is experienced for the time period of 10 to 15 seconds. The acceleration is zero for the remaining 5 seconds of the run.

The filter model is given by

$$\begin{bmatrix} x(k+1) \\ v(k+1) \\ a(k+1) \end{bmatrix} = \begin{bmatrix} 1 & T & T^2/2 \\ 0 & 1 & T \\ 0 & 0 & 1 \end{bmatrix} \begin{bmatrix} x(k) \\ v(k) \\ a(k) \end{bmatrix} + \begin{bmatrix} T^3/6 \\ T^2/2 \\ T \end{bmatrix} w(k) \qquad (4.1\text{-}2a)$$

$$z(k) = [1\ 0\ 0] \begin{bmatrix} x(k) \\ v(k) \\ a(k) \end{bmatrix} + v(k) \qquad (4.1\text{-}2b)$$

The only difference between the true model and the filter model is the input to the model. The true model is driven by a deterministic input. The filter model is driven by a stochastic process that is used to model the unknown deterministic input to the true model. The stochastic process is a zero-mean, uncorrelated, gaussian process with a covariance matrix Q.

Since the white noise process is used to account for the unknown input, some general observations can be made.

1. If the input to the true system is small, then the uncertainty that the process noise must account for is small. For these circumstances the value of Q should be small.

2. If the input to the true system is large, then the uncertainty that the process noise must account for is large. For these circumstances the value of Q should be large.

In general, the value of Q should be proportional to the magnitude of the input squared. This presents an obvious problem. If the time initiation, duration and the magnitude of the input is unknown, then how can the value of Q be selected? One method is for the designer to select an average value of Q a-priori and use this constant value throughout the tracking period. This method is examined in this section

The a-priori approach to the selection of Q requires the designer to select a value of Q and use this constant value throughout the tracking period. To determine what the effect of Q is on tracking ability, three values of Q are investigated.

1. Q=10.37 $(ft/sec^3)^2$ (mild maneuver)
2. Q=1037 $(ft/sec^3)^2$ (moderate maneuver)
3. Q=9332 $(ft/sec^3)^2$ (violent maneuver)

The value of $\sqrt{Q}$ represents the acceleration derivative or jerk of the aircraft. These values assume a 0-g to 1-g (i.e. 32.2 ft/sec^2) change in acceleration assuming a constant level of jerk. The mild maneuver occurs in 10 seconds, while the moderate and violent maneuvers occur in 1 second and 0.333 seconds respectively.

These three values were used in the LKF equations to track the aircraft motion. In all these cases, the deterministic input u(k) was as described above.

Figures 4-1 through 4-3 depict the graphical results for the case Q = 10.37 $(ft/sec^3)^2$. Figure 4-1 shows the true acceleration versus the estimated acceleration.

For the first five seconds when the aircraft is not accelerating, the estimates are excellent. After the aircraft begins to accelerate the estimation accuracy falls off dramatically. The acceleration estimate lags the true acceleration by approximately seven seconds. It is also obvious that after aircraft acceleration has been initiated, that the estimator is not providing an unbiased estimate of acceleration, so the value of Q = 10.37 $(ft/sec^3)^2$ is not yielding a satisfactory estimator. Figures 4-2 and 4-3 show the associated acceleration errors and position errors for this value of Q. The error is defined as the true value minus the estimated value. Figure 4-2 shows the effect of the acceleration estimation lag on the acceleration error. The acceleration estimation lag produces a clear trend in the acceleration errors. A more satisfactory estimator would produce random errors, and therefore no predictable trend would be seen. Figure 4-3 shows the position errors versus time and again the graph contains an obvious error trend indicating nonoptimal estimation.

Figures 4-4 through 4-6 depict the results for the moderate maneuver value of Q = 1037 $(ft/sec^3)^2$. Figure 4-4 shows the true acceleration versus estimated acceleration. Compared to the first case, the estimates for the first five seconds when the aircraft is not accelerating, shows that the estimate variance has increased. However, there is an improvement in tracking capability when an acceleration occurs. Although the estimated acceleration value still lags the true value, the lag time has decreased from seven seconds in the first case to two to three seconds when Q is increased to the moderate maneuver level. Examination of Figure 4-5 still shows large nonrandom acceleration errors around five, ten, and 15 seconds (i.e. points where acceleration levels change), but the errors occur for a far shorter period of time. The same general statement can be made for Figure 4-6, which shows positional errors versus time for this case.

Figures 4-7 through 4-9 show the results for the case when Q = 9332 $(ft/sec^3)^2$. Again, the estimation variance for the first five seconds of nonaccelerating flight shows a marked increase over the first two cases. However, as in the second case the time lag has decreased to one or two seconds. Examination of Figures 4-8 and 4-9 (acceleration errors and position errors versus time) again confirm that increased values of Q reduces time lags, but increase the error variance associated with the estimates.

In addition to the graphs of Figures 4-1 through 4-9, two additional figures of merit were computed. The first figure of merit is the root mean square (RMS) value of the error in position and acceleration estimates for the twenty second trajectory. The twenty second trajectory is sampled at 30 times per second, thereby yielding 600 data points. The RMS values for position (ε_x) and acceleration (ε_a) are calculated as

$$\varepsilon_x = \left[\frac{1}{600} \sum_{k=1}^{600} ((x(k) - \hat{x}(k))^2 \right]^{1/2}$$

$$\varepsilon_a = \left[\frac{1}{600} \sum_{k=1}^{600} ((a(k) - \hat{a}(k))^2 \right]^{1/2}$$

where $\hat{x}$ and $\hat{a}$ are the filtered estimates at the time of a position measurement.

The second figure of merit was the maximum error that occurred in position ($\varepsilon_{x_{max}}$) and acceleration ($\varepsilon_{a_{max}}$) for the twenty second trajectory. These values were determined from the graphs of position and acceleration errors versus time.

The values for these figures of merit are shown in Table 4-1.

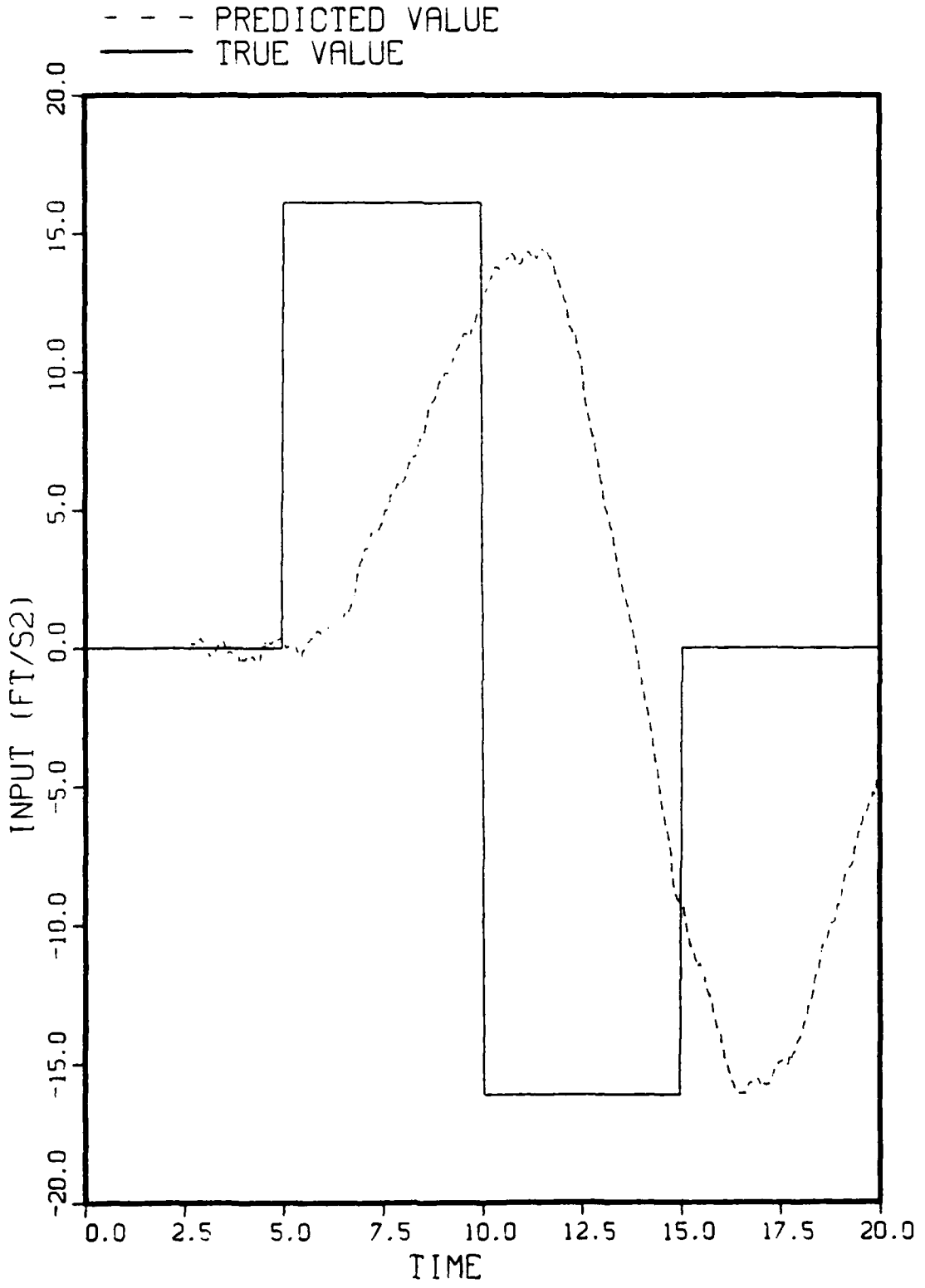

Figure 4-1 $\alpha - \beta - \gamma$ Tracker Acceleration Estimate (Q = 10.37)

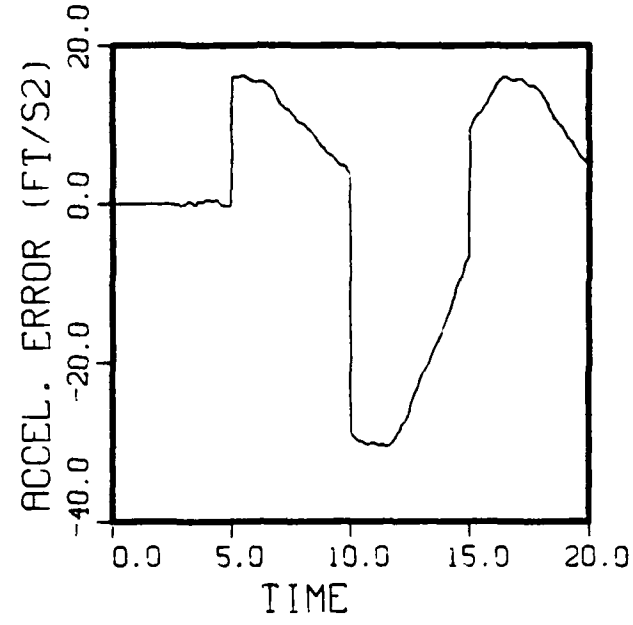

Figure 4-2 $\alpha - \beta - \gamma$ Tracker Acceleration Error (Q = 10.37)

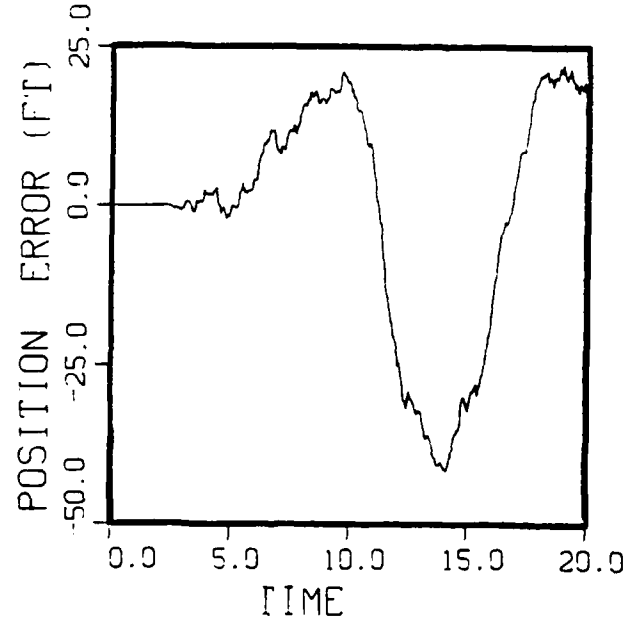

Figure 4-3 $\alpha - \beta - \gamma$ Tracker Position Error (Q = 10.37)

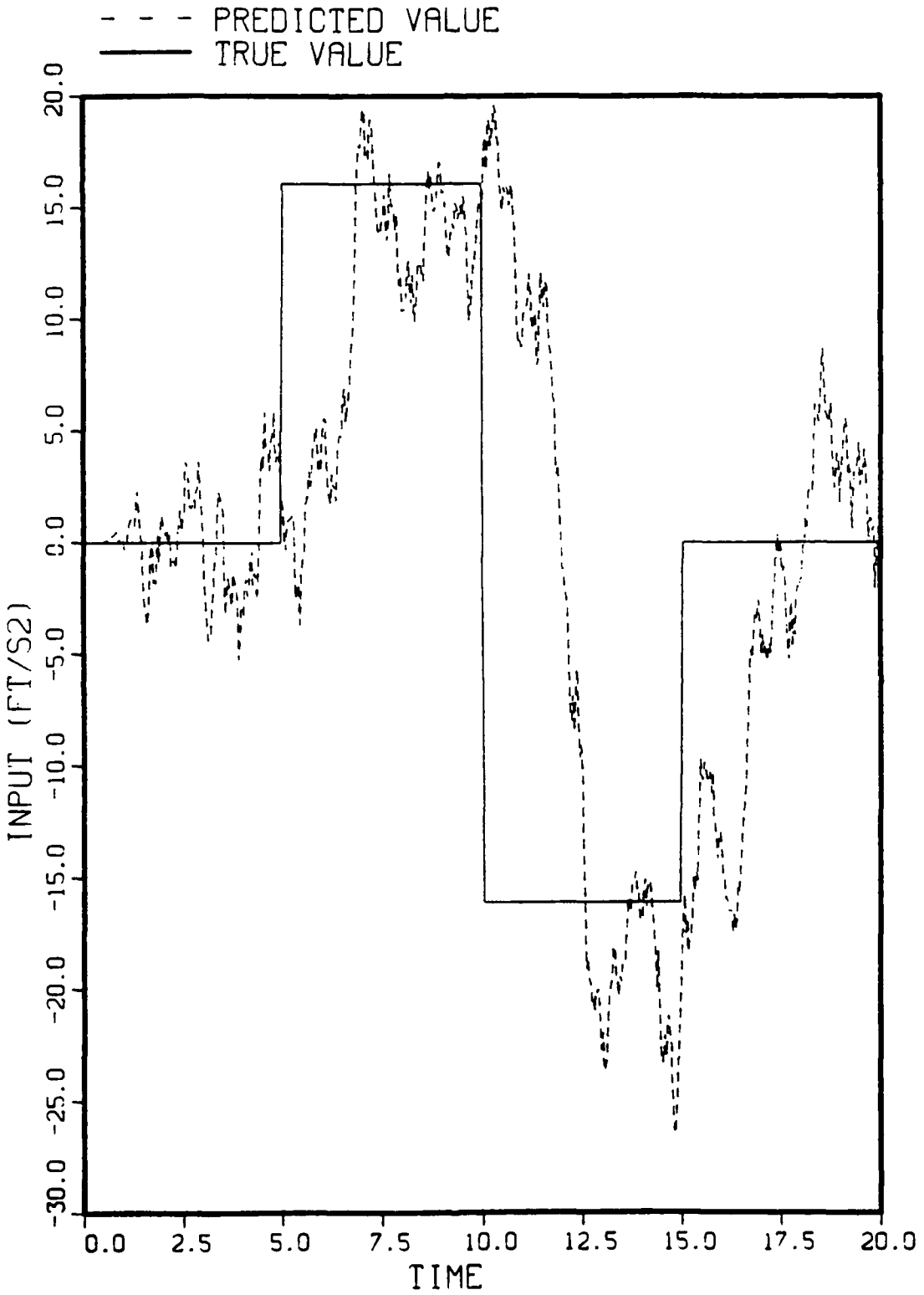

Figure 4-4 $\alpha - \beta - \gamma$ Tracker Acceleration Estimate (Q = 1037)

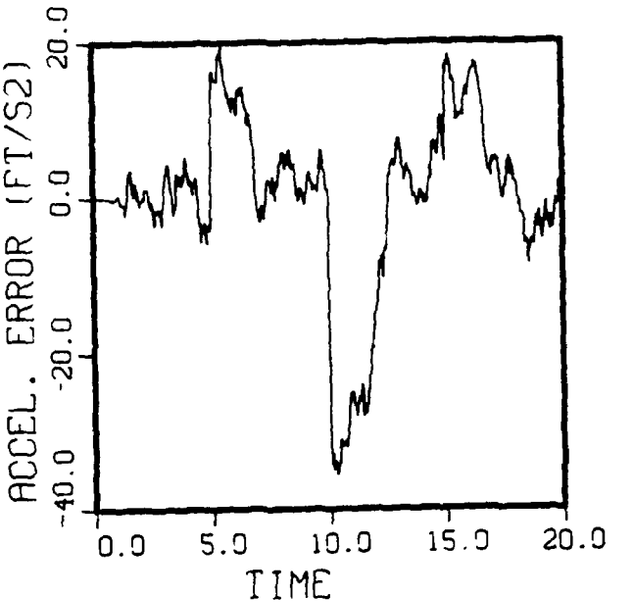

Figure 4-5 $\alpha - \beta - \gamma$ Tracker Acceleration Error (Q = 1037)

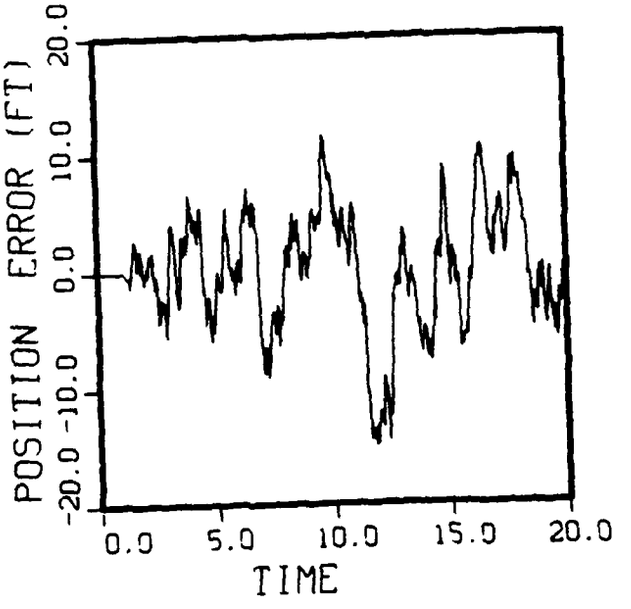

Figure 4-6 $\alpha - \beta - \gamma$ Tracker Position Error (Q = 1037)

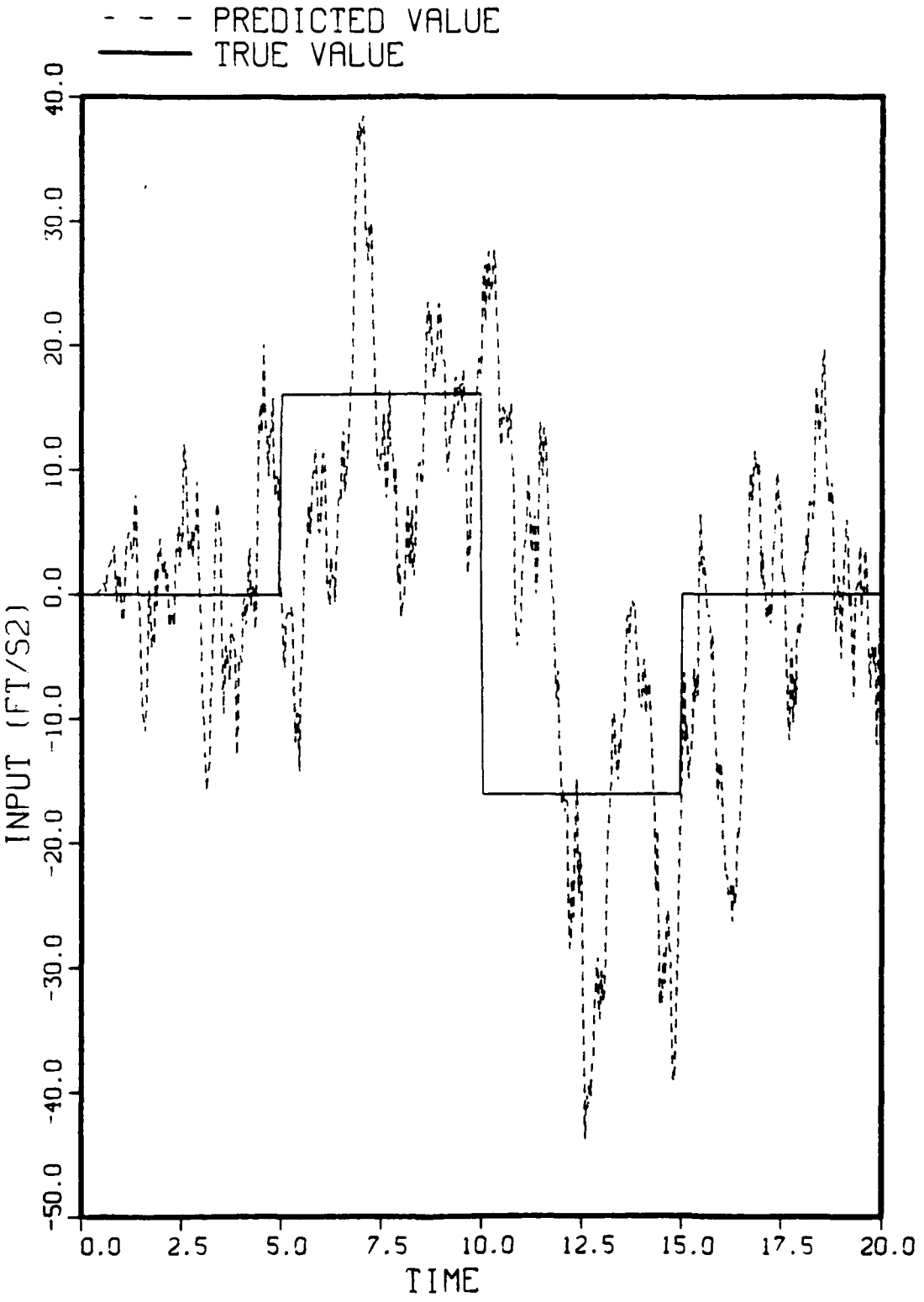

Figure 4-7 $\alpha - \beta - \gamma$ Tracker Acceleration Estimate (Q = 9332)

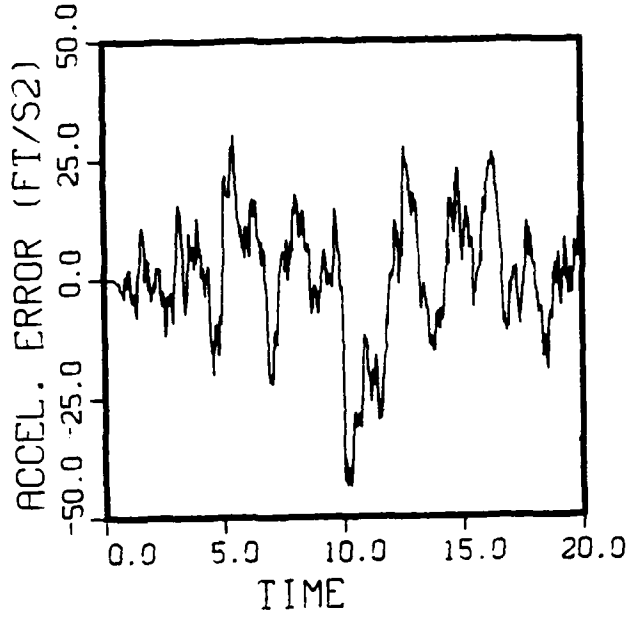

Figure 4-8 $\alpha - \beta - \gamma$ Tracker Acceleration Error (Q = 9332)

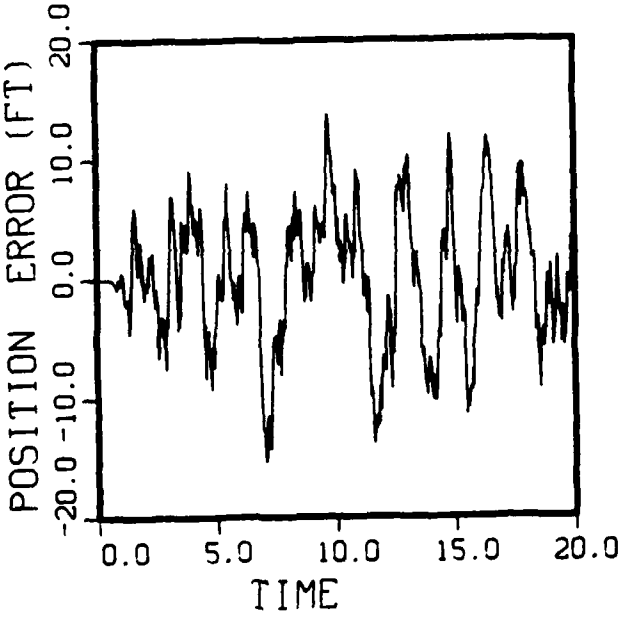

Figure 4-9 $\alpha - \beta - \gamma$ Tracker Position Error (Q = 9332)

Table 4-1 Error Values for α–β–γ Tracking Filter

	ε_x (ft)	ε_a (ft/s^2)	$\varepsilon_{x_{max}}$ (ft)	$\varepsilon_{a_{max}}$ (ft/s^2)
Q = 10.37	18.13	14.86	-42	-31
Q = 1037	5.00	11.16	-15	-36
Q = 9332	5.53	12.98	-15	-44

Examination of Table 4-1 shows that increasing Q from 10.37 to 1037 reduces ε_x and $\varepsilon_{x_{max}}$ significantly. Increasing Q to 9332 increases ε_a and $\varepsilon_{a_{max}}$.

The results from Figures 4-1 through 4-9 and Table 4-1 reveals the significant impact the selection of Q has on tracking performance. In general, the higher the value of Q, the faster the tracker responds to changes in acceleration, although a penalty is paid in error variances associated with the estimates. The increase in error variance is particularly acute if the aircraft acceleration values are zero or very small. The conclusion that can be drawn is that if acceleration values are low then values of Q should also be low and vice versa. If an average value of Q is chosen, then one can expect good tracking performance for moderate maneuvers, and degraded tracker performance for mild or violent maneuvers. These results are consistent with the results of the nonlinear trackers using radar only measurements, where the estimation accuracy was highly dependent upon the selection of the process noise.

4.2 $\alpha - \delta$ Tracking Filters

The $\alpha - \delta$ model (Andrisani; 1985) combines the straight forward approach of the linear $\alpha - \beta - \gamma$ model, with the additional orientation information used with the nonlinear model. In this way, the benefits of the orientation information can be thoroughly analyzed. This analysis will then provide insight into which parameters and variables are vital and which parameters and variables may be neglected in the nonlinear model. Like the $\alpha - \beta - \gamma$ model, the $\alpha - \delta$ model considers motion only along one of the inertial coordinate axes. The example considered will be a hovering helicopter performing a bank to translate maneuver. A hovering helicopter moves sidewards by rolling to one side or the other. This maneuver tilts the lift vector which is created by the spinning of the helicopter's rotor. The tilting of the lift vector creates a side force and therefore a side acceleration. For small bank angles (ϕ), the following continuous linear state space representation may be used

$$\begin{bmatrix} \dot{x} \\ \ddot{x} \\ \dot{\phi} \\ \dot{p} \end{bmatrix} = \begin{bmatrix} 0 & 1 & 0 & 0 \\ 0 & 0 & g & 0 \\ 0 & 0 & 0 & 1 \\ 0 & 0 & 0 & 0 \end{bmatrix} \begin{bmatrix} x \\ \dot{x} \\ \phi \\ p \end{bmatrix} + \begin{bmatrix} 0 \\ 0 \\ 0 \\ L_\delta \end{bmatrix} \delta \qquad (4.2\text{-}1)$$

where ϕ is the bank angle, p is the bank angle rate, and $L_\delta \delta$ represents the input that is used to bank the helicopter.

Analyzing the above continuous model reveals that the translation motion is treated as an $\alpha - \beta$ model, (i.e. considers only position and velocity states) and the rotational motion is also treated as an $\alpha - \beta$ model. The coupling of the two motions comes from the g term which represents the side acceleration that develops when the helicopter banks to translate.

Examination of the state equations reveals that the x-acceleration is proportional to the bank angle ϕ (i.e. $\ddot{x} = g\phi$). The $\alpha - \beta - \gamma$ formulation is predicated on the fact that there is only a measurement of the position state. The $\alpha - \delta$ model is based

on using a position measurement, x, and orientation measurement ϕ. Since ϕ is proportional to $\ddot{x}$ a great deal more information is provided to the tracker concerning the motion of the helicopter. This clearly points out the benefits of incorporating orientation measurements into a tracking algorithm.

The discrete model which generates true values of position (x), velocity (v), bank angle (ϕ), and bank angle rate (p) is given as

$$\begin{bmatrix} x(k+1) \\ v(k+1) \\ \phi(k+1) \\ p(k+1) \end{bmatrix} = \begin{bmatrix} 1 & T & cT^2/2 & cT^3/6 \\ 0 & 1 & cT & cT^2/2 \\ 0 & 0 & 1 & T \\ 0 & 0 & 0 & 1 \end{bmatrix} \begin{bmatrix} x(k) \\ v(k) \\ \phi(k) \\ p(k) \end{bmatrix} + \begin{bmatrix} cT^4/24 \\ cT^3/6 \\ T^2/2 \\ T \end{bmatrix} \delta(k) \qquad (4.2\text{-}2a)$$

$$\begin{bmatrix} z_x(k) \\ z_\phi(k) \end{bmatrix} = \begin{bmatrix} 1 & 0 & 0 & 0 \\ 0 & 0 & 1 & 0 \end{bmatrix} \begin{bmatrix} x(k) \\ v(k) \\ \phi(k) \\ p(k) \end{bmatrix} + \begin{bmatrix} v_x(k) \\ v_\phi(k) \end{bmatrix} \qquad (4.2\text{-}2b)$$

where the value of c corresponds to a modified gravity constant to account for angular values of degrees as opposed to radians (i.e. c = (32.17 ft/sec^2)/(57.3 degree/radian) = .562), T is the sampling period for the discretization process, and L_δ is chosen to be 1.

The white gaussian noise that is corrupting the two measurements has the following statistics

$$E\{v_x\} = 0$$

$$E\{v_x(i)v_x(j)^T\} = 225\delta_{ij}(ft^2)$$

$$E\{v_\phi\} = 0$$

$$E\{v_\phi(i)v_\phi(j)^T\} = .25\delta_{ij}(degrees^2)$$

The maneuver that is tracked is the same maneuver tracked by the $\alpha - \beta - \gamma$ filter. This corresponds to the helicopter remaining unbanked and not translating for 5 seconds, and then banking a positive 28.64 degrees for the next 5 seconds. This is followed by a bank of negative 28.64 degrees for the next five seconds and finally returning to a level ($\phi = 0$) orientation for the final 5 seconds of the trajectory. This results in a x-translation of 400 feet in the 10 second period that the helicopter is maneuvering.

The filter model used in this analysis is

$$\begin{bmatrix} x(k+1) \\ v(k+1) \\ \phi(k+1) \\ p(k+1) \end{bmatrix} = \begin{bmatrix} 1 & T & cT^2/2 & cT^3/6 \\ 0 & 1 & cT & cT^2/2 \\ 0 & 0 & 1 & T \\ 0 & 0 & 0 & 1 \end{bmatrix} \begin{bmatrix} x(k) \\ v(k) \\ \phi(k) \\ p(k) \end{bmatrix} + \begin{bmatrix} cT^4/24 \\ cT^3/6 \\ T^2/2 \\ T \end{bmatrix} w(k) \qquad (4.2\text{-}3a)$$

$$\begin{bmatrix} z_x(k) \\ z_\phi(k) \end{bmatrix} = \begin{bmatrix} 1 & 0 & 0 & 0 \\ 0 & 0 & 1 & 0 \end{bmatrix} \begin{bmatrix} x(k) \\ v(k) \\ \phi(k) \\ p(k) \end{bmatrix} + \begin{bmatrix} v_x(k) \\ v_\phi(k) \end{bmatrix} \qquad (4.2\text{-}3b)$$

where w(k) is a zero-mean, uncorrelated, gaussian noise sequence with variance Q.

Again, three values of Q were examined. They are

1. Q = .2025 $(rad/sec^2)^2$ (mild maneuver)
2. Q = 3.24 $(rad/sec^2)^2$ (moderate maneuver)
3. Q = 2025 $(rad/sec^2)^2$ (violent maneuver)

The values of Q are based on a constant angular acceleration 0^o to 90^o banked maneuver. Q = .2025 $(rad/sec^2)^2$ corresponds to this maneuver being performed in 20 seconds. Q = 3.24 and 2025 $(rad/sec^2)^2$ correspond to a maneuver time of 10 and 2 seconds respectively.

The same analysis which was performed for the $\alpha - \beta - \gamma$ filter is now performed on the $\alpha - \delta$ filter. This analysis clearly shows how the $\alpha - \delta$ filter outperforms the $\alpha - \beta - \gamma$ filter.

Figures 4-10 through 4-12 shows graphically the results for the case when Q = .2025 $(rad/sec^2)^2$. Figure 4-10 reveals that for this low level of Q the estimated linear acceleration lags the true acceleration by approximately one second. Figures 4-11 and 4-12 provide the corresponding graphs for the acceleration and positional errors. Both figures clearly show nonrandom error trends for extended periods of time. The conclusion is that Q = .2025 $(rad/sec^2)^2$ is inappropriate for the maneuvering portion of this trajectory.

Figure 4-13 through 4-15 provides the results for Q = 3.24 $(rad/sec^2)^2$ level of process noise. Figure 4-13 reveals an improved transient response for acceleration estimation. The acceleration errors shown in Figure 4-14 contain the same error trends found in the previous case (i.e. Q = .2025), although the magnitudes of the errors have decreased slightly. Figure 4-15 shows that the position estimates now lag the true values, where before they were leading the true value.

Figure 4-16 through 4-18 shows the results for Q = 2025 $(rad/sec^2)^2$. For this case there is almost no lag in the estimation of the acceleration state. The acceleration error trends occur for a shorter duration, and positional errors appear to be similar to the previous case.

To determine how the values of Q affect the tracking performance to the total trajectory period; RMS error values and maximum error values were calculated. The results of these calculations are found in Table 4-2.

A comparison of Tables 4-1 and 4-2 shows that with the selection of appropriate values of Q, the $\alpha - \delta$ tracker clearly outperforms the $\alpha - \beta - \gamma$ tracker. It is also clear from Table 4-2 that the $\alpha - \delta$ tracking performance is less sensitive to The Q value selection. This result is consistent with the results found with the nonlinear trackers.

Table 4-2 Error Values for $\alpha - \delta$ Tracking Filter

	ε_x (ft)	ε_a (ft/s^2)	$\varepsilon_{x_{max}}$ (ft)	$\varepsilon_{a_{max}}$ (ft/s^2)
Q = .2025	4.53	5.29	-7.0	-30
Q = 3.24	0.36	3.55	0.9	-28
Q = 2025	0.39	1.23	1.0	-16

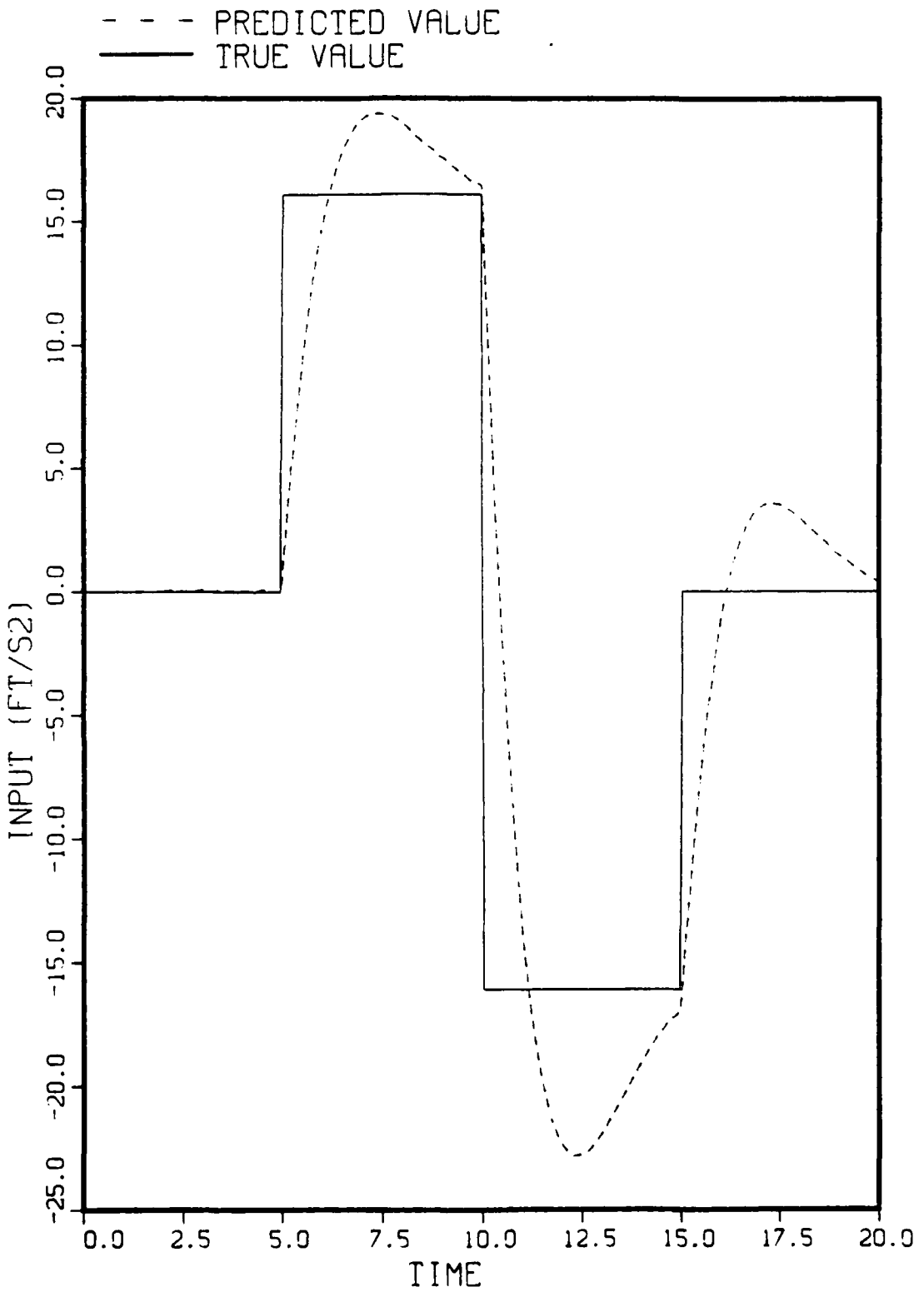

Figure 4-10 $\alpha - \delta$ Tracker Acceleration Estimate (Q = .2025)

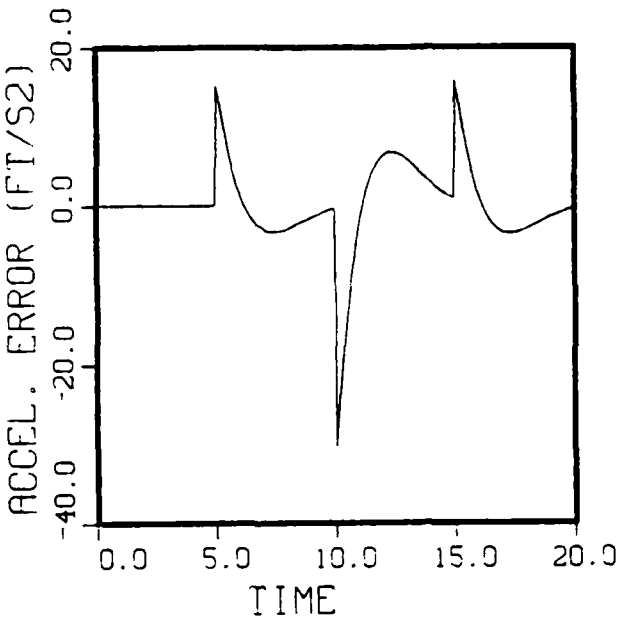

Figure 4-11 $\alpha - \delta$ Tracker Acceleration Error (Q = .2025)

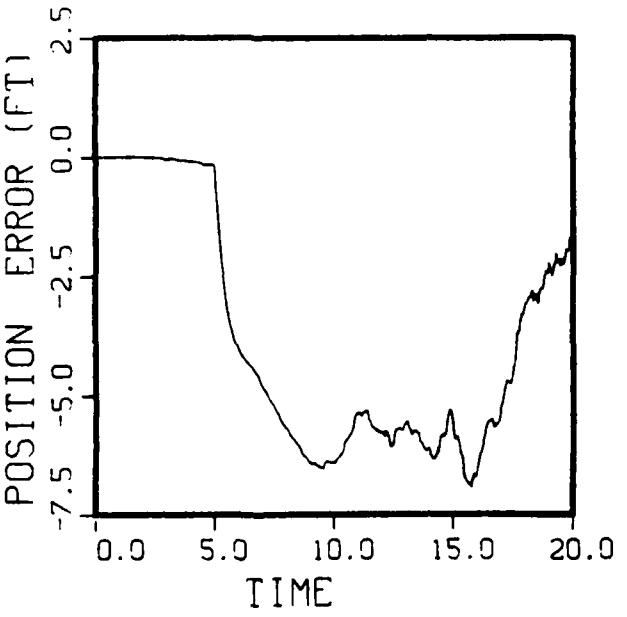

Figure 4-12 $\alpha - \delta$ Tracker Position Error (Q = .2025)

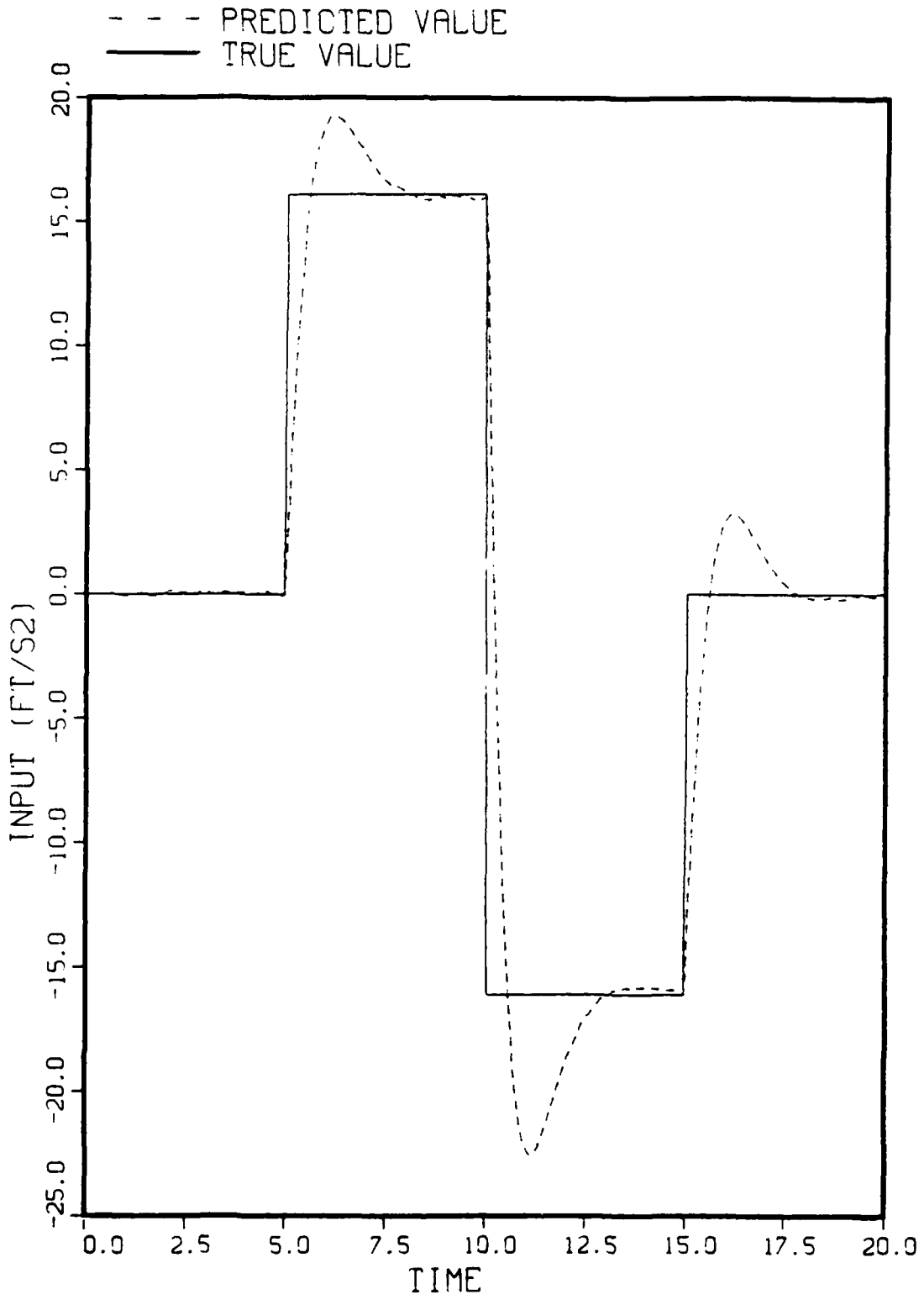

Figure 4-13 $\alpha - \delta$ Tracker Acceleration Estimate (Q = 3.24)

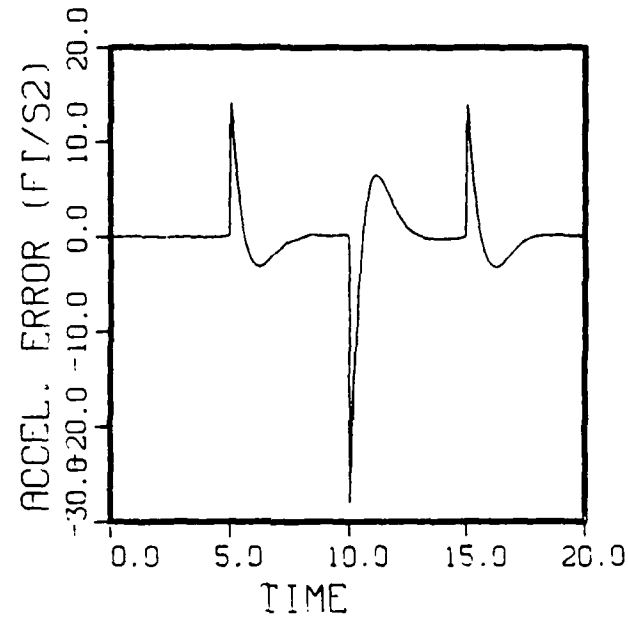

Figure 4-14 $\alpha - \delta$ Tracker Acceleration Error (Q = 3.24)

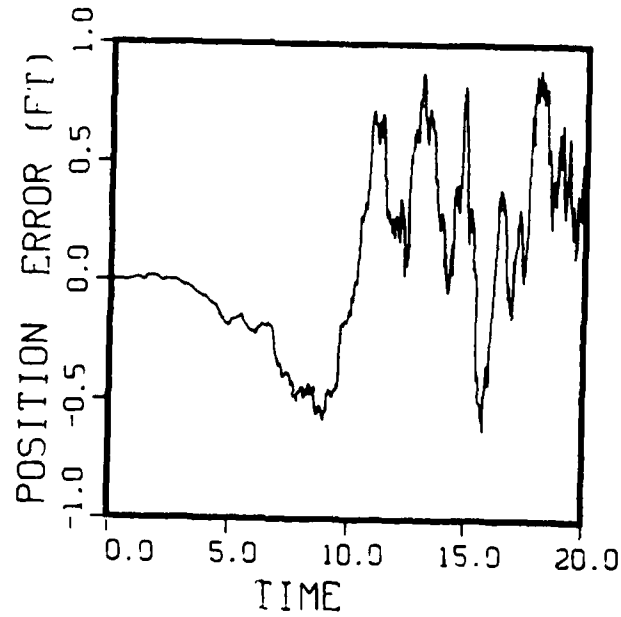

Figure 4-15 $\alpha - \delta$ Tracker Position Error (Q = 3.24)

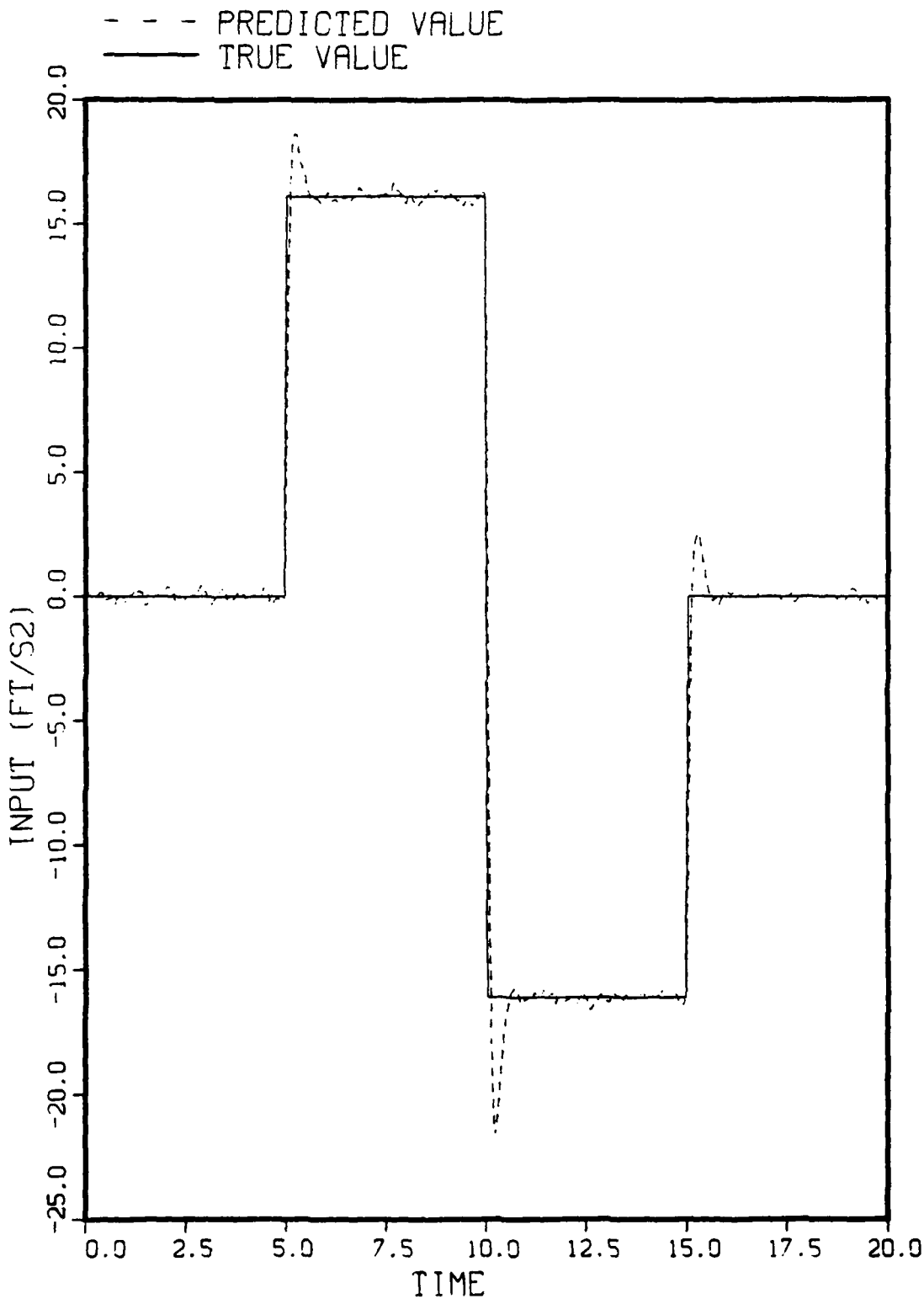

Figure 4-16 $\alpha - \delta$ Tracker Acceleration Estimate (Q = 2025)

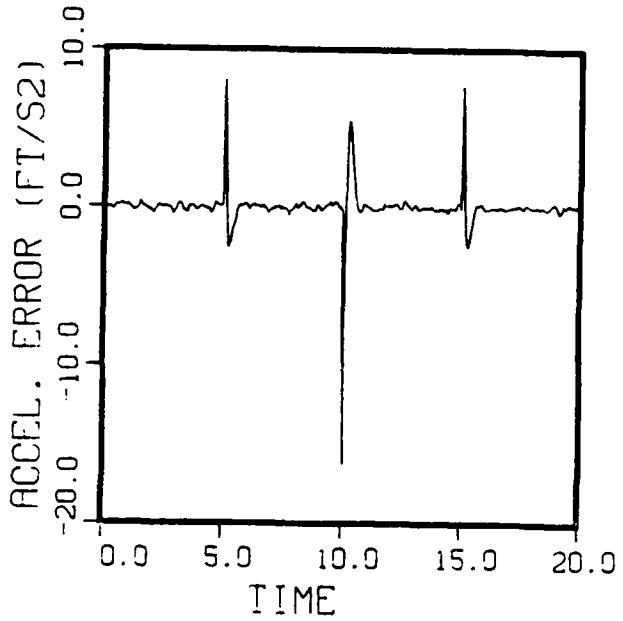

Figure 4-17 $\alpha - \delta$ Tracker Acceleration Error (Q = 2025)

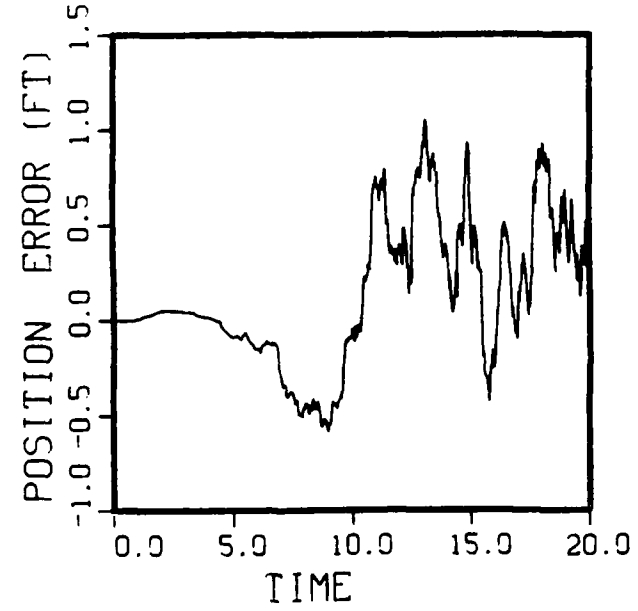

Figure 4-18 $\alpha - \delta$ Tracker Position Error (Q = 2025)

4. Summary

This chapter investigates the improvements that are accrued when orientation information is included in a linear tracking model. The linear tracker that incorporates orientation information (i.e. $\alpha - \delta$ tracker) outperforms the point-mass tracker (i.e. $\alpha - \beta - \gamma$ tracker). In addition, the $\alpha - \delta$ tracker is more robust in terms of sensitivity to the selection of the process noise level. These results correlate nicely with the far more extensive nonlinear analysis performed in Chapter 3.

CHAPTER 5
OBSERVER DESIGN FOR SYSTEMS WITH UNKNOWN EXOGENOUS INPUTS

5.1 Introduction

In general, system observers are used to estimate state time histories for systems with an incomplete set of system state measurements and unknown initial conditions. The design of observers with these condition is predicated on having a known model of the system, and complete access to the system exogenous inputs. Under these circumstances, the performance of the system observer is well known and documented [Luenberger; 1971].

The target *trajectory estimation problem* is severely handicapped, due to the fact that the system exogenous inputs are generally unknown. With incomplete knowledge concerning the system inputs, the question of the selection of the observer gains becomes critical. This chapter addresses this problem for both the continuous and discrete observers. The solution leads to the implementation of a Kalman filter with infinite process noise which has previously been referred to a Fisher filter [Schweppe; 1975].

5.2 Continuous Observer Design

The basic approach for the observer design with unknown exogenous inputs is to model the unknown inputs as states of the system. This requires augmenting the state vector and the associated dynamics matrix.

Figure 5-1 represents the time domain block diagram for the augmented observer implementation. The concatenation of the state and input estimates results in the n + m augmented state vector as shown.

The governing equations for the system depicted in Figure 5-1 are

System Dynamics

$$\dot{x}(t) = Fx(t) + Gu(t) \tag{5.1-1a}$$

$$z(t) = H_1 x(t) \tag{5.1-1b}$$

Observer Dynamics

$$\dot{\hat{x}}^a(t) = F^a \hat{x}^a(t) + Kr(t) \tag{5.1-2a}$$

$$r(t) = z(t) - H_2 \hat{x}^a(t) \tag{5.1-2b}$$

where

$$\hat{x}^a = \begin{bmatrix} \hat{x} \\ \hat{u} \end{bmatrix}$$

$$F^a = \begin{bmatrix} F & G \\ 0 & 0 \end{bmatrix} \quad K = \begin{bmatrix} K_x \\ K_u \end{bmatrix} \quad H_2 = \begin{bmatrix} H_1 & 0 \end{bmatrix}$$

where $x \in R^n$ = system state vector, $u \in R^m$ = unknown exogenous input vector. The observer vector $\hat{x}^a \in R^{n+m}$ represents the state vector estimate. The vectors $z \in R^l$ and $r \in R^l$ represent the system measurements and residuals. For the purposes of the present analysis, the system is assumed to have as many inputs as outputs (i.e. l = m). The associated matrices are dimensioned to ensure compatibility.

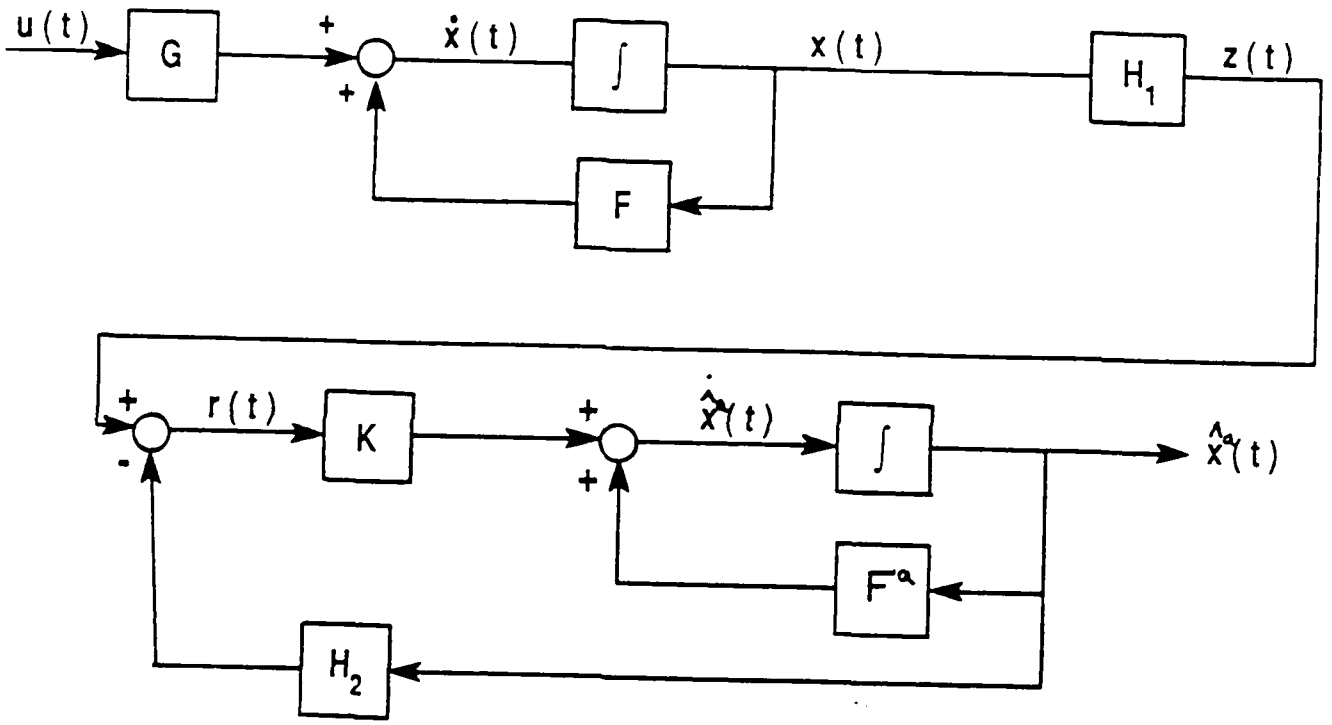

Figure 5-1 Continuous Augmented Observer

In order to determine the accuracy of the input estimation, it is necessary to find the overall transfer function matrix between u(t) and $\hat{u}(t)$. As shown in Figure 5-2, this requires that intermediate transfer functions be found.

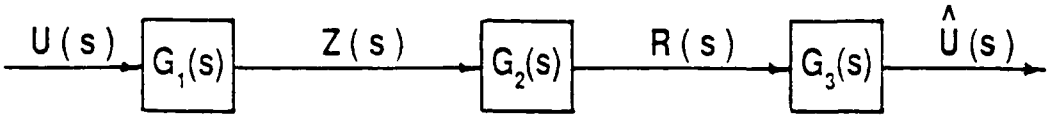

Figure 5-2 Continuous Frequency Domain Transfer Function Matrices

The transfer function matrices (TFM) depicted in Figure 5-2 represent the appropriate Laplace transform input/output relationships. The overall input/output transfer function matrix is

$$\frac{\hat{U}(s)}{U(s)} = G_3(s)G_2(s)G_1(s) \qquad (5.1\text{-}3)$$

The individual transfer function matrices must be determined from the system shown in Figure 5-1, and described by equations 5.1-1 and 5.1-2.

$G_1(s)$ Transfer Function Matrix

The G_1 (s) TFM represents the input/output relationship between U(s) and Z(s). This is found in a straightforward fashion by applying Laplace transforms to equations 5-1.1a and 5.1-1b.

$$\frac{Z(s)}{U(s)} = G_1(s) = H_1(sI - F)^{-1}G \tag{5.1-4}$$

$G_2(s)$ Transfer Function Matrix

The G_2 TFM represents the input/output relationship between Z(s) and R(s). The Laplace transform of equation 5.1-2a and 5.1-2b yields

$$\hat{X}^a(s) = (sI - F^a)^{-1}KR(s) \tag{5.1-5}$$

$$R(s) = Z(s) - H_2\hat{X}^a(s) \tag{5.1-6}$$

Combining equations 5.1-5 and 5.1-6 provides

$$\frac{R(s)}{Z(s)} = G_2(s) = \left[I + H_2(sI - F^a)^{-1}K\right]^{-1} \tag{5.1-7}$$

$G_3(s)$ Transfer Function Matrix

The G_3 TFM represents the input/output relationship between $\hat{U}(s)$ and R(s). Recalling that

$$\hat{x}^a(t) = [\hat{x}(t)\ \ \hat{u}(t)]^T \tag{5.1-8}$$

then

$$\hat{u}(t) = H_3\hat{x}^a(t) \tag{5.1-9}$$

where

$$H_3=[0\ \ I_m]$$

Premultiplying both sides of equation 5.1-5 by H_3 and substituting the Laplace transformation of equation 5.1-9 results in

$$\frac{\hat{U}(s)}{R(s)} = G_3(s) = H_3(sI - F^a)^{-1}K \tag{5.1-10}$$

Combining equations 5.1-3, 5.1-4, 5.1-7 and 5.1-10 results in

$$\frac{\hat{U}(s)}{U(s)} = \left[H_3(sI - F^a)^{-1}K\right]\left[I + H_2(sI - F^a)^{-1}K\right]^{-1}\left[H_1(sI - F)^{-1}G\right] \tag{5.1-11}$$

Equation 5.1-11 gives the m x m TFM between estimates of the system inputs and the actual system inputs. Ideally, this matrix should be the identity matrix indicating perfect estimates of the system input. However, the system structure may preclude achieving a perfect estimate without time lag.

Examination of equation 5.1-11 shows that, in fact, if the overall transfer matrix is the identity matrix, then the combined G_3 (s) and G_2 (s) TFM can be viewed as the left inverse TFM of G_1 (s). Wolovich [1974] shows that this left inverse exists if and only if the rank (G_1 (s)) = m. Therefore the existence of the left inverse requires $m \leq l$. If the left inverse is used, then the combined G_3 (s) G_2 (s) TFM can be viewed as performing system deconvolution.

The general rule of thumb [Luenberger; 1971] for observer gain selection is to select values that ensure that the observer dynamics are significantly faster than the system dynamics. To achieve this end, the designer evaluates the observer eigenvalues to determine their location in the left half s-plane for the continuous case. However, if the observer is to be used as an integral part of a system controller, the stability margins ensured under full state feedback are no longer guaranteed. In fact, as shown by Doyle and Stein [1979] for the continuous case, the resulting stability margins may be wholly unacceptable. Under these conditions, the stability margins can be recovered by selecting the gains based on a Kalman filter implementation with the process noise

strength asymptotically approaching infinity. A filter designed with this condition is referred to as a Fisher filter, and as will be demonstrated, yields an ideal augmented observer for systems with unknown exogenous inputs.

In order to evaluate the effects of infinite process noise intensities on the TFM of equation 5.1-11, parameterize the observer gain as a function of a scalar q such that

$$\lim_{q\to\infty}\frac{K}{q}=G^{a}W \tag{5.1-12}$$

where $G^{a}=[\,0\;\;I_m\,]^{T}$ and W is any non-singular m x m matrix. Substituting equation 5.1-12 into equation 5.1-11 results in

$$\lim_{q\to\infty}\frac{\hat{U}(s)}{U(s)}=\lim_{q\to\infty}\left[H_3(sI-F^{a})^{-1}\frac{K}{q}\right]\left[\frac{I}{q}+H_2(sI-F^{a})^{-1}\frac{K}{q}\right]^{-1}\cdot \left[H_1(sI-F)^{-1}G\right] \tag{5.1-13}$$

$$=\left[H_3(sI-F^{a})^{-1}G^{a}W\right]\left[H_2(sI-F^{a})^{-1}G^{a}W\right]^{-1}\cdot \left[H_1(sI-F)^{-1}G\right] \tag{5.1-14}$$

Since W is assumed non-singular, equation 5.1-14 simplifies to

$$\lim_{q\to\infty}\frac{\hat{U}(s)}{U(s)}=\left[H_3(sI-F^{a})^{-1}G^{a}\right]\left[H_2(sI-F^{a})^{-1}G^{a}\right]^{-1}\cdot \left[H_1(sI-F)^{-1}G\right] \tag{5.1-15}$$

It is now shown that the TFM given by equation 5.1-15 simplifies to

$$\lim_{q\to\infty}\frac{\hat{U}(s)}{U(s)}=I_m \tag{5.1-16}$$

To demonstrate that equation 5.1-15 simplifies to equation 5.1-16, let equation 5.1-15 be rewritten as

$$\lim_{q\to\infty}\frac{\hat{U}(s)}{U(s)} = G_3'(s)G_2'(s)G_1(s) \tag{5.1-17}$$

where

$$G_3'(s) = H_3(sI - F^a)^{-1}G^a \tag{5.1-18}$$

$$G_2'(s) = \left[H_2(sI - F^a)^{-1}G^a\right]^{-1} \tag{5.1-19}$$

$$G_1(s) = H_1(sI - F)^{-1}G \tag{5.1-20}$$

Recall that the above matrices are partitioned as

$$F^a = \begin{bmatrix} F & G \\ 0 & 0 \end{bmatrix} \quad G^a = \begin{bmatrix} 0 \\ I_m \end{bmatrix}$$

$$H_2 = \begin{bmatrix} H_1 & 0 \end{bmatrix} \quad H_3 = \begin{bmatrix} 0 & I_m \end{bmatrix}$$

The $G_3'(s)$ TFM is obtained as follows.

$$G_3'(s) = H_3(sI - F^a)^{-1}G^a$$

$$= \begin{bmatrix} 0 & I_m \end{bmatrix} \begin{bmatrix} (sI - F)^{-1} & \frac{1}{s}(sI - F)^{-1}G \\ 0 & \frac{1}{s}I \end{bmatrix} \begin{bmatrix} 0 \\ I_m \end{bmatrix}$$

$$G_3'(s) = \frac{1}{s}I_m \tag{5.1-21}$$

The $G_2'(s)$ transfer function is found as follows

$$G_2'(s) = \left[H_2(sI - F^a)^{-1}G^a\right]^{-1}$$

$$= \left\{ \begin{bmatrix} H_1 & 0 \end{bmatrix} \begin{bmatrix} (sI - F)^{-1} & \frac{1}{s}(sI - F)^{-1}G \\ 0 & \frac{1}{s}I \end{bmatrix} \begin{bmatrix} 0 \\ I_m \end{bmatrix} \right\}^{-1}$$

$$G_2'(s) = s\left[H_1(sI - F)^{-1}G\right]^{-1} \tag{5.1-22}$$

Combining equations 5.1-17, 5.1-20, 5.1-21, and 5.1-22, demonstrates that

$$\lim_{q\to\infty} \frac{\hat{U}(s)}{U(s)} = I_m \tag{5.1-16}$$

It is now shown that for a square (i.e. m = l) minimum phase system, a Kalman filter implementation with infinite process noise will yield the values for K shown in equation 5.1-12. This proof is attributable to Doyle and Stein [1979]. Using the continuous Kalman filter notation previously defined, let

$$K(q) = P(q)H^T R^{-1} \tag{5.1-23}$$

with P(q) defined by the continuous algebraic Ricatti equation

$$FP + PF^T + Q(q) - PH^T R^{-1} HP = 0 \tag{5.1-24}$$

Let the process noise be represented as

$$Q(q) = Q_o + q^2 GVG^T \tag{5.1-25}$$

where Q_o represents the nominal plant noise and V is any positive definite symmetric matrix. Note that for q = 0 the filter gains are simply the nominal Kalman filter gains.

To examine the effect on the filter gains as q asymptotically approaches infinity, divide both sides of equation 5.1-24 by q^2

$$F\left(\frac{P}{q^2}\right) + \left(\frac{P}{q^2}\right)F^T + \frac{Q_o}{q^2} + GVG^T$$

$$-q^2\left(\frac{P}{q^2}\right)H^T R^{-1} H\left(\frac{P}{q^2}\right) = 0 \tag{5.1-26}$$

Kwakernaak and Sivan [1972] demonstrate that

$$\lim_{q\to\infty}\left(\frac{P}{q^2}\right) = 0 \tag{5.1-27}$$

whenever the transfer function $H(sI - F)^{-1}G$ has no right half plane zeroes.

Therefore,

$$\lim_{q\to\infty} q^2\left(\frac{P}{q^2}\right)H^t R^{-1} H\left(\frac{P}{q^2}\right) = GVG^T \tag{5.1-28}$$

or in terms of equation 5.1-23

$$\lim_{q\to\infty} \frac{KRK^T}{q^2} = GVG^T \tag{5.1-29}$$

For this to hold requires

$$\lim_{q\to\infty} \frac{K}{q} = GV^{1/2}(R^{1/2})^{-1} \tag{5.1-30}$$

Since it has been assumed that both V and R are positive definite matrices then the matrix W from equation 5.1-12 exists and is invertible.

Verification of the augmented observer approach is performed with a steady state $\alpha - \beta - \gamma$ tracking filter. The point-mass model dynamics are

$$\dot{x}(t) = \begin{bmatrix} 0 & 0 \\ 0 & 1 \end{bmatrix} x(t) + \begin{bmatrix} 0 \\ 1 \end{bmatrix} u(t) \tag{5.1-31a}$$

$$z(t) = \begin{bmatrix} 1 & 0 \end{bmatrix} x(t) \tag{5.1-31b}$$

This model has position and velocity as elements of the state vector, with an acceleration input. In the filter implementation, only position measurements are available.

Using this model leads to the following augmented observer matrices.

$$F^a = \begin{bmatrix} 0 & 1 & 0 \\ 0 & 0 & 1 \\ 0 & 0 & 0 \end{bmatrix} \quad G^a = \begin{bmatrix} 0 \\ 0 \\ 1 \end{bmatrix}$$

$$H_2 = \begin{bmatrix} 1 & 0 & 0 \end{bmatrix}$$

$$H_3 = \begin{bmatrix} 0 & 0 & 1 \end{bmatrix}$$

Since the model describes a single input-single output relationship, the TFM of equation 5.1-17 simplifies to a scalar transfer function. Substituting the observer matrices into equations 5.1-18, 5.1-19, and 5.1-20 gives

$$G_3'(s) = H_3(sI - F^a)^{-1}G^a \tag{5.1-32}$$

$$= \begin{bmatrix} 0 & 0 & 1 \end{bmatrix} \begin{bmatrix} \frac{1}{s} & \frac{1}{s^2} & \frac{1}{s^3} \\ 0 & \frac{1}{s} & \frac{1}{s^2} \\ 0 & 0 & \frac{1}{s} \end{bmatrix} \begin{bmatrix} 0 \\ 0 \\ 1 \end{bmatrix}$$

$$G_3'(s) = \frac{1}{s} \tag{5.1-33}$$

$$G_2'(s) = \left[H_2(sI - F^a)^{-1}G^a \right]^{-1} \tag{5.1-34}$$

$$= \left\{ \begin{bmatrix} 1 & 0 & 0 \end{bmatrix} \begin{bmatrix} \frac{1}{s} & \frac{1}{s^2} & \frac{1}{s^3} \\ 0 & \frac{1}{s} & \frac{1}{s^2} \\ 0 & 0 & \frac{1}{s} \end{bmatrix} \begin{bmatrix} 0 \\ 0 \\ 1 \end{bmatrix} \right\}^{-1}$$

$$G_2'(s) = s^3 \tag{5.1-35}$$

$$G_1(s) = H_1(sI - F)^{-1}G \tag{5.1-36}$$

$$= \begin{bmatrix} 1 & 0 \end{bmatrix} \begin{bmatrix} \frac{1}{s} & \frac{1}{s^2} \\ 0 & \frac{1}{s} \end{bmatrix} \begin{bmatrix} 0 \\ 1 \end{bmatrix}$$

$$G_1(s) = \frac{1}{s^2} \tag{5.1-37}$$

Combining the results of equations 5.1-17, 5.1-32, 5.1-34, and 5.1-37 confirms the the achievement of a unity TFM.

$$\frac{\hat{U}(s)}{U(s)} = G_3'(s)G_2'(s)G_1(s) = 1 \tag{5.1-38}$$

5.3 Discrete Observer Design

The discrete augmented observer design is accomplished using a procedure that parallels the continuous observer design. Figure 5-3 represents the time domain block diagram for the augmented observer implementation. The concatenation of the state and input estimates results in the n+m augmented state vector as shown.

The governing equations for the system depicted in Figure 5-3 are

System Dynamics

$$x(k+1) = \Phi x(k) + \Gamma u(k) \tag{5.2-1a}$$

$$z(k) = H_1 x(k) \tag{5.2-1b}$$

Observer Dynamics

$$\bar{x}^a(k+1) = \Phi^a \hat{x}^a(k) \tag{5.2-2a}$$

$$\hat{x}^a(k+1) = \bar{x}^a(k+1) + K\ r(k+1) \tag{5.2-2b}$$

$$r(k+1) = z(k+1) - H_2 \bar{x}^a(k+1) \tag{5.2-2c}$$

where

$$\bar{x}^a = \begin{bmatrix} \bar{x} \\ \bar{u} \end{bmatrix} \qquad \hat{x}^a = \begin{bmatrix} \hat{x} \\ \hat{u} \end{bmatrix}$$

$$\Phi^a = \begin{bmatrix} \Phi & \Gamma \\ 0 & I_m \end{bmatrix} \quad K = \begin{bmatrix} K_x \\ K_u \end{bmatrix} \quad H_2 = \begin{bmatrix} H_1 & 0 \end{bmatrix}$$

where $x \in R^n$ = system state vector, $u \in R^m$ = unknown exogenous input vector. The observer vectors $\bar{x}^a$ and $\hat{x}^a \in R^{n+m}$ represent the state vector estimate. The vectors

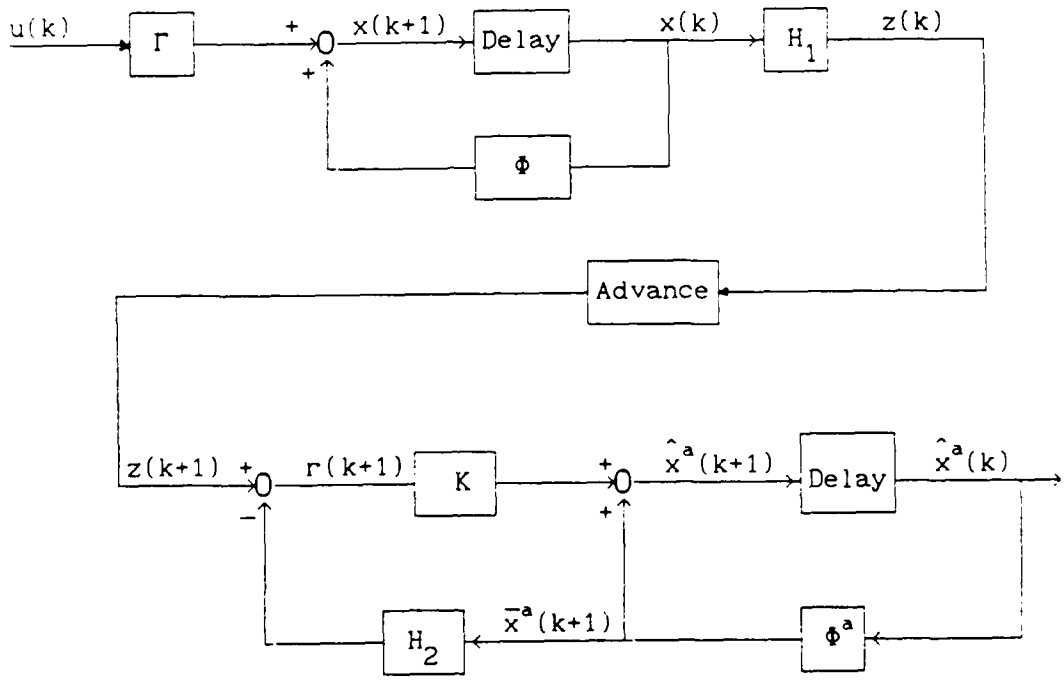

Figure 5-3 Discrete Augmented Observer

$z \in R^l$ and $r \in R^l$ represent the system measurements and residuals. For the purposes of the present analysis, the system is assumed to have as many inputs as outputs (i.e. l = m). The associated matrices are dimensioned to ensure compatibility.

In order to determine the accuracy of the input estimation, it is necessary to find the overall transfer function matrix between u(k) and $\hat{u}(k)$. As shown in Figure 5-4, this requires that intermediate transfer functions be found.

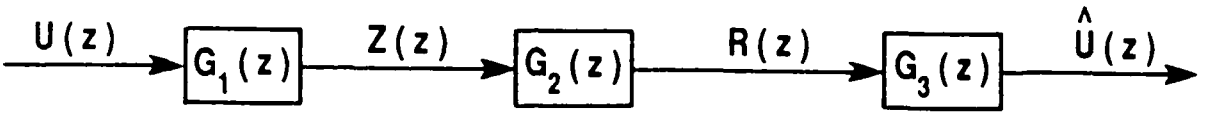

Figure 5-4 Discrete Frequency Domain Transfer Function Matrices

The transfer function matrices (TFM) depicted in Figure 5.4 represent the appropriate z-transform input/output relationships. The overall input/output transfer function matrix is

$$\frac{\hat{U}(z)}{U(z)} = G_3(z)G_2(z)G_1(z) \qquad (5.2\text{-}3)$$

The individual transfer function matrices must be determined from the system shown in Figure 5-3, and described by equations 5.2-1 and 5.2-2.

$G_1(z)$ Transfer Function Matrix

The G_1 (z) TFM represents the input/output relationship between U(z) and Z(z). This is found in a straightforward fashion by applying z-transforms to equations 5.2-1a and 5.2-1b.

$$\frac{Z(z)}{U(z)} = G_1(z) = H_1(zI - \Phi)^{-1}\Gamma \tag{5.2-4}$$

$G_2(z)$ Transfer Function Matrix

The G_2 TFM represents the input/output relationship between Z(z) and R(z). The z-transform of equation 5.2-2c yields

$$R(z) = Z(z) - H_2\bar{X}^a(z) \tag{5.2-5}$$

Combining equations 5.2-2a and 5.2-2b provides

$$\hat{x}^a(k+1) = \Phi^a\hat{x}^a(k) + Kr(k+1) \tag{5.2-6}$$

$$\hat{X}^a(z) = (zI - \Phi^a)^{-1}KzR(z) \tag{5.2-7}$$

Premultiplying equation 5.2-7 by $H_2\Phi^a$ gives

$$H_2\bar{X}^a(z) = H_2\Phi^a(zI - \Phi^a)^{-1}KR(z) \tag{5.2-8}$$

Substituting equation 5.2-8 into equation 5.2-5 results in

$$\frac{R(z)}{Z(z)} = G_2(z) = \left[I + H_2\Phi^a(zI - \Phi^a)^{-1}K\right]^{-1} \tag{5.2-9}$$

$G_3(z)$ Transfer Function Matrix

The G_3 TFM represents the input/output relationship between $\hat{U}(z)$ and R(z). Recalling that

$$\hat{x}^a(k) = [\hat{x}(k)\ \ \hat{u}(k)]^T \tag{5.2-10}$$

then

$$\hat{u}(k) = H_3 \hat{x}^a(k) \tag{5.2-11}$$

where $H_3 = [\,0 \quad I_m\,]$

Premultiplying equation 5.2-7 by H_3 gives

$$\frac{\hat{U}(z)}{R(z)} = G_3(z) = H_3(zI - \Phi^a)^{-1}K\ z \tag{5.2-12}$$

Combining equations 5.2-3, 5.2-4, 5.2-9, and 5.2-12 results in

$$\frac{\hat{U}(z)}{U(z)} = \left[H_3(zI - \Phi^a)^{-1}K\ z\right]\left[I + H_2\Phi^a(zI - \Phi^a)^{-1}K\right]^{-1} \cdot \left[H_1(zI - \Phi)^{-1}\Gamma\right] \tag{5.2-13}$$

Equation 5.2-13 gives the m x m TFM between estimates of the system inputs and the actual system inputs. Ideally, this matrix should be the identity matrix indicating perfect estimates of the system input. However, the system structure may preclude achieving a perfect estimate without time delay.

As was the case with the continuous observer, the designer selects observer gain values that ensure that the observer dynamics are significantly faster than the system dynamics. To achieve this end, the designer evaluates the observer eigenvalues to determine their location in the unit circle of the z-plane for the discrete case. However, if the observer is to be used as an integral part of a system controller, the stability margins ensured under full state feedback are no longer guaranteed. The stability margins can be recovered by selecting the gains based on a Kalman filter implementation with the process noise strength asymptotically approaching infinity. A filter designed with this condition yields a dead-beat augmented observer for systems with unknown exogenous inputs.

In order to evaluate the effects of K on the TFM of equation 5.2-13, first parameterize K as a function of a scalar q such that K = K(q). Select K so that

$$\lim_{q \to \infty} K = \Gamma^a W \tag{5.2-14}$$

where $\Gamma^a = [\ \Gamma \quad I_m\ ]^T$ and W is any non-singular m x m matrix. Substituting equation 5.2-14 into equation 5.2-13 results in

$$\lim_{q \to \infty} \frac{\hat{U}(z)}{U(z)} = \left[zH_3(zI - \Phi^a)^{-1}\Gamma^a W \right] \left[I + H_2\Phi^a(zI - \Phi^a)^{-1}\Gamma^a W \right]^{-1} \cdot \left[H_1(zI - \Phi)^{-1}\Gamma \right] \tag{5.2-15}$$

Since W is assumed non-singular, equation 5.2-15 simplifies to

$$\lim_{q \to \infty} \frac{\hat{U}(z)}{U(z)} = \left[zH_3(zI - \Phi^a)^{-1}\Gamma^a \right] \left[W^{-1} + H_2\Phi^a(zI - \Phi^a)^{-1}\Gamma^a \right]^{-1} \left[H_1(zI - \Phi)^{-1}\Gamma \right] \tag{5.2-16}$$

It is now shown that the TFM given by equation 5.2-16 simplifies to

$$\lim_{q \to \infty} \frac{\hat{U}(z)}{U(z)} = \frac{1}{z} I_m \tag{5.2-17}$$

To demonstrate that equation 5.2-16 collapses to equation 5.2-17, let equation 5.2-16 be rewritten as

$$\lim_{q \to \infty} \frac{\hat{U}(z)}{U(z)} = G_3'(z)G_2'(z)G_1(z) \tag{5.2-18}$$

where

$$G_3'(z) = zH_3(zI - \Phi^a)^{-1}\Gamma^a \tag{5.2-19}$$

$$G_2'(z) = \left[W^{-1} + H_2\Phi^a(zI - \Phi^a)^{-1}\Gamma^a \right]^{-1} \tag{5.2-20}$$

$$G_1(z) = H_1(zI - \Phi)^{-1}\Gamma \tag{5.2-21}$$

Recall that the above matrices are partitioned as

$$\Phi^a = \begin{bmatrix} \Phi & \Gamma \\ 0 & I_m \end{bmatrix} \qquad \Gamma^a = \begin{bmatrix} \Gamma \\ I_m \end{bmatrix}$$

$$H_2 = \begin{bmatrix} H_1 & 0 \end{bmatrix} \qquad H_3 = \begin{bmatrix} 0 & I_m \end{bmatrix}$$

Substituting in the partitioned matrices for Γ^a and H_2 with W = $(H_1\Gamma)^{-1}$ (which is assumed to be full rank) results in

$$K = \begin{bmatrix} \Gamma \\ I_m \end{bmatrix} (H_1\Gamma)^{-1}$$

The G_3' TFM is obtained as follows.

$$G_3' = zH_3(zI - \Phi^a)^{-1}\Gamma^a$$

$$= z\begin{bmatrix} 0 & I_m \end{bmatrix} \begin{bmatrix} (zI - \Phi)^{-1} & (zI - \Phi)^{-1}\Gamma(zI - I_m)^{-1} \\ 0 & (zI - I_m)^{-1} \end{bmatrix} \begin{bmatrix} \Gamma \\ I_m \end{bmatrix}$$

$$G_3' = z\,(zI - I_m)^{-1} \tag{5.2-22}$$

The G_2' transfer function is found by first evaluating

$$H_2\Phi^a(zI - \Phi^a)^{-1}\Gamma^a =$$

$$\begin{bmatrix} H_1 & 0 \end{bmatrix} \begin{bmatrix} \Phi & \Gamma \\ 0 & I_m \end{bmatrix} \begin{bmatrix} (zI - \Phi)^{-1} & (zI - \Phi)^{-1}\Gamma(zI - I_m)^{-1} \\ 0 & (zI - I_m)^{-1} \end{bmatrix} \begin{bmatrix} \Gamma \\ I_m \end{bmatrix}$$

$$= H_1\Phi(zI - \Phi)^{-1}\Gamma\left\{ I_m + (zI - I_m)^{-1} \right\} + H_1\Gamma(zI - I_m)^{-1}$$

Using the identities

$$I_m + (zI - I_m)^{-1} = z\,(zI - I_m)^{-1}$$

$$H_1\Gamma(zI - I_m)^{-1} = H_1(zI - I_n)^{-1}\Gamma$$

results in

$$H_2\Phi^a(zI-\Phi^a)^{-1}\Gamma^a =$$

$$\left\{zH_1\Phi(zI-\Phi)^{-1}\Gamma + H_1\Gamma\right\}(zI-I_m)^{-1}$$

Adding W^{-1} and taking the inverse results in

$$G_2' = \left\{H_1\Gamma + (zH_1\Phi(zI-\Phi)^{-1}\Gamma + H_1\Gamma)((zI-I_m)^{-1})\right\}^{-1}$$

$$= (zI-I_m)\left\{H_1(zI + z\Phi(zI-\Phi)^{-1})\Gamma\right\}^{-1}$$

Noting that

$$zI + z\Phi(zI-\Phi)^{-1} = \left\{z(zI-\Phi) + z\Phi\right\}(zI-\Phi)^{-1}$$

$$= z^2(zI-\Phi)^{-1}$$

then

$$G_2' = z^{-2}(zI-I_m)(H_1(zI-\Phi)^{-1}\Gamma)^{-1} \qquad (5.2\text{-}23)$$

Combining equations 5.2-18, 5.2-21, 5.2-22, and 5.2-23, demonstrates that

$$\lim_{q\to\infty}\frac{\hat{U}(z)}{U(z)} = \frac{1}{z}I_m \qquad (5.2\text{-}17)$$

To determine the Kalman filter behavior as process noise levels approach infinity (i.e. a Fisher filter), examine a square (m = 1) minimum phase system. The minimum phase requirements ensures a dead-beat respo ıse [Kwakernaak and Sivan; 1972]. The state gain and covariance equations for the standard Kalman filter are :

Predicted Error Covariance

$$M = \Phi^a P \Phi^{aT} + \Gamma^a Q \Gamma^{aT} \qquad (5.2\text{-}24)$$

Kalman Gain

$$K = MH_2^T(H_2MH_2^T + R)^{-1} \tag{5.2-25}$$

Filtered Error Covariance

$$P = (I - KH_2)M \tag{5.2-26}$$

where

M = predicted state error covariance matrix prior to system measurement.

P = filtered state error covariance matrix at time of system measurement.

Substituting equation 5.2-25 into 5.2-26 gives

$$P = M - MH_2^T(H_2MH_2^T+R)^{-1}H_2M \tag{5.2-27}$$

Substituting equation 5.2-27 into equation 5.2-24 produces the discrete Ricatti equation governing the predicted error covariance.

$$M = \Phi^a M \Phi^{a^T} - \Phi^a MH_2^T(H_2MH_2^T + R)^{-1}H_2M\Phi^{a^T} + \Gamma^a Q \Gamma^{a^T} \tag{5.2-28}$$

Let Q = $Q_0 + q^2$ I, and divide equation 5.2-28 by q^2

$$\frac{M}{q^2} = \Phi^a \frac{M}{q^2}\Phi^{a^T} - \Phi^a \frac{M}{q^2}H_2^T(H_2\frac{M}{q^2}H_2^T + \frac{R}{q^2})^{-1}H_2\frac{M}{q^2}\Phi^{a^T}$$

$$+ \Gamma^a(\frac{Q_0}{q^2} + I)\Gamma^{a^T} \tag{5.2-29}$$

Taking the limit as q approaches infinity gives

$$M_\infty = \Phi^a M_\infty \Phi^{a^T} - \Phi^a M_\infty H_2^T(H_2M_\infty H_2^T)^{-1}H_2M_\infty\Phi^{a^T} + \Gamma^a\Gamma^{a^T} \tag{5.2-30}$$

where $M_\infty = \lim_{q\to\infty}\frac{M}{q^2}$

Now assume $M_\infty = \Gamma^a\Gamma^{a^T}$ and substitute this into equation 5.2-30

$$\Gamma^a\Gamma^{a^T} = \Phi^a\left\{\Gamma^a\Gamma^{a^T} - \Gamma^a\Gamma^{a^T}H_2^T(H_2\Gamma^a\Gamma^{a^T}H_2^T)^{-1}H_2\Gamma^a\Gamma^{a^T}\right\}\Phi^{a^T} + \Gamma^a\Gamma^{a^T} \tag{5.2-31}$$

If $H_2\Gamma^a$ is square and full rank, then $M_\infty = \Gamma^a\Gamma^{a^T}$ is a satisfactory solution.

The resulting gain for the Fisher filter is found by multiplying and dividing the right hand side of equation 5.2-25 by q^2 and taking the limit which leads to

$$K = M_\infty H_2^T (H_2 M_\infty H_2^T)^{-1} \tag{5.2-32}$$

Substituting $M_\infty = \Gamma^a \Gamma^{aT}$ results in

$$K = \Gamma^a (H_2 \Gamma^a)^{-1} \tag{5.2-33}$$

Therefore, the selection of the gains based on a Fisher filter satisfies the parameterization of K shown in equation 5.2-14.

The verification of the augmented observer approach is now shown for the discrete $\alpha - \beta - \gamma$ tracking filter. The point-mass model dynamics are

$$x(k+1) = \begin{bmatrix} 1 & T \\ 0 & 1 \end{bmatrix} x(k) + \begin{bmatrix} T^2/2 \\ T \end{bmatrix} u(k) \tag{5.2-34a}$$

$$z(k) = \begin{bmatrix} 1 & 0 \end{bmatrix} x(k) \tag{5.2-34b}$$

This model has position and velocity as elements of the state vector, with an acceleration input that is assumed constant over the sampling period T. In the filter implementation, only position measurements are available.

Using this model leads to the following observer matrices.

$$\Phi^a = \begin{bmatrix} 1 & T & T^2/2 \\ 0 & 1 & T \\ 0 & 0 & 1 \end{bmatrix} \quad \Gamma^a = \begin{bmatrix} T^2/2 \\ T \\ 1 \end{bmatrix} \quad K = \begin{bmatrix} \alpha \\ \beta \\ \gamma \end{bmatrix} \tag{5.2-35}$$

Since the model describes a single input-single output relationship, the TFM of equation 5.2-13 simplifies to a scalar transfer function. Substituting the observer matrices into equations 5.2-4, 5.2-9, and 5.2-12 gives

$$G_1(z) = \frac{(T^2/2)(z+1)}{(z-1)^2}$$

$$G_2(z) = \frac{(z-1)^3}{z^3 - (3 - \alpha - \beta T - \gamma T^2/2)z^2 + (3 - 2\alpha - \beta T + \gamma T^2/2)z + (\alpha - 1)}$$

$$G_3(z) = \frac{\gamma z}{z - 1}$$

Combining these transfer functions results in

$$\frac{\hat{U}(z)}{U(z)} = \frac{\gamma(T^2/2)z(z+1)}{z^3 - (3 - \alpha - \beta T - \gamma T^2/2)z^2 + (3 - 2\alpha - \beta T + \gamma T^2/2)z + (\alpha - 1)}$$

Kalata [1984] provides tracker gain equations for this model. Using his results, a process noise limit analysis can be performed to evaluate the Fisher filter gains. This leads to

$$\alpha = 1$$

$$\beta = 2/T$$

$$\gamma = 2/T^2$$

Substituting these gains values into the input estimator transfer function provides

$$\frac{\hat{U}(z)}{U(z)} = \frac{1}{z} \tag{5.2-35}$$

Gleason and Andrisani [1985] determined closed form solutions to the above model with $\Gamma^a = [T^3/6 \;\; T^2/2 \;\; T]$. Note that this is the time integral of the input matrix suggested by equation 5.2-35 . The infinite process noise analysis leads to differing gain values which will not lead to a pure time delay transfer function. Therefore, the selection of Γ^a will affect the overall TFM found in equation 5.2-13.

5.4 Summary

This chapter details an improved methodology for continuous and discrete observer design for systems with unknown exogenous inputs. The methodology requires that the state vector be augmented with the unknown inputs. When the input

dynamics are appropriately modeled, and the augmented filter is implemented as a Kalman filter with infinite process noise levels (i.e. A Fisher filter), then the resulting input estimates to true input transfer functions are demonstrated to be unity in the continuous case, and unity with a sampling period delay in the discrete case. Previously, observer design was based on the rule of thumb of selecting the gains to ensure that the observer dynamics were "faster" than the system dynamics. This chapter presents a systematic method for selecting the gains when unknown exogenous inputs exist. The drawback to this method is the high observer bandwidth that results when a Fisher filter is implemented. Under these conditions, extensive noise corruption of the input estimates can occur. Therefore, the designer must make an appropriate tradeoff between observer response time and the degree of permissible noise degradation.

The methodology is presented in a generalized format. The analytical demonstrations of the method is shown using typical tracking filter implementation for systems with unknown inputs.

CHAPTER 6
TRACKING FILTER ERROR COVARIANCE ANALYSIS

6.1 Introduction

The nonlinear models developed in Chapter 3 requires tuning the process noise to account for unknown inputs and structural dissimilarities between the various order trackers. This chapter investigates an error covariance analysis tool for variable order trackers. The approach takes advantage of the generalized upper triangular structure of many tracking models. This leads to a single equation that describes the difference in the error covariance histories for higher order trackers versus a reduced order tracker. This in turn, leads to method for selecting process noise levels to achieve "error covariance equivalent tracking filters". The selection of the process noise accounts for the structural differences between trackers. Both continuous and discrete error covariance analysis techniques are developed. The techniques are then applied to the analytical closed form solutions found by previous researchers. The validity of the results is confirmed with these closed form solutions.

6.2 Continuous Error Covariance Analysis

To generalize the approach taken herein, we will work with the same general model structure, and examine two models referred to as a higher order model (HOM), and a reduced order model (ROM). As examples of a higher order model and a reduced order model, the $\alpha-\beta-\gamma$ tracking filter corresponds to the HOM, and the $\alpha-\beta$ tracking filter qualifies as the ROM.

HIGHER ORDER MODEL (HOM)

$$\begin{bmatrix}\dot{x}_1\\ \dot{x}_2\end{bmatrix} = \begin{bmatrix}F_{11} & F_{12}\\ 0 & F_{22}\end{bmatrix}\begin{bmatrix}x_1\\ x_2\end{bmatrix} + \begin{bmatrix}w_1\\ w_2\end{bmatrix} \; ; \; \begin{bmatrix}w_1\\ w_2\end{bmatrix} \; \tilde{} N\left(\begin{bmatrix}0\\ 0\end{bmatrix} \; , \; \begin{bmatrix}Q_{11} & Q_{21}\\ Q_{21} & Q_{22}\end{bmatrix}\right) \tag{6.2-1a}$$

$$z = \begin{bmatrix}H_1 & H_2\end{bmatrix}\begin{bmatrix}x_1\\ x_2\end{bmatrix} + v \quad ; \; v \; \tilde{} N(0,r) \tag{6.2-1b}$$

REDUCED ORDER MODEL (ROM)

$$\dot{\bar{x}}_1 = F_{11}\bar{x}_1 + \bar{w} \quad ; \; \bar{w} \; \tilde{} N(0,\bar{Q}) \tag{6.2-2a}$$

$$z = H_1\bar{x}_1 + v \quad ; \; v \; \tilde{} N(0,r) \tag{6.2-2b}$$

where w_1, w_2 and v are white noise Gaussian noise inputs with the notation representing [Gelb; 1974]

$$E\{v(t)\} = 0$$

$$E\{v(t)v(\tau)^T\} = R\,\delta(t-\tau)$$

where $\delta(t-\tau)$ is the Dirac delta function.

The partitioning of the HOM is done to emphasize that the HOM states consist of those states which are identical to the states of the ROM (i.e. x_1), and those states which are in addition to the states of the ROM (i.e. x_2). States denoted with a bar (i.e. $\bar{x}_1$) are generated by the ROM as shown, while those without the bar are generated by the HOM. It is important to note that both models use the same measurement sequences, but can use different input noise sequences, denoted by w_1 and w_2 for thc HOM, and by $\bar{w}$ for the ROM.

The tracking filters for these models are standard Kalman filters based on the appropriate motion model that is selected and are given as follows.

HOM TRACKING FILTER

$$\begin{bmatrix} \dot{\hat{x}}_1 \\ \dot{\hat{x}}_2 \end{bmatrix} = \begin{bmatrix} F_{11} & F_{12} \\ 0 & F_{22} \end{bmatrix} \begin{bmatrix} \hat{x}_1 \\ \hat{x}_2 \end{bmatrix} + \begin{bmatrix} K_1 \\ K_2 \end{bmatrix} \left(z - \begin{bmatrix} H_1 & H_2 \end{bmatrix} \begin{bmatrix} \hat{x}_1 \\ \hat{x}_2 \end{bmatrix} \right) \tag{6.2-3a}$$

$$\begin{bmatrix} K_1 \\ K_2 \end{bmatrix} = \begin{bmatrix} P_{11} & P_{12} \\ P_{12}^T & P_{22} \end{bmatrix} \begin{bmatrix} H_1^T \\ H_2^T \end{bmatrix} R^{-1} \tag{6.2-3b}$$

$$\begin{bmatrix} \dot{P}_{11} & \dot{P}_{12} \\ \dot{P}_{12}^T & \dot{P}_{22} \end{bmatrix} = \begin{bmatrix} F_{11} & F_{12} \\ 0 & F_{22} \end{bmatrix} \begin{bmatrix} P_{11} & P_{12} \\ P_{12}^T & P_{22} \end{bmatrix} + \begin{bmatrix} P_{11} & P_{12} \\ P_{12}^T & P_{22} \end{bmatrix} \begin{bmatrix} F_{11}^T & 0 \\ F_{12}^T & F_{22}^T \end{bmatrix} + \begin{bmatrix} Q_{11} & Q_{12} \\ Q_{21} & Q_{22} \end{bmatrix} - \begin{bmatrix} P_{11} & P_{12} \\ P_{12}^T & P_{22} \end{bmatrix} \begin{bmatrix} H_1^T \\ H_2^T \end{bmatrix} R^{-1} \begin{bmatrix} H_1 & H_2 \end{bmatrix} \begin{bmatrix} P_{11} & P_{12} \\ P_{12}^T & P_{22} \end{bmatrix} \tag{6.2-3c}$$

ROM TRACKING FILTER

$$\dot{\bar{\hat{x}}}_1 = F_{11}\bar{\hat{x}}_1 + \bar{K}\left\{ z - H_1\bar{\hat{x}}_1 \right\} \tag{6.2-4a}$$

$$\bar{K} = \bar{P}H_1^T R^{-1} \tag{6.2-4b}$$

$$\dot{\bar{P}} = F_{11}\bar{P} + \bar{P}F_{11}^T + \bar{Q} - \bar{P}H_1^T R^{-1} H_1 \bar{P} \tag{6.2-4c}$$

For the above tracking filters the following definitions apply.

K_1 = HOM Kalman gain applied to the states of x_1

K_2 = HOM Kalman gain applied to the states of x_2

$\bar{K}$ = ROM Kalman gain applied to the states of $\bar{x}_1$

$$P(t)_{ij} = E\left\{ [x_i(t) - \hat{x}_i(t)]\,[x_j(t) - \hat{x}_j(t)]^T \right\} \quad i=1,2 \;\; j=1,2$$

$$\bar{P}(t) = E\left\{ [x_1(t) - \hat{\bar{x}}_1(t)]\, [x_1(t) - \hat{\bar{x}}_1(t)]^T \right\}$$

It should be noted that P_{11} and $\bar{P}$ corresponds to the error covariances of the states contained in x_1 given x_2 for the HOM and and the states in x_1 for the ROM. Under certain conditions, (i.e. by the judicious selection of Q_{11} and $\bar{Q}$) the error covariance of the ROM ($\bar{P}$) can be equated to the error covariance of the HOM (P_{11}).

The equating of the error covariances for the HOM and ROM is achieved by analyzing the equations for each. Examining the individual components of the error covariance equations gives

$$\dot{P}_{11} = F_{11}P_{11} + F_{12}P_{12}^T + P_{11}F_{11}^T + P_{12}F_{12}^T + Q_{11} - \mathbf{P}_{11} \tag{6.2-5}$$

$$\dot{P}_{12} = F_{11}P_{12} + F_{12}P_{22} + P_{12}F_{22}^T + Q_{12} - \mathbf{P}_{12} \tag{6.2-6}$$

$$\dot{P}_{12}^T = P_{12}^T F_{11}^T + P_{22}F_{12}^T + F_{22}P_{12}^T + Q_{21} - \mathbf{P}_{21} \tag{6.2-7}$$

$$\dot{P}_{22} = F_{22}P_{22} + P_{22}F_{22}^T + Q_{22} - \mathbf{P}_{22} \tag{6.2-8}$$

$$\dot{\bar{P}} = F_{11}\bar{P} + \bar{P}F_{11}^T + \bar{Q} - \bar{P}H_1^T R^{-1} H_1 \bar{P} \tag{6.2-9}$$

where

$$\mathbf{P}_{11} = P_{11}H_1^T R^{-1} H_1 P_{11} + P_{12}H_2^T R^{-1} H_1 P_{11} + P_{11}H_1^T R^{-1} H_2 P_{12}^T + P_{12}H_2^T R^{-1} H_2 P_{12}^T \tag{6.2-10}$$

$$\mathbf{P}_{12} = P_{11}H_1^T R^{-1} H_1 P_{12} + P_{12}H_2^T R^{-1} H_1 P_{12} + P_{11}H_1^T R^{-1} H_2 P_{22} + P_{12}H_2^T R^{-1} H_2 P_{22} \tag{6.2-11}$$

$$\mathbf{P}_{21} = P_{12}^T H_1^T R^{-1} H_1 P_{11} + P_{22}H_2^T R^{-1} H_1 P_{11} + P_{12}^T H_1^T R^{-1} H_2 P_{12}^T + P_{22}H_2^T R^{-1} H_2 P_{12}^T \tag{6.2-12}$$

$$\mathbf{P}_{22} = P_{12}^T H_1^T R^{-1} H_1 P_{12} + P_{22}H_2^T R^{-1} H_1 P_{12} + P_{12}^T H_1^T R^{-1} H_2 P_{22} + P_{22}H_2^T R^{-1} H_2 P_{22} \tag{6.2-13}$$

To determine the differences between the error covariances of the equivalent HOM and ROM states, we define $\Delta P = P_{11} - \bar{P}$, and carry out this operation on the above equations.

$$\Delta \dot{P} = F_{11}\Delta P + \Delta P F_1^T \tag{6.2-14}$$
$$+\left\{ Q_{11} - \bar{Q} + F_{12}P_{12}^T + P_{12}F_{12}^T - \mathbf{P}_{11} + \bar{P}H_1^T R^{-1} H_1 \bar{P} \right\}$$

The above matrix differential equation describes the error covariance difference for the common states in the HOM and ROM. The solution of this equation yields the time history of this error covariance difference ($\Delta P(t)$).

Obviously $\Delta P(t)$ is dependent upon the term in brackets which may be viewed as a forcing function for the matrix differential equation. Now, if the initial conditions on the common state error covariance are identical (i.e. $\bar{P}(0) = P_{11}(0)$) and the forcing function can be made identically zero, then $\Delta P(t)$ = 0 for all time, which implies $P_{11}(t) = \bar{P}(t)$ for all time. This possibility is now examined for the $\alpha - \beta$ and $\alpha - \beta - \gamma$ tracking filters.

Recall that the $\alpha - \beta$ filter uses the states of position and velocity, while the $\alpha - \beta - \gamma$ filter uses the states of position, velocity, and acceleration. Both tracking filters are supplemented with measurements of position. In equation form these models are given as

$\alpha - \beta$ Tracking Filter

$$\begin{bmatrix} \dot{x}(t) \\ \ddot{x}(t) \end{bmatrix} = \begin{bmatrix} 0 & 1 \\ 0 & 0 \end{bmatrix} \begin{bmatrix} x(t) \\ \dot{x}(t) \end{bmatrix} + \begin{bmatrix} 0 \\ w_v \end{bmatrix} \quad ; \; w_v \sim N(0, q_v) \tag{6.2-15a}$$

$$z = \begin{bmatrix} 1 & 0 \end{bmatrix} \begin{bmatrix} x(t) \\ \dot{x}(t) \end{bmatrix} + v_v \quad ; \; v_v \sim N(0, r) \tag{6.2-15b}$$

where w_v and v_v are zero-mean uncorrelated Gaussian noise sources with noise intensity of q_v and r, respectively.

$\alpha - \beta - \gamma$ Tracking Filter

$$\begin{bmatrix} \dot{x}(t) \\ \ddot{x}(t) \\ \dddot{x}(t) \end{bmatrix} = \begin{bmatrix} 0 & 1 & 0 \\ 0 & 0 & 1 \\ 0 & 0 & 0 \end{bmatrix} \begin{bmatrix} x(t) \\ \dot{x}(t) \\ \ddot{x}(t) \end{bmatrix} + \begin{bmatrix} 0 \\ 0 \\ w_a \end{bmatrix} \quad ; \; w_a \tilde{} N(0,q_a) \tag{6.2-16a}$$

$$z = \begin{bmatrix} 1 & 0 & 0 \end{bmatrix} \begin{bmatrix} x(t) \\ \dot{x}(t) \\ \ddot{x}(t) \end{bmatrix} + v_a \quad ; \; v_a \tilde{} N(0,r) \tag{6.2-16b}$$

where w_a and v_a are zero-mean uncorrelated gaussian noise sources of intensity q_a and r respectively.

For these $\alpha - \beta$ and $\alpha - \beta - \gamma$ class of tracking filters we have the following matrices.

$$F_{11} = \begin{bmatrix} 0 & 1 \\ 0 & 0 \end{bmatrix} \quad F_{12} = \begin{bmatrix} 0 \\ 1 \end{bmatrix} \quad F_{22} = 0$$

$$H_1 = \begin{bmatrix} 1 & 0 \end{bmatrix} \quad H_2 = 0$$

$$Q_{11} = \begin{bmatrix} 0 & 0 \\ 0 & 0 \end{bmatrix} \quad Q_{12} = \begin{bmatrix} 0 & 0 \end{bmatrix} \quad Q_{22} = q$$

$$R = r$$

(Note : lower case variables denote scalars)

Substituting these values into the appropriate equations gives the following relationships.

$$\dot{\Delta P} = F_{11}\Delta P + \Delta P F_{11}^T + Q_{11} - \bar{Q} \tag{6.2-17}$$

$$+ F_{12}P_{12}^T + P_{12}F_{12}^T - P_{11}H_1^T R^{-1} H_1 P_{11} + \bar{P}H_1^T R^{-1} H_1 \bar{P}$$

Substituting $\bar{P} = P_{11} - \Delta P$ into the above gives

$$\Delta\dot{P} = (F_{11} - P_{11}H_1^T R^{-1}H_1)\Delta P + \Delta P(F_1^T - H_1^T R^{-1}H_1 P_{11}) \qquad (6.2\text{-}18)$$

$$+ \Delta P H_1^T R^{-1}H_1 \Delta P$$

$$+ \left\{ Q_{11} - \bar{Q} + F_{12}P_2^T + P_{12}F_2^T \right\}$$

Again, we note that if $\Delta P(0) = 0$, and the term in brackets can be driven to zero, then the error covariance $\Delta P(t) = 0$ for all time. This requires

$$\bar{Q} = Q_{11} + F_{12}P_2^T + P_{12}F_2^T \qquad (6.2\text{-}19)$$

To verify the results of this equation, we use the results found in Fitzgerald [1981]. For the $\alpha - \beta - \gamma$ tracking filter, Fitzgerald found the following steady state error covariances.

$$P_{11} = \begin{bmatrix} 2(qr^5)^{1/6} & 2(qr^2)^{1/3} \\ 2(qr^2)^{1/3} & 3(qr)^{1/2} \end{bmatrix} \quad P_{12} = \begin{bmatrix} (qr)^{1/2} \\ 2(q^2r)^{1/3} \end{bmatrix}$$

Solving for $\bar{Q}$ gives

$$\bar{Q} = \begin{bmatrix} \bar{q}_{11} & \bar{q}_{12} \\ \bar{q}_{21} & \bar{q}_{22} \end{bmatrix} = \begin{bmatrix} 0 & 0 \\ 0 & 0 \end{bmatrix} + \begin{bmatrix} 0 \\ 1 \end{bmatrix} \begin{bmatrix} (qr)^{1/2} & 2(q^2r)^{1/3} \end{bmatrix}$$

$$+ \begin{bmatrix} (qr)^{1/2} \\ 2(q^2r)^{1/3} \end{bmatrix} \begin{bmatrix} 0 & 1 \end{bmatrix}$$

The resulting elements of $\bar{Q}$ are

$$\bar{q}_{11} = 0$$

$$\bar{q}_{12} = (qr)^{1/2}$$

$$\bar{q}_{22} = 4(q^2 r)^{1/3}$$

Substituting this process noise intensity matrix into the matrix differential equation for $\bar{P}$ yields the identical steady state solution to P_{11}, again confirming the results. A similar analysis for an $\alpha - \beta$, and an α tracking filter can also be performed.

Examination of the above results reveals a $\bar{Q}$ that is not a positive semi-definite matrix, but is in fact indefinite. The indefiniteness is due to the cross correlation terms that are introduced. The choice of this $\bar{Q}$ still leads to achieving a positive definite error covariance for the ROM. Kailath and Ljung [1976] demonstrate that the asymptotic behavior of the general constant coefficient matrix Ricatti differential equation does not necessitate a positive semi-definite Q for convergence of the Ricatti equation to converge to a positive definite solution. Although exact error covariance equivalence will not occur if the cross covariance terms are set to zero, in many cases good results will be achieved.

It is also noted that since the steady state error covariance values are equivalent, an examination of the Kalman gain equations shows that the corresponding steady state Kalman gains are equal. Tracking filters with equivalent steady state Kalman gains for position and velocity states are evaluated in the frequency domain by Andrisani [1985].

6.3 Discrete Error Covariance Analysis

As with the continuous error covariance analysis, a generalized approach is taken, in order to take advantage of the upper triangular structure of the discrete dynamic models associated with tracking filters. The generalized results are then verified analytically using steady state closed form solutions for tracking filters. The results are also verified numerically and graphically using higher order tracking filters.

The development of the discrete error covariance analysis is more difficult and complex due to the two part (predicted/filtered) estimates associated with discrete Kalman filters. For the discrete error covariance analysis, only the equations for the gains and the error covariances need be considered. In order to facilitate the analysis, it is convenient to develop the error covariance in terms of a matrix Ricatti difference equation that is solely a function of the predicted error covariances.

The Kalman filter equations for the error covariances and gains are

Predicted Equations

$$M(k+1) = \Phi P(k)\Phi^T + \Gamma Q \Gamma^T \tag{6.3-1}$$

Filtered Equations

$$K(k+1) = M(k+1)H^T[HM(k+1)H^T + R] \tag{6.3-2}$$

$$P(k+1) = [I - K(k+1)H]M(k+1) \tag{6.3-3}$$

where

M(k+1) = predicted state error covariance at time k+1 given measurements to time k.

P(k+1) = filtered state error covariance at time k+1 given measurements to time k+1.

K(k+1) = filter gain at time k+1

Substituting a delayed filtered state error covariance equation into the predicted state error covariance equation results in a discrete time matrix Ricatti equation for the predicted state error covariance.

$$M(k+1) = \Phi M(k)\Phi^T - \Phi M(k)H^T[HM(k)H^T + R]^{-1}HM(k)\Phi^T + \Gamma Q \Gamma^T \tag{6.3-4}$$

To exploit the structural nature of the previously described tracking filters, it is noted that all models used here result in an upper triangular matrices to describe vehicular motion.

Generalizing the approach taken herein , we will work with the same general model structure and examine two models referred to as a higher order model (HOM), and a reduced order model (ROM). The models have the following general structure

Higher Order Model (HOM)

$$x(k+1) = \Phi x(k) + \Gamma w(k) \quad w(k) \sim N(0, Q(k)) \tag{6.3-5a}$$

$$z(k) = Hx(k) + v(k) \quad v(k) \sim N(0, R) \tag{6.3-5b}$$

where the matrices Φ, Γ, H, and R are time invariant. The system is partitioned in the following manner

$$x(k) = \begin{bmatrix} x_1(k) \\ x_2(k) \end{bmatrix} \qquad \Phi = \begin{bmatrix} \Phi_{11} & \Phi_{12} \\ 0 & \Phi_{22} \end{bmatrix}$$

$$\Gamma = \begin{bmatrix} \Gamma_1 \\ \Gamma_2 \end{bmatrix} \qquad H = \begin{bmatrix} H_1 & 0 \end{bmatrix}$$

Reduced Order Model (ROM)

$$\bar{x}_1(k+1) = \Phi_{11}\bar{x}_1(k) + \bar{\Gamma}\bar{w}(k) \quad \bar{w}(k) \sim N(0, \bar{Q}(k)) \tag{6.3-6a}$$

$$z(k) = H_1\bar{x}_1(k) + v(k) \quad v(k) \sim N(0, R) \tag{6.3-6b}$$

The partitioning of the HOM is done to emphasize that the HOM states consist of those states which are identical to the states of the ROM (i.e. x_1), and those states which are in addition to the ROM (i.e. x_2). States denoted by the over-bar (i.e. $\bar{x}_1$) are generated by the ROM as shown, while those without the over-bar are generated by the HOM. It is important to note that both models use the same measurement sequence, but can use different process noise sequences denoted by w(k) for the HOM and $\bar{w}(k)$ for the ROM.

Using the HOM and the ROM in the Kalman filter results in the equations detailed in Tables 6-1 and 6-2.

Table 6-1 HOM Tracking Filter

Predicted Equations

$$\begin{bmatrix} M_{11}(k+1) & M_{12}(k+1) \\ M_{12}^T(k+1) & M_{22}(k+1) \end{bmatrix} = \begin{bmatrix} \Phi_{11} & \Phi_{12} \\ 0 & \Phi_{22} \end{bmatrix} \begin{bmatrix} M_{11}(k) & M_{12}(k) \\ M_{12}^T(k) & M_{22}(k) \end{bmatrix} \begin{bmatrix} \Phi_{11}^T & 0 \\ \Phi_{12}^T & \Phi_{22}^T \end{bmatrix} + \begin{bmatrix} \Gamma_1 \\ \Gamma_2 \end{bmatrix} Q \begin{bmatrix} \Gamma_1^T & \Gamma_2^T \end{bmatrix} -$$

$$\begin{bmatrix} \Phi_{11} & \Phi_{12} \\ 0 & \Phi_{22} \end{bmatrix} \begin{bmatrix} M_{11}(k) & M_{12}(k) \\ M_{12}^T(k) & M_{22}(k) \end{bmatrix} \begin{bmatrix} H_1^T \\ 0 \end{bmatrix} \mathbf{M} \begin{bmatrix} H_1 & 0 \end{bmatrix} \begin{bmatrix} M_{11}(k) & M_{12}(k) \\ M_{12}^T(k) & M_{22}(k) \end{bmatrix} \begin{bmatrix} \Phi_{11}^T & 0 \\ \Phi_{12}^T & \Phi_{22}^T \end{bmatrix}$$

$$\mathbf{M} = \left[\begin{bmatrix} H_1 & 0 \end{bmatrix} \begin{bmatrix} M_{11}(k) & M_{12}(k) \\ M_{12}^T(k) & M_{22}(k) \end{bmatrix} \begin{bmatrix} H_1^T \\ 0 \end{bmatrix} + R \right]^{-1}$$

$$= \left[H_1 M_{11}(k) H_1^T + R \right]^{-1}$$

Filtered Equations

$$\begin{bmatrix} K_1(k+1) \\ K_2(k+1) \end{bmatrix} = \begin{bmatrix} M_{11}(k+1) & M_{12}(k+1) \\ M_{12}^T(k+1) & M_{22}(k+1) \end{bmatrix} \begin{bmatrix} H_1^T \\ 0 \end{bmatrix} \left[H_1 M_{11}(k) H_1^T + R \right]^{-1}$$

$$\begin{bmatrix} P_{11}(k+1) & P_{12}(k+1) \\ P_{12}^T(k+1) & P_{22}(k+1) \end{bmatrix} = \left[\begin{bmatrix} I & 0 \\ 0 & I \end{bmatrix} - \begin{bmatrix} K_1(k+1) \\ K_2(k+1) \end{bmatrix} \begin{bmatrix} H_1 & 0 \end{bmatrix} \right] \begin{bmatrix} M_{11}(k+1) & M_{12}(k+1) \\ M_{12}^T(k+1) & M_{22}(k+1) \end{bmatrix}$$

where

K_1 = HOM Kalman gain applied to the states of x_1

K_2 = HOM Kalman gain applied to the states of x_2

Table 6-2 ROM Tracking Filter

Predicted Equations

$$\bar{M}(k+1) = \Phi_{11}\bar{M}(k)\Phi_{11}^T - \Phi_{11}\bar{M}(k)H_1^T\,\overline{\mathbf{M}}H\bar{M}(k)\Phi_{11}^T + \bar{\Gamma}\bar{Q}\bar{\Gamma}^T$$

$$\overline{\mathbf{M}} = [H_1\bar{M}(k)H_1^T + R]^{-1}$$

Filtered Equations

$$\bar{K}(k+1) = \bar{M}(k+1)H_1^T[H_1\bar{M}(k+1)H_1^T + R]^{-1}$$

$$\bar{P}(k+1) = [I - \bar{K}(k+1)H_1]\bar{M}(k+1)$$

where

$\bar{K}$ = ROM Kalman gain applied to the states of $\bar{x}_1$

Carrying out the matrix operations in Tables 6-1 and 6-2 for the predicted error covariances gives

$$\begin{aligned} M_{11}(k+1) &= \Phi_{11}M_{11}(k)\Phi_{11}^T + \Phi_{12}M_{12}^T(k)\Phi_{11}^T \\ &\quad + \Phi_{11}M_{12}(k)\Phi_{12}^T + \Phi_{12}M_{22}(k)\Phi_{12}^T \\ &\quad - \Phi_{11}M_{11}(k)H_1^T\mathbf{M}H_1M_{11}(k)\Phi_{11}^T \\ &\quad - \Phi_{11}M_{11}(k)H_1^T\mathbf{M}H_1M_{12}(k)\Phi_{12}^T \\ &\quad - \Phi_{12}M_{12}^T(k)H_1^T\mathbf{M}H_1M_{11}(k)\Phi_{11}^T \\ &\quad - \Phi_{12}M_{12}^T(k)H_1^T\mathbf{M}H_1M_{12}(k)\Phi_{12}^T \\ &\quad + \Gamma_1Q(k)\Gamma_1^T \end{aligned} \tag{6.3-7}$$

$$\begin{aligned} M_{12}(k) &= \Phi_{11}M_{12}(k)\Phi_{22}^T + \Phi_{12}M_{22}(k)\Phi_{22}^T \\ &\quad - [\Phi_{11}M_{11}(k) + \Phi_{12}M_{12}^T(k)]H_1^T\mathbf{M}H_1M_{12}(k)\Phi_{22}^T \\ &\quad + \Gamma_1Q(k)\Gamma_2^T \end{aligned} \tag{6.3-8}$$

$$\begin{aligned} M_{22}(k) &= \Phi_{22}M_{22}(k)\Phi_{22}^T \\ &\quad + \Phi_{22}M_{12}^T(k)H_1^T\mathbf{M}H_1M_{12}(k)\Phi_{22}^T \\ &\quad + \Gamma_2Q(k)\Gamma_2^T \end{aligned} \tag{6.3-9}$$

$$\bar{M}(k+1) = \Phi_{11}\bar{M}(k)\Phi_{11}^T - \Phi_{11}\bar{M}(k)H_1^T\bar{\mathbf{M}}H_1\bar{M}(k)\Phi_{11}^T + \bar{\Gamma}\bar{Q}(k)\bar{\Gamma}^T \tag{6.3-10}$$

To determine the difference between the error covariances of equivalent HOM and ROM states, we define $\Delta M = M_{11} - \bar{M}$ and carry out this operation on the above equations.

$$\begin{aligned}\Delta M(k+1) &= \Phi_{11}\Delta M(k)\Phi_{f1}^T + \Phi_{12}M_{f2}^T(k)\Phi_{f1}^T \\ &+ \Phi_{11}M_{12}(k)\Phi_{f2}^T + \Phi_{12}M_{22}(k)\Phi_{f2}^T \\ &- \Phi_{11}M_{11}(k)H_f^T\mathbf{M}H_1M_{11}(k)\Phi_{f1}^T \\ &+ \Phi_{11}\overline{M}(k)H_f^T\overline{\mathbf{M}}H_1\overline{M}(k)\Phi_{f1}^T \\ &- \Phi_{11}M_{11}(k)H_f^T\mathbf{M}H_1M_{12}(k)\Phi_{f2}^T \\ &- \Phi_{12}M_{f2}^T(k)H_f^T\mathbf{M}H_1M_{11}(k)\Phi_{f1}^T \\ &- \Phi_{12}M_{f2}^T(k)H_f^T\mathbf{M}H_1M_{12}(k)\Phi_{f2}^T \\ &+ \Gamma_1Q(k)\Gamma_f^T - \overline{\Gamma}\overline{Q}(k)\overline{\Gamma}^T \end{aligned} \tag{6.3-11}$$

Substituting $\overline{M}(k) = M_{11}(k) - \Delta M(k)$ in the fourth line of equation 6.3-11 results in

$$\begin{aligned}\Delta M(k+1) &= \Phi_{11}\Delta M(k)\Phi_{f1}^T + \Phi_{12}M_{f2}^T(k)\Phi_{f1}^T \\ &+ \Phi_{11}M_{12}(k)\Phi_{f2}^T + \Phi_{12}M_{22}(k)\Phi_{f2}^T \\ &- \Phi_{11}M_{11}(k)H_f^T[\mathbf{M} - \overline{\mathbf{M}}]H_1M_{11}(k)\Phi_{f1}^T \\ &- \Phi_{11}M_{11}(k)H_f^T\overline{\mathbf{M}}H_1\Delta M(k)\Phi_{f1}^T \\ &- \Phi_{11}\Delta M(k)H_f^T\overline{\mathbf{M}}H_1M_{11}(k)\Phi_{f1}^T \\ &+ \Phi_{11}\Delta M(k)H_f^T\overline{\mathbf{M}}H_1\Delta M(k)\Phi_{f1}^T \\ &- \Phi_{11}M_{11}(k)H_f^T\mathbf{M}H_1M_{12}(k)\Phi_{f2}^T \\ &- \Phi_{12}M_{f2}^T(k)H_f^T\mathbf{M}H_1M_{11}(k)\Phi_{f1}^T \\ &- \Phi_{12}M_{f2}^T(k)H_f^T\mathbf{M}H_1M_{12}(k)\Phi_{f2}^T \\ &+ \Gamma_1Q(k)\Gamma_f^T - \overline{\Gamma}\overline{Q}(k)\overline{\Gamma}^T \end{aligned} \tag{6.3-12}$$

By noting that

$$\mathbf{M}(k) - \overline{\mathbf{M}}(k) = [H_1M_{11}(k)H_f^T + R]^{-1} - [H_1\overline{M}(k)H_f^T + R]^{-1} \tag{6.3-13}$$

and performing pre and post multiplication by $[H_1\overline{M}(k)H_f^T + R]$ and $[H_1M_{11}(k)H_f^T + R]$ respectively gives

$$[H_1\bar{M}(k)H_1^T + R]\,[\mathbf{M}(k) - \bar{\mathbf{M}}(k)]\,[H_1 M_{11}(k)H_1^T + R]$$
$$= [H_1\bar{M}(k)H_1^T + R - H_1 M_{11}(k)H_1^T - R]$$
$$= H_1[\bar{M}(k) - M_{11}(k)]H_1^T = -H_1[\Delta M(k)]H_1^T \qquad (6.3\text{-}14)$$

Reversing the procedure by pre and post multiplying by $[H_1\bar{M}(k)H_1^T + R]^{-1}$ and $[H_1 M_{11}(k)H_1^T + R]^{-1}$ respectively gives

$$\mathbf{M} - \bar{\mathbf{M}} = -\bar{\mathbf{M}}H_1\Delta M(k)H_1^T\mathbf{M} \qquad (6.3\text{-}15)$$

Substituting this relationship into the previous equation for $\Delta M(k+1)$ and combining terms yields

$$\begin{aligned}\Delta M(k+1) = \Phi_{11}[&\Delta M(k)\\ &+ M_{11}(k)H_1^T\bar{\mathbf{M}}H_1\Delta M(k)H_1^T\mathbf{M}H_1M_{11}(k)\\ &- M_{11}(k)H_1^T\bar{\mathbf{M}}H_1\Delta M(k)\\ &- \Delta M(k)H_1^T\bar{\mathbf{M}}H_1M_{11}(k)\\ &+ \Delta M(k)H_1^T\bar{\mathbf{M}}H_1\Delta M(k)]\Phi_{11}^T\\ &+ \Phi_{12}[M_{12}^T(k) - M_{12}^T(k)H_1^T\mathbf{M}H_1M_{11}(k)]\Phi_{11}^T\\ &+ \Phi_{11}[M_{12}(k) - M_{11}(k)H_1^T\mathbf{M}H_1M_{12}(k)]\Phi_{12}^T\\ &+ \Phi_{12}[M_{22}(k) - M_{12}^T(k)H_1^T\mathbf{M}H_1M_{12}(k)]\Phi_{12}^T\\ &+ \Gamma_1 Q(k)\Gamma_1^T - \bar{\Gamma}\bar{Q}(k)\bar{\Gamma}^T \qquad (6.3\text{-}16)\end{aligned}$$

The above matrix difference equation describes the error covariance difference for the common states in the HOM and the ROM. The solution of this equation yields the time history of ΔM.

Obviously $\Delta M(k+1)$ is a function of $\Delta M(k)$, and the remaining terms not containing a $\Delta M(k)$ may be viewed as the forcing function for the matrix difference equation. Now if the initial conditions on the common state error covariances are identical (i.e. $\bar{M}(0) = M_{11}(0)$) and the forcing function can be made identically zero, then $\Delta M(k) = 0$ for all $k \geq 0$ which implies $M_{11}(k) = \bar{M}(k)$ for all $k \geq 0$, which is the requirement for an error covariance equivalent model. To achieve this, requires that the forcing function be precisely zero or

$$\begin{aligned}\bar{\Gamma}\bar{Q}(k)\bar{\Gamma}^T &= \Phi_{12}[M^T_{12}(k) - M^T_{12}(k)H^T_1\mathbf{M}H_1M_{11}(k)]\Phi^T_{11} \\ &+ \Phi_{11}[M_{12}(k) - M_{11}(k)H^T_1\mathbf{M}H_1M_{12}(k)]\Phi^T_{12} \\ &+ \Phi_{12}[M_{22}(k) - M^T_{12}(k)H^T_1\mathbf{M}H_1M_{12}(k)]\Phi^T_{12} \\ &+ \Gamma_1Q(k)\Gamma^T_1 \end{aligned} \tag{6.3-17}$$

The above equation can be solved for $\bar{\Gamma}\bar{Q}(k)\bar{\Gamma}^T$ in order to force ΔM (k) = 0 for all k ≥ 0. This solution is a function of the predicted state error covariances. Simplification is achieved by substituting the filtered state error covariances for the predicted state error covariances.

Recall

$$P(k) = M(k) - M(k)H^T[HM(k)H^T + R]^{-1}HM(k) \tag{6.3-18}$$

Carrying out the partitioned matrix multiplication from Table 1 gives

$$P_{11}(k) = M_{11}(k) - M_{11}(k)H^T_1\mathbf{M}(k)H_1M_{11}(k) \tag{6.3-19}$$

$$P_{12}(k) = M_{12}(k) - M_{11}(k)H^T_1\mathbf{M}(k)H_1M_{12}(k) \tag{6.3-20}$$

$$P^T_{12}(k) = M^T_{12}(k) - M^T_{12}(k)H^T_1\mathbf{M}(k)H_1M_{11}(k) \tag{6.3-22}$$

$$P_{22}(k) = M_{22}(k) - M^T_{12}(k)H^T_1\mathbf{M}(k)H_1M_{12}(k) \tag{6.3-22}$$

Substituting these relationships into the forcing function based on the predicted state error covariances provides the solution in terms of the filtered state error covariance.

$$\begin{aligned}\bar{\Gamma}\bar{Q}(k)\bar{\Gamma}^T &= \Phi_{12}P^T_{12}(k)\Phi^T_{11} + \Phi_{11}P_{12}(k)\Phi^T_{12} + \\ &\Phi_{12}P_{22}(k)\Phi^T_{12} + \Gamma_1Q(k)\Gamma^T_1 \end{aligned} \tag{6.3-23}$$

In order to verify these results, the discrete error covariance analysis is applied to the previously developed tracking filters. The application of error covariance equivalent model will be demonstrated using the analytical steady state results of Friedland [1973]. An $\alpha - \beta$ filter will be used to obtain a position error covariance α filter.

For an $\alpha - \beta$ filter the following steady state relationships hold

$$\Phi_{11} = 1 \quad \Gamma_1 = \frac{T^2}{2} \quad H_1 = 1$$

$$\Phi_{12} = T \quad \Gamma_2 = T = \bar{\Gamma}$$

$$\Phi_{22} = 1$$

$$Q = \sigma_a^2 \quad \bar{Q} = \bar{\sigma}_a^2$$

$$R = \sigma_x^2$$

$$M = \begin{bmatrix} m_{11} & m_{12} \\ m_{12}^T & m_{22} \end{bmatrix}$$

$$m_{11} = \frac{\sigma_x^2}{r^2}\sqrt{1+2r}\ [\sqrt{1+2r} + 1]^2$$

$$m_{12} = \frac{\sigma_x \sigma_a T}{2r}[\sqrt{1+2r} + 1]^2$$

$$m_{22} = \frac{\sigma_a^2 T^2}{2}[\sqrt{1+2r} + 1]$$

$$P = \begin{bmatrix} p_{11} & p_{12} \\ p_{12}^T & p_{22} \end{bmatrix}$$

$$p_{11} = \frac{\sigma_x^2}{r^2}\sqrt{1+2r}\ [\sqrt{1+2r} + 1]^2$$

$$p_{12} = \frac{\sigma_x \sigma_a T}{2r}[\sqrt{1+2r} + 1]^2$$

$$p_{22} = \frac{\sigma_a^2 T^2}{2}[\sqrt{1+2r} + 1]$$

where

$$r = \frac{4\sigma_x}{T^2 \sigma_a}$$

Substituting these relationships into the equation for determining $\bar{\Gamma}\bar{Q}\bar{\Gamma}^T$ using the filtered error covariances gives

$$T^2\bar{\sigma}_a^2 = \frac{\sigma_x \sigma_a T^2}{r}[\sqrt{1+2r} - 1]^2$$

$$+ \frac{\sigma_a^2 T^4}{2}[\sqrt{1+2r} - 1]$$

$$+ \frac{T^4}{4}\sigma_a^2$$

Solving for $\bar{\sigma}_a^2$ gives

$$\bar{\sigma}_a^2 = \frac{\sigma_x \sigma_a}{r}[1+2r]$$

To verify that this process noise covariance yields identical predicted position error covariance, we examine the steady state scalar Ricatti equation for an α tracker.

$$\bar{m} = \bar{m} - \frac{\bar{m}^2}{\bar{m} + \sigma_x^2} + T^2\bar{\sigma}_a^2$$

Solving for $\bar{m}$ gives

$$\bar{m} = \frac{T^2\bar{\sigma}_a^2}{2} + \frac{1}{2}\sqrt{(T^2\bar{\sigma}_a^2)^2 + 4T^2\bar{\sigma}_a^2\sigma_x^2}$$

Substituting for $\bar{\sigma}_a^2$ and performing the necessary algebraic manipulations results in

$$\bar{m} = 2\frac{\sigma_x^2}{r^2}\sqrt{1+2r}\ [\sqrt{1+2r} + r + 1]$$

Expanding m_{11} will show that $m_{11} = \bar{m}$.

To examine the difference in time responses between the HOM and ROM using a time-invariant process noise, we investigate an $\alpha - \beta - \gamma$ tracking filter and an error covariance equivalent $\alpha - \beta$ tracking filter.

Selecting a process noise covariance of $\sigma_j^2 = 100$ and T = 1/30, the $\alpha - \beta - \gamma$ matrices and steady state filtered error covariance matrices are

$$\Phi_{11} = \begin{bmatrix} 1 & T \\ 0 & 1 \end{bmatrix} \quad \Gamma_1 = \begin{bmatrix} \frac{T^3}{6} \\ \frac{T^2}{2} \end{bmatrix} \quad H_1 = \begin{bmatrix} 1 & 0 \end{bmatrix}$$

$$\Phi_{12} = \begin{bmatrix} \frac{T^2}{2} \\ T \end{bmatrix} \quad \Gamma_2 = T$$

$$\Phi_{22} = 1$$

$$P = \begin{bmatrix} 6.449 & 6.448 & 3.224 \\ 6.448 & 9.781 & 6.557 \\ 3.224 & 6.557 & 6.611 \end{bmatrix}$$

Substituting these values into the equations for $\bar{Q}$ provides

$$\bar{\Gamma}\bar{Q}\bar{\Gamma}^T = \begin{bmatrix} .0038 & .1185 \\ .1185 & .4445 \end{bmatrix}$$

Figures 6-1 through 6-3 depict the filtered error covariance time responses for the HOM $\alpha - \beta - \gamma$ filter and the ROM $\alpha - \beta$ filter. In all three cases the steady state filter error covariance responses converge to identical values, with the $\alpha - \beta$ filter achieving steady state values sooner than the $\alpha - \beta - \gamma$ filter.

6.4 Summary

This chapter outlines a methodology for determining the effects on the error covariance history of variable dimension models. The methodology is accomplished for both continuous and discrete models. The continuous methodology leads to a single differential equation that describes the error covariance difference between the common states of a higher order model (HOM) and a reduced order model (ROM). The discrete methodology leads to a single difference equation that describes the predicted error covariance differences between common states of the HOM and ROM. Analysis of these equations results in a means for selecting the process noise level for a ROM such that an error covariance equivalent model is achieved for both the continuous and discrete time cases.

The continuous/discrete methodology is developed for systems with generalized upper triangular dynamic matrices. The methodology is demonstrated with steady state analytical and numerical examples for common tracking filters.

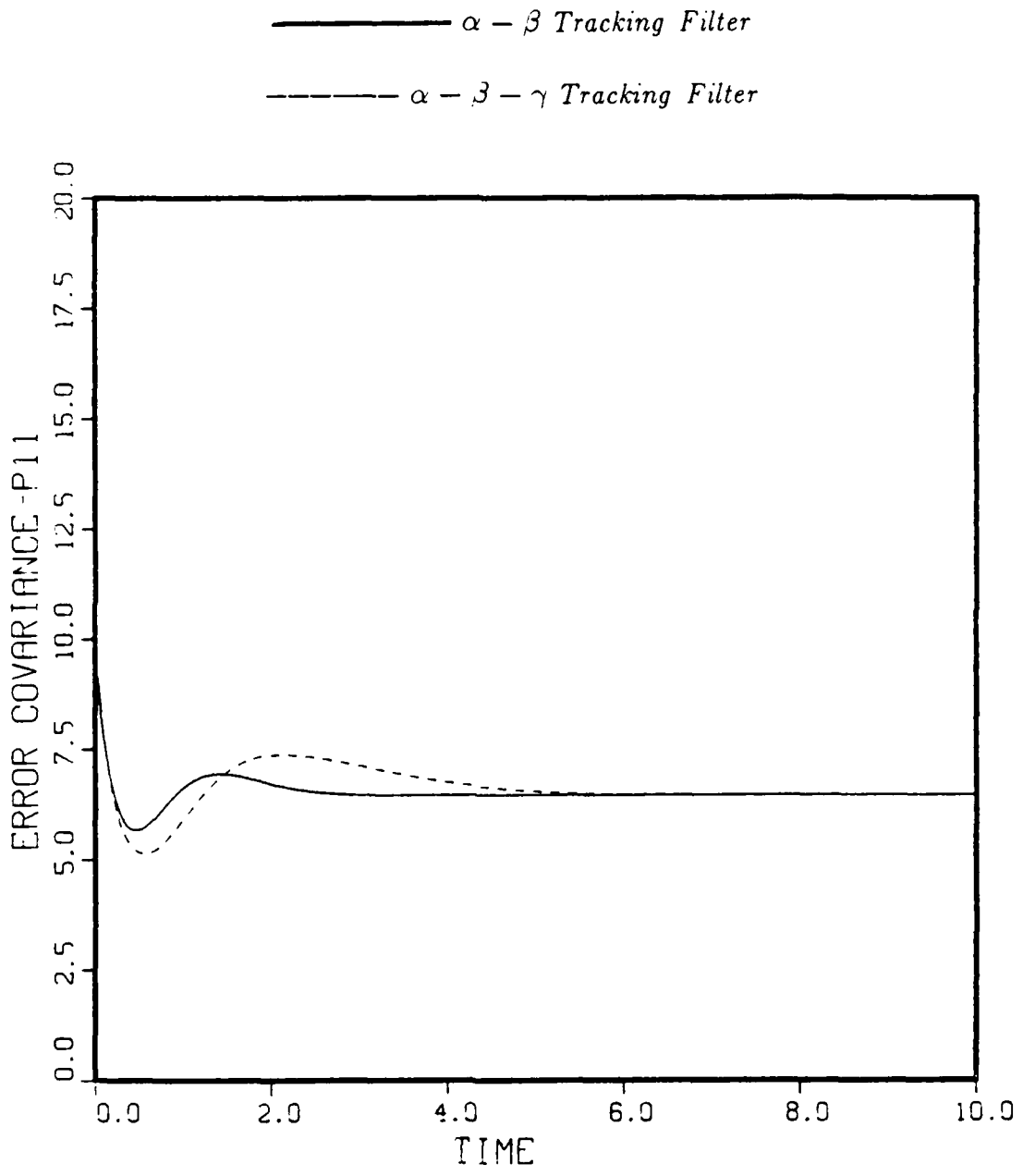

Figure 6-1 P_{11} Time History

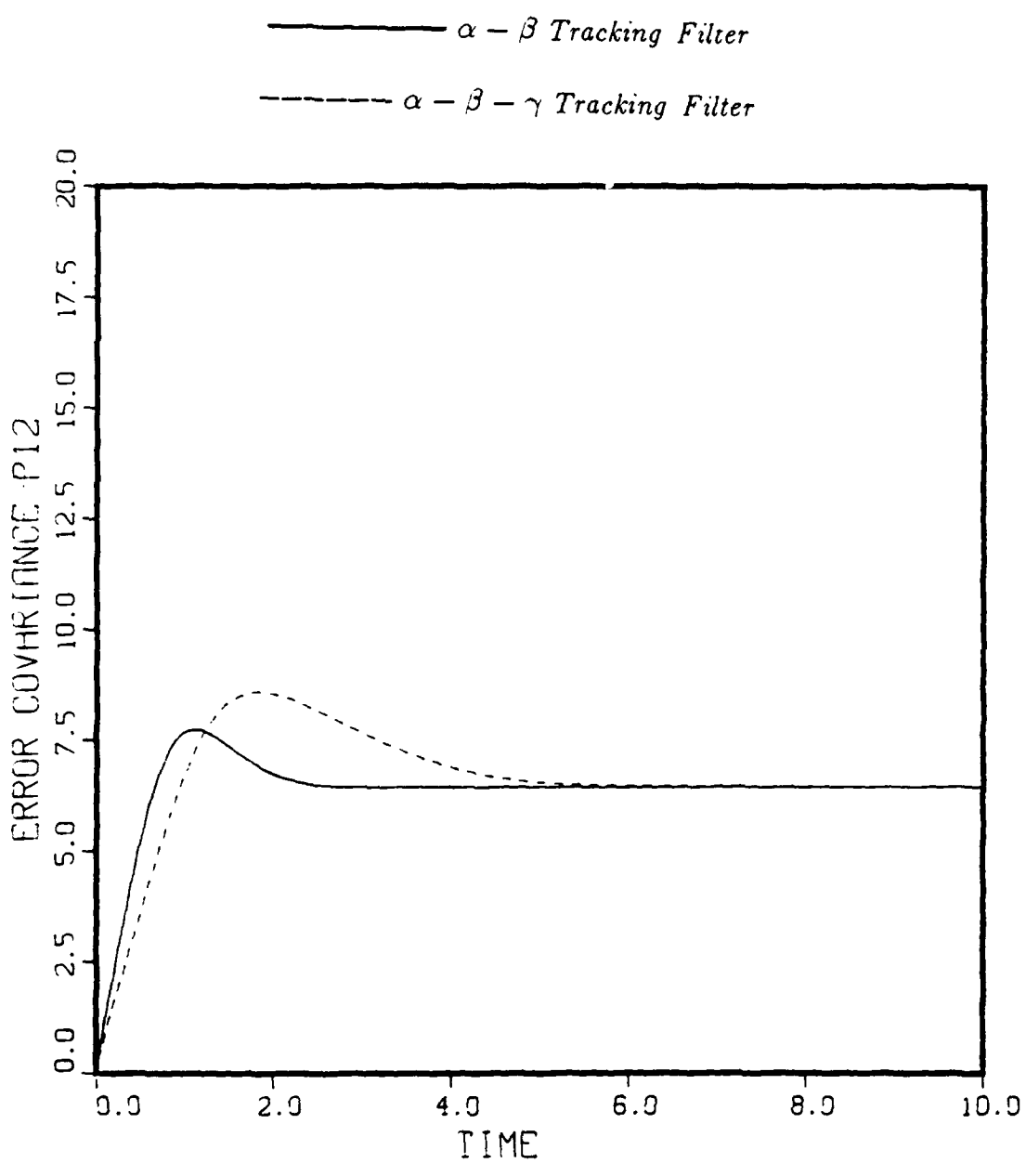

Figure 6-2 P_{12} Time History

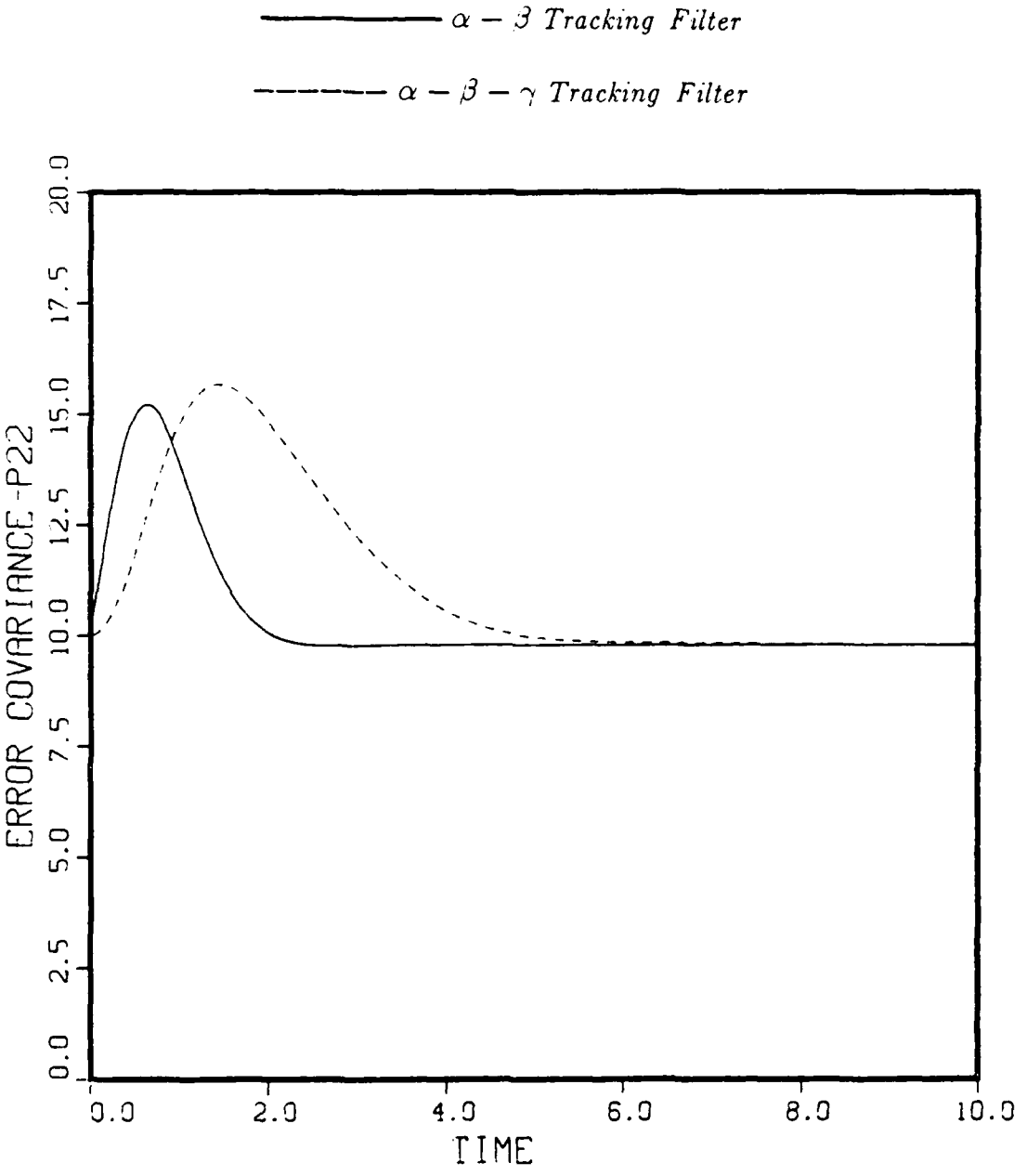

Figure 6-3 P_{22} Time History

CHAPTER 7
CONSTANT GAIN ANALYSIS FOR DISCRETE TRACKING FILTERS

7.1 Introduction

Vehicle tracking is often accomplished with a three state $\alpha - \beta - \gamma$ tracking filter, where the states are position, velocity, and acceleration. Implementing this filter requires the following design parameters:

1. Measurement sampling period (T)
2. Process noise covariance (q)
3. Measurement noise covariance (r)

These design parameters in conjunction with the system dynamics are used solve the associated time-varying tracking filter gain and error covariance equations.

In order to reduce computational burdens, these filters are frequently used with constant gains. The constant gains are obtained by using the steady state results of the tracking filter gain and error covariance equations. However, if the design parameters are changed, the tracking filter gains and error covariance equations must be rerun to find new steady state solutions.

This chapter examines the steady state error covariance equations and determines a closed form solution for the error covariance between the position and acceleration states. This is accomplished by symbolically solving a steady state matrix Ricatti equation and solving for the desired error covariance element. This results in a quartic equation for the error covariance between position and acceleration which is solely dependent on the design parameters (T, q, r). The appropriate solution of this quartic is found using MACSYMA [1985]. MACSYMA is an interactive computer

program written in LISP used to symbolically solve unwieldy mathematical problems. Once the quartic solution is obtained, the remaining elements of the error covariance matrix are easily calculated, and likewise for the filter gains.

The closed form solutions to the gains of the $\alpha - \beta - \gamma$ tracking filter facilitates a limiting analysis. The limiting analysis is useful in the derivation of the Fischer filters that were discussed in previous chapters. The state space representation for the three state $\alpha - \beta - \gamma$ tracking filter is given as

$$x(k+1) = \Phi x(k) + \Gamma w(k) \tag{7.1-1a}$$

$$z(k) = Hx(k) + v(k) \tag{7.1-1b}$$

where x(k) is a vector composed of position, velocity and acceleration; w(k)is a discrete zero-mean white noise sequence with covariance q accounting for modeling uncertainties; z(k) is a position measurement that is corrupted with a discrete zero-mean white noise sequence, v(k) that has covariance of r, and

$$\Phi = \begin{bmatrix} 1 & T & T^2/2 \\ 0 & 1 & T \\ 0 & 0 & 1 \end{bmatrix} \quad \Gamma = \begin{bmatrix} T^3/6 \\ T^2/2 \\ T \end{bmatrix}$$

$$H = \begin{bmatrix} 1 & 0 & 0 \end{bmatrix}$$

The Kalman filter equations for the error covariances and gains are

Predicted Equations

$$M(k+1) = \Phi P(k) \Phi^T + \Gamma q \Gamma^T \tag{7.1-2}$$

Filtered Equations

$$K(k+1) = M(k+1) H^T [HM(k+1) H^T + r] \tag{7.1-3}$$

$$P(k+1) = [I - K(k+1) H] M(k+1) \tag{7.1-4}$$

where

M(k+1) = predicted state error covariance at time k+1 given measurements to time k.

P(k+1) = filtered state error covariance at time k+1 given measurements to time k+1.

K(k+1) = filter gain at time k+1

Substituting a delayed filtered state error covariance equation into the predicted state error covariance equation results in a discrete time matrix Ricatti equation for the filtered state error covariance.

$$M(k+1) = \Phi M(k)\Phi^T - \Phi M(k)H^T[HM(k)H^T + r]^{-1}HM(k)\Phi^T \qquad (7.1\text{-}5)$$
$$+ \Gamma q \Gamma^T$$

7.2 Steady State Gain Determination

Since only steady state values are needed, the increment notation is not needed, and the filtered error covariance equation becomes

$$M = \Phi M \Phi^T - \Phi M H^T[HMH^T + r]^{-1}HM\Phi^T$$
$$+ \Gamma q \Gamma^T$$

with

$$M = \begin{bmatrix} m_{11} & m_{12} & m_{13} \\ m_{21} & m_{22} & m_{23} \\ m_{31} & m_{32} & m_{33} \end{bmatrix}$$

Expanding this equation in terms of its individual elements results in nine nonlinear equation and nine unknowns. However, due to the symmetric nature of the Ricatti equation only six nonlinear equation are need to solve for six unknowns. These equations are presented in Table 7-1.

Table 7-1 Filtered Error Covariance Equations

$$m_{11} = m_{11} + 2Tm_{12} + T^2m_{13} + T^2m_{22} + T^3m_{23} + (T^4/4)m_{33}$$

$$- \frac{m_{11}^2 + 2Tm_{11}m_{12} + T^2m_{12}^2}{m_{11} + r}$$

$$- \frac{T^2m_{11}m_{13} + T^3m_{12}m_{13} + (T^4/4)m_{13}^2}{m_{11} + r}$$

$$+ \frac{qT^6}{36} \qquad (7.2\text{-}1)$$

$$m_{12} = m_{12} + Tm_{13} + Tm_{22} + (3T^2/2)m_{23} + (T^3/2)m_{33}$$

$$- \frac{m_{11}m_{12} + Tm_{11}m_{13} + Tm_{12}^2 + (3T^2/2)m_{12}m_{13} + (T^3/2)m_{13}^2}{m_{11} + r}$$

$$+ \frac{qT^5}{12} \qquad (7.2\text{-}2)$$

$$m_{13} = m_{13} + Tm_{23} + (T^2/2)m_{33}$$

$$- \frac{m_{11}m_{13} + Tm_{12}m_{13} + (T^2/2)m_{13}^2}{m_{11} + r} + \frac{qT^4}{6} \qquad (7.2\text{-}3)$$

$$m_{22} = m_{22} + 2Tm_{23} + T^2m_{33}$$

$$- \frac{m_{12}^2 + 2Tm_{12}m_{13} + T^2m_{13}^2}{m_{11} + r} + \frac{qT^4}{4} \qquad (7.2\text{-}4)$$

$$m_{23} = m_{23} + Tm_{33} - \frac{m_{12}m_{13} + Tm_{13}^2}{m_{11} + r} + \frac{qT^3}{2} \qquad (7.2\text{-}5)$$

$$m_{33} = m_{33} - \frac{m_{13}^2}{m_{11} + r} + qT^2 \qquad (7.2\text{-}6)$$

Obtaining a closed form solution for these equations requires isolating individual error covariances elements. This is achieved by performing cancellations and algebraic manipulation of the equations (7.2-1) through (7.2-6). The isolation of individual elements is best achieved by starting with equation (7.2-6), and performing necessary algebraic manipulations with appropriate cancellations and substitutions. This procedure is repeated with equation (7.2-5), then (7.2-4), etc.. The results of this isolation process is presented in Table 7-2.

Analysis of these six equations and the equations governing the tracker gains reveals that the elements m_{11}, m_{12}, and m_{13} are key elements to solve for. As shown in the Table 7-2, these elements are isolated in equations (7.2-7), (7.2-10), and (7.2-12) which are now repeated.

$$m_{11} = \frac{m_{13}^2}{qT^2} - r \tag{7.2-7}$$

$$m_{11} = \frac{12m_{12}^2 + T^2 m_{13}^2}{24m_{13}} \tag{7.2-10}$$

$$m_{12} = \frac{(m_{11} + (T/2)m_{12})^2}{2T(m_{11} + r)} - \frac{qT^5}{288} \tag{7.2-12}$$

Table 7-2 Modified Filtered Error Covariance Equations

$$m_{11} = \frac{m_{f3}^2}{qT^2} - r \tag{7.2-7}$$

$$m_{33} = qT\frac{m_{12}}{m_{13}} + \frac{qT^2}{2} \tag{7.2-8}$$

$$m_{23} = \frac{qT(m_{f2}^2 + Tm_{12}m_{13} + T^2m_{f3}^2)}{2m_{f3}^2} - \frac{3qT^3}{8} \tag{7.2-9}$$

$$m_{11} = \frac{12m_{f2}^2 + T^2m_{f3}^2}{24m_{13}} \tag{7.2-10}$$

$$\begin{aligned} m_{22} = \frac{qT}{m_{f3}^2}(&m_{11}m_{12} + Tm_{11}m_{13} + Tm_{f2}^2 \\ &+ (3T^2/2)m_{12}m_{13} + (5T^3/12)m_{f3}^2) \\ &- m_{13} - (3T/2)m_{23} - (T^2/2)m_{33} \end{aligned} \tag{7.2-11}$$

$$m_{12} = \frac{(m_{11} + (T/2)m_{12})^2}{2T(m_{11} + r)} - \frac{qT^5}{288} \tag{7.2-12}$$

The three nonlinear equations and three unknowns can be solved for the m_{13} element, resulting in a quartic equation with coefficients that are functions only of the design parameters T, q, and r. The quartic equation governing m_{13} is

$$m_{13}^4 - \left[\sqrt{b^2/9 + 16c} + b\right] m_{13}^3 + \left[b^2/9 + 6c\right] m_{13}^2 + \left[bc - c\sqrt{b^2/9 + 16c}\right] m_{13} + c^2 = 0 \qquad (7.2\text{-}13)$$

where

$$b = qT^4/2$$

$$c = qrT^2$$

Using MACSYMA it is possible to solve this equation for the appropriate root of the above quartic equation. The solution is given by

$$m_{13} = \frac{\sqrt{144c + b^2}+3b}{12} + \frac{\sqrt{6}}{36\sqrt{d}} \qquad (7.2\text{-}14)$$

$$+ \frac{\sqrt{6}}{36\sqrt{d}}\left[36\sqrt{6}(b^3+b^2\sqrt{144c + b^2} + 18bc)d^{3/2} + (27b\sqrt{144c + b^2} + 33b^2)d - 1\right]^{1/2}$$

where

$$z = 1458c^{3/2}\sqrt{729c + 2b^2} + 39366c^2 + 486b^2c + b^4$$

$$y = 2b^{2/3}z^{2/3} + (9b\sqrt{144c + b^2}+11b^2)z^{1/3} + b^{1/3}(648bc + 2b^3)$$

$$d = z^{1/3}/y$$

Once element m_{13} is evaluated, then elements m_{11} and m_{12} are respectively found from equations 7.2-7 and 7.2-10 as

$$m_{11} = \frac{m_{13}^2}{qT^2} - r \qquad (7.2\text{-}7)$$

$$m_{12} = \sqrt{2m_{13}m_{11} - (T^2/12)m_{13}^2} \tag{7.2-15}$$

The remaining elements of the predicted error covariance matrix are found from the equations in Table 7-2.

Once the key predicted error covariance elements m_{11}, m_{12}, and m_{13} are known, the gains for position (α), velocity (β), and acceleration (γ) can be determined. Expanding the elements of the Kalman filter gain equation gives

$$K = \begin{bmatrix} \alpha & \beta & \gamma \end{bmatrix}^T$$

$$\alpha = \frac{m_{11}}{m_{11} + r} \tag{7.2-16}$$

$$\beta = \frac{m_{12}}{m_{11} + r} \tag{7.2-17}$$

$$\gamma = \frac{m_{13}}{m_{11} + r} \tag{7.2-18}$$

Expanding the elements of the Kalman filter filtered error covariance equation results in

$$P = \begin{bmatrix} p_{11} & p_{12} & p_{13} \\ p_{21} & p_{22} & p_{23} \\ p_{31} & p_{32} & p_{33} \end{bmatrix}$$

$$p_{11} = (1 \quad \alpha)m_{11} \tag{7.2-19}$$

$$p_{12} = (1 - \alpha)m_{12} \tag{7.2-20}$$

$$p_{13} = (1 - \alpha)m_{13} \tag{7.2-21}$$

$$p_{22} = -\beta m_{12} + m_{22} \tag{7.2-22}$$

$$p_{23} = -\beta m_{13} + m_{23} \tag{7.2-23}$$

$$p_{33} = -\gamma m_{13} + m_{33} \tag{7.2-24}$$

The above equations are easily calculated in a short program which allows the user to input the design parameters T, q, r, and calculate all error covariances and gains without having to exercise the Kalman filter equations until a steady state value is achieved. In addition, as will be shown later, these equations provide a meaningful way to perform a limiting analysis for the filter gains.

The equations for the predicted error covariance elements m_{11}, m_{12}, and m_{13}, and the filter gains α, β, and γ were evaluated in a simple computational algorithm to evaluate gain behavior graphically. Using the tracking index ($\Lambda^2 = T^4 q / r$) defined by Kalata [1984], plots are obtained for for α, β, and γ versus Λ^2. These plots are presented in Figures 7-1 through 7-3. It should be noted that Kalata used a slightly modified Γ matrix for his $\alpha - \beta - \gamma$ tracker, but the nature of the α versus Λ^2 plots are quite similar. In addition, three dimensional plots are presented that display α, β, and γ gain surfaces as a function of q and r. These results are presented in Figures 7-4 through 7-6 and correspond to T=10.

Examining Figures 7-1 through 7-6 reveals that the gains approach zero in the limit as q approaches zero and r approaches ∞ as expected. In addition, the gains approach limiting values as q approaches ∞ and r approaches zero. These limiting values will now be examined with the aid of the closed form solution equations.

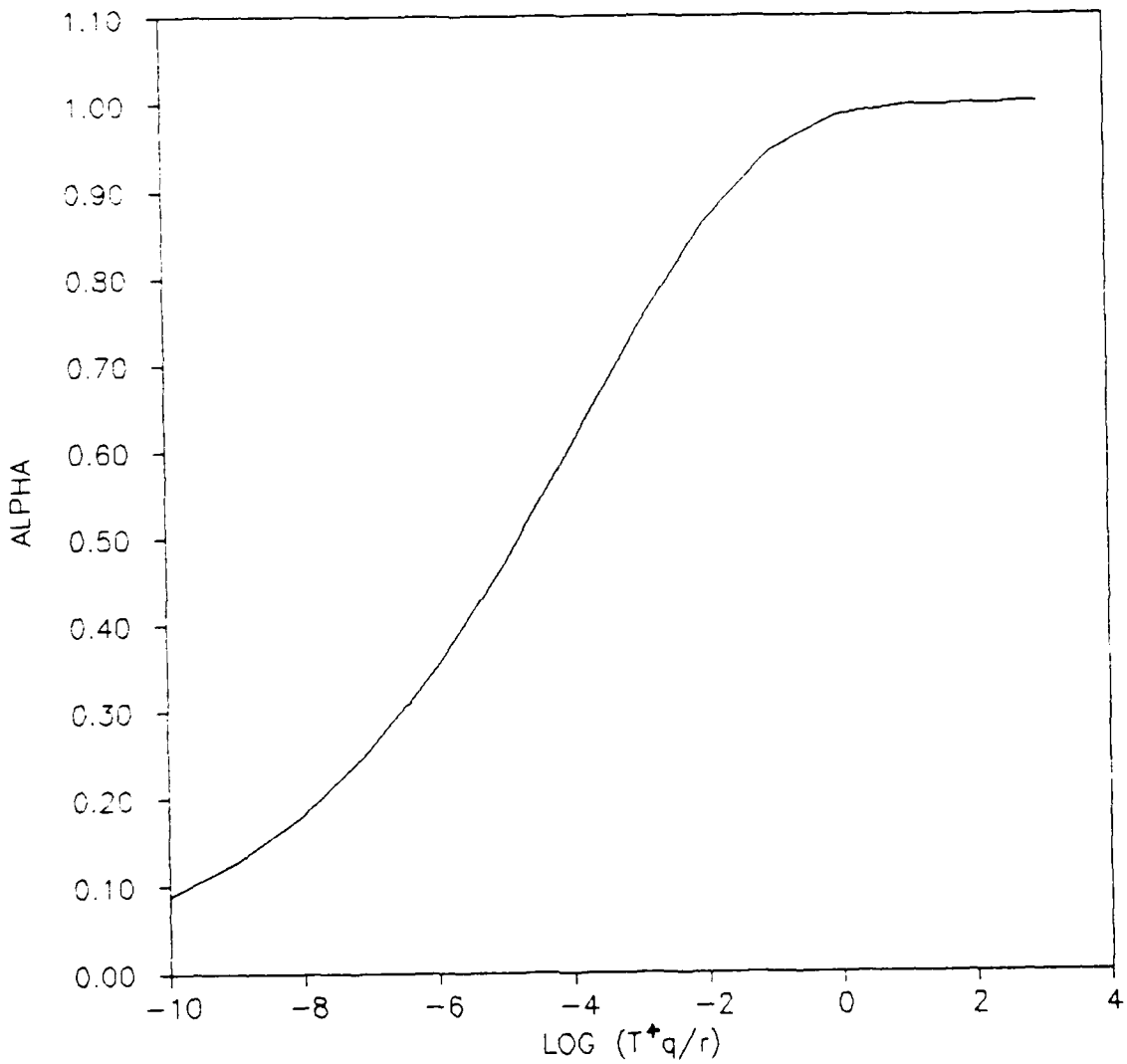

Figure 7-1 α versus Tracking Index (Λ^2)

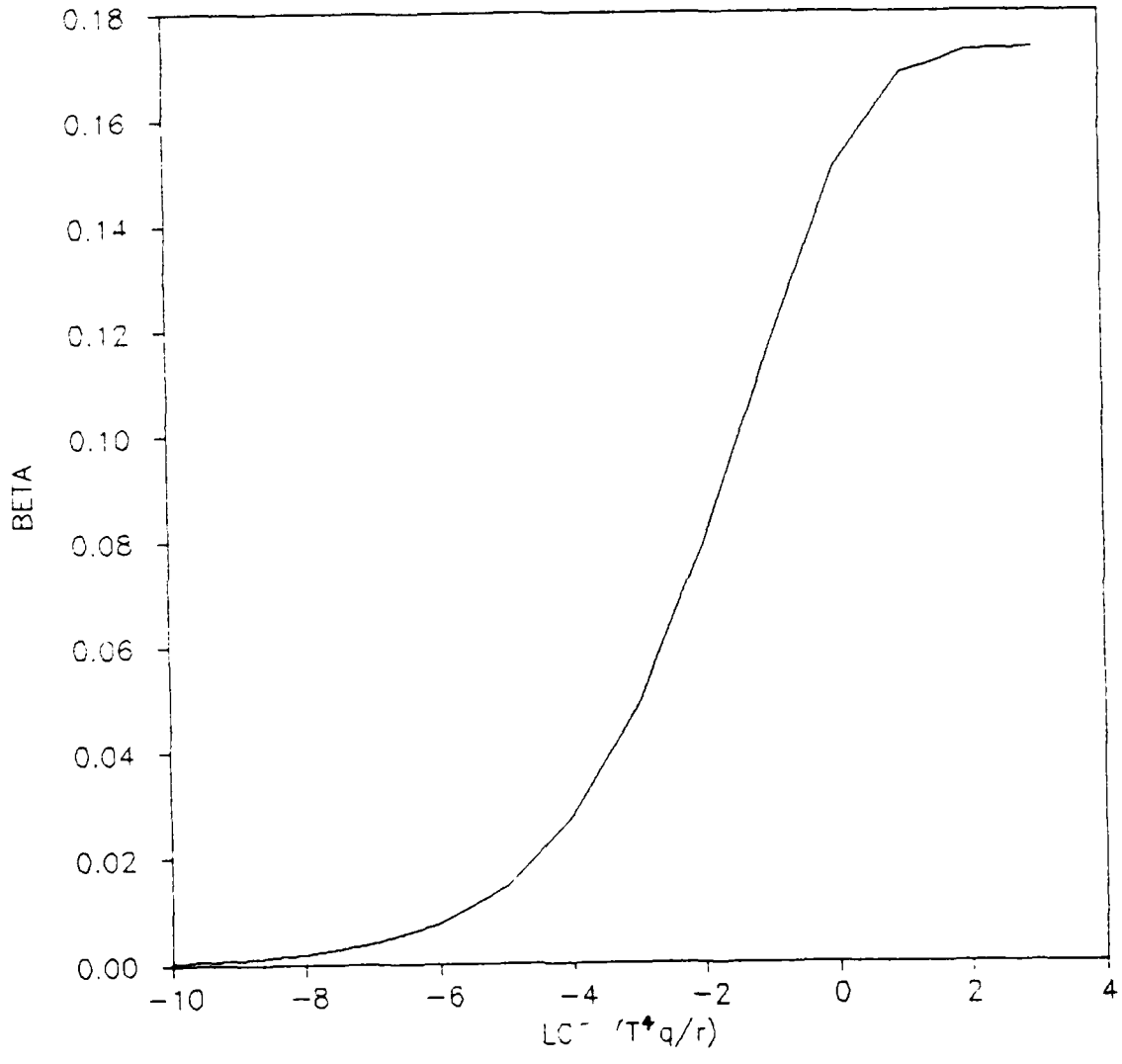

Figure 7-2 β versus Tracking Index (Λ^2)

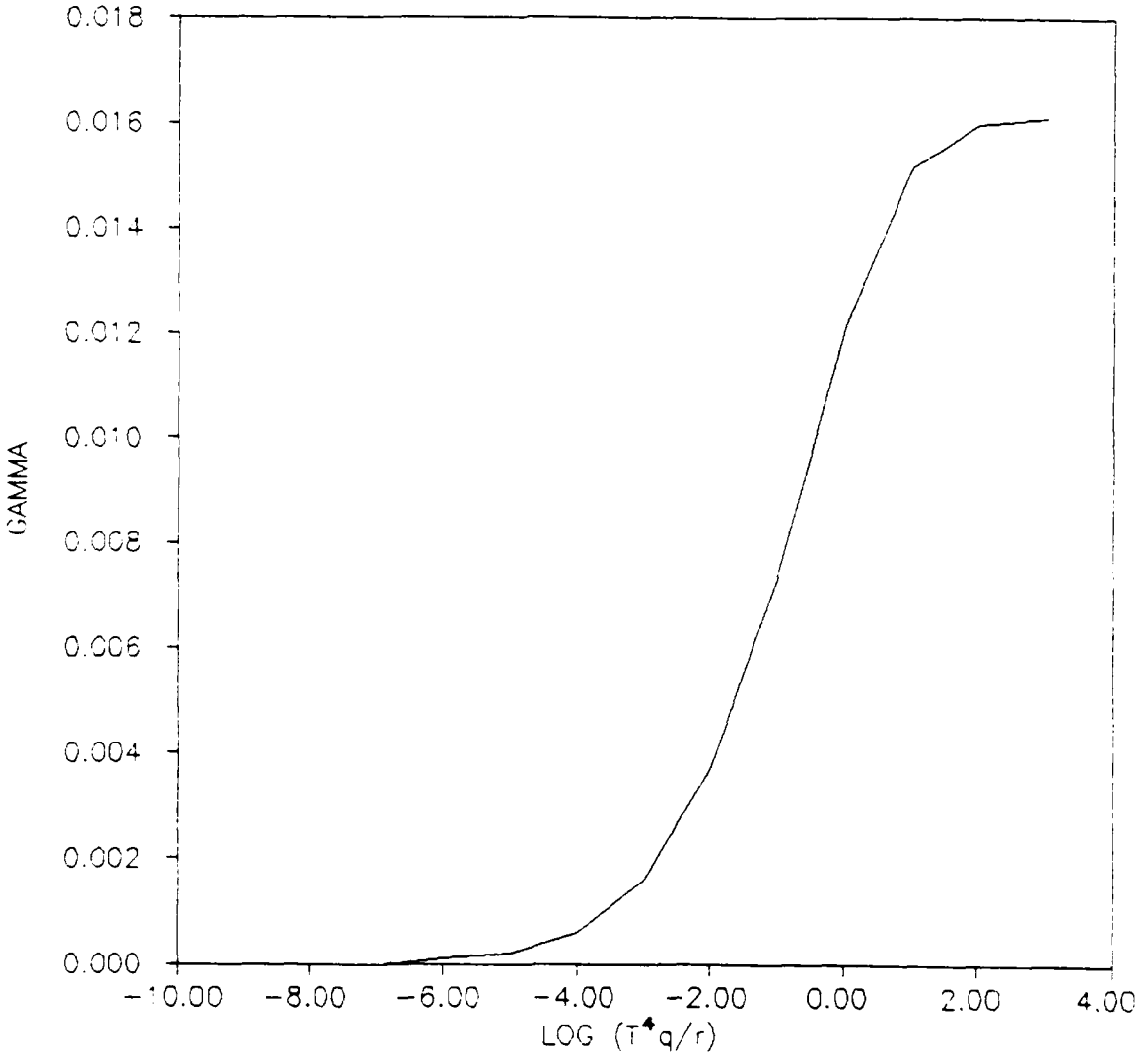

Figure 7-3 γ versus Tracking Index (Λ^2)

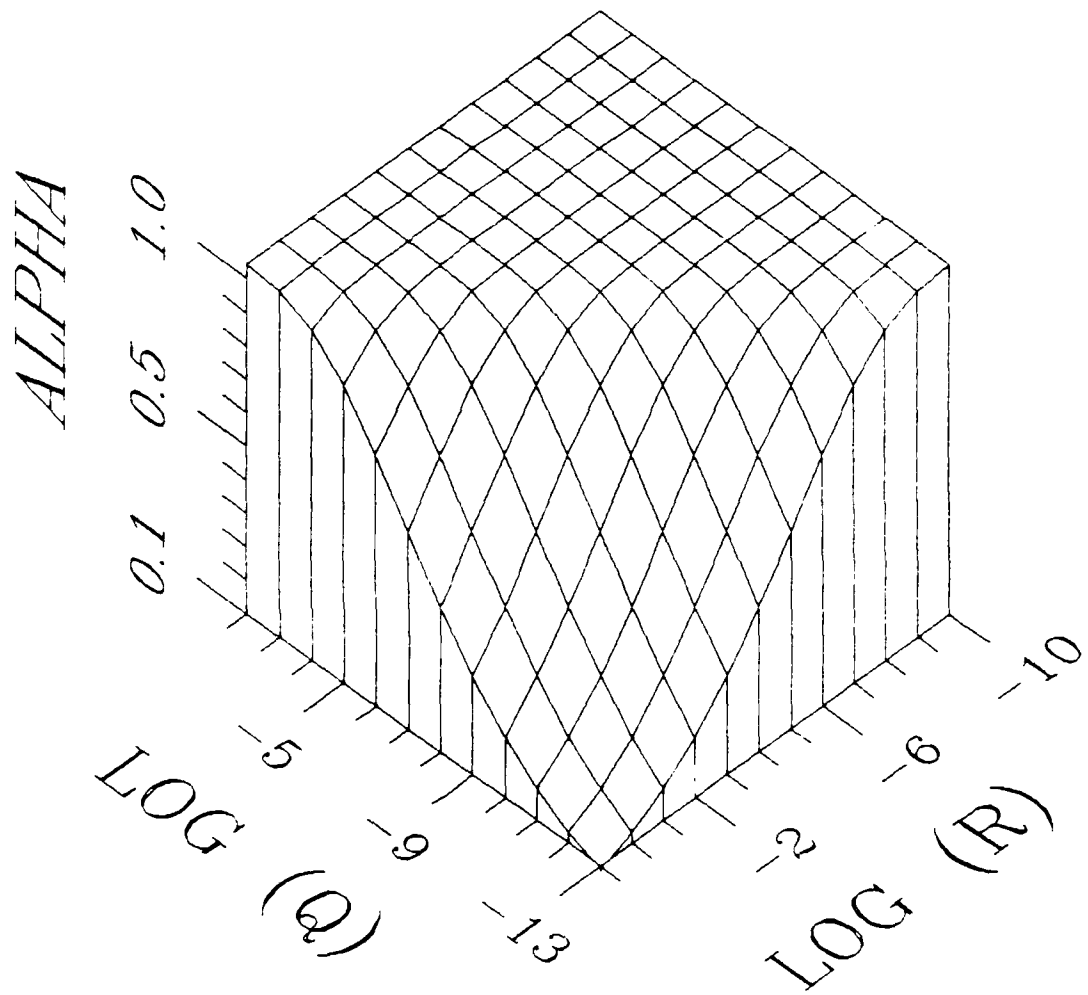

Figure 7-4 Position Gain (α) Surface (T = 10s)

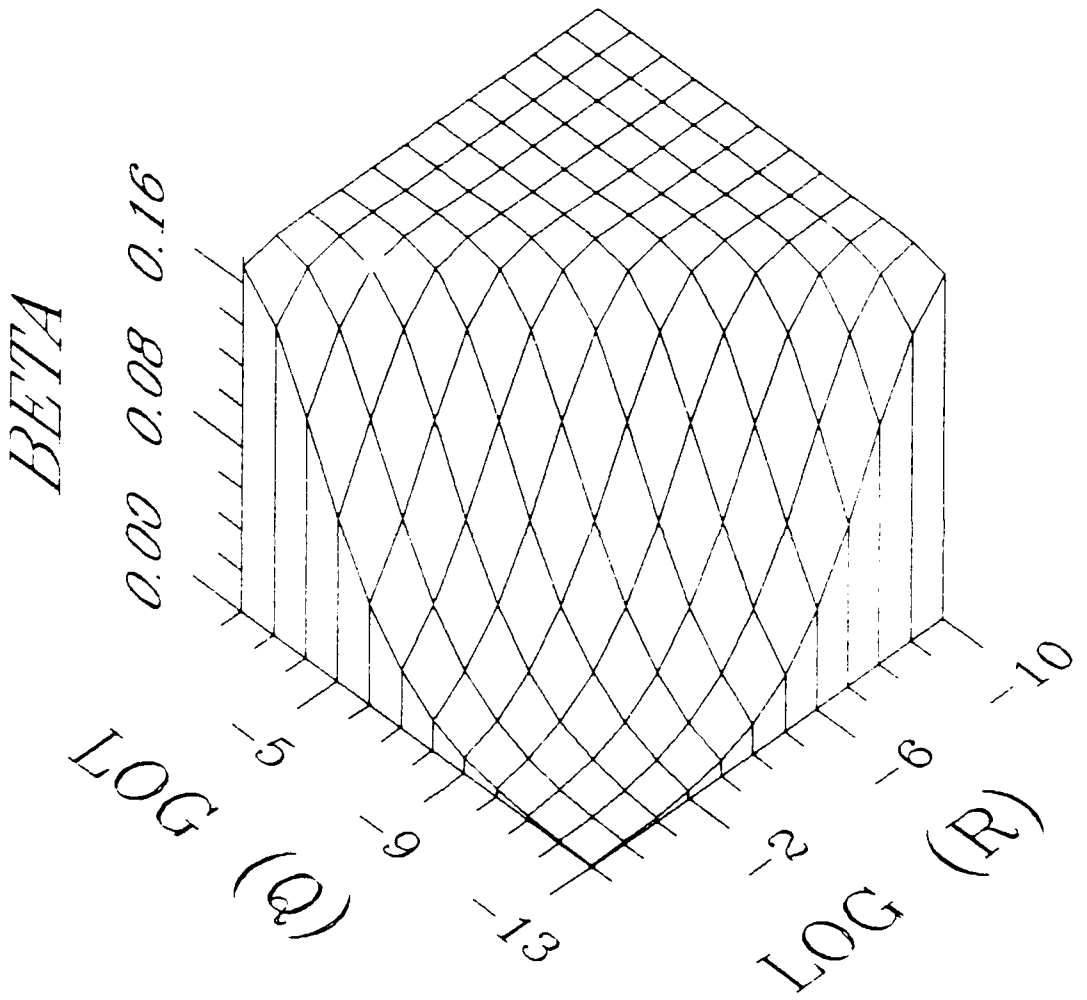

Figure 7-5 Velocity Gain (β) Surface (T = 10s)

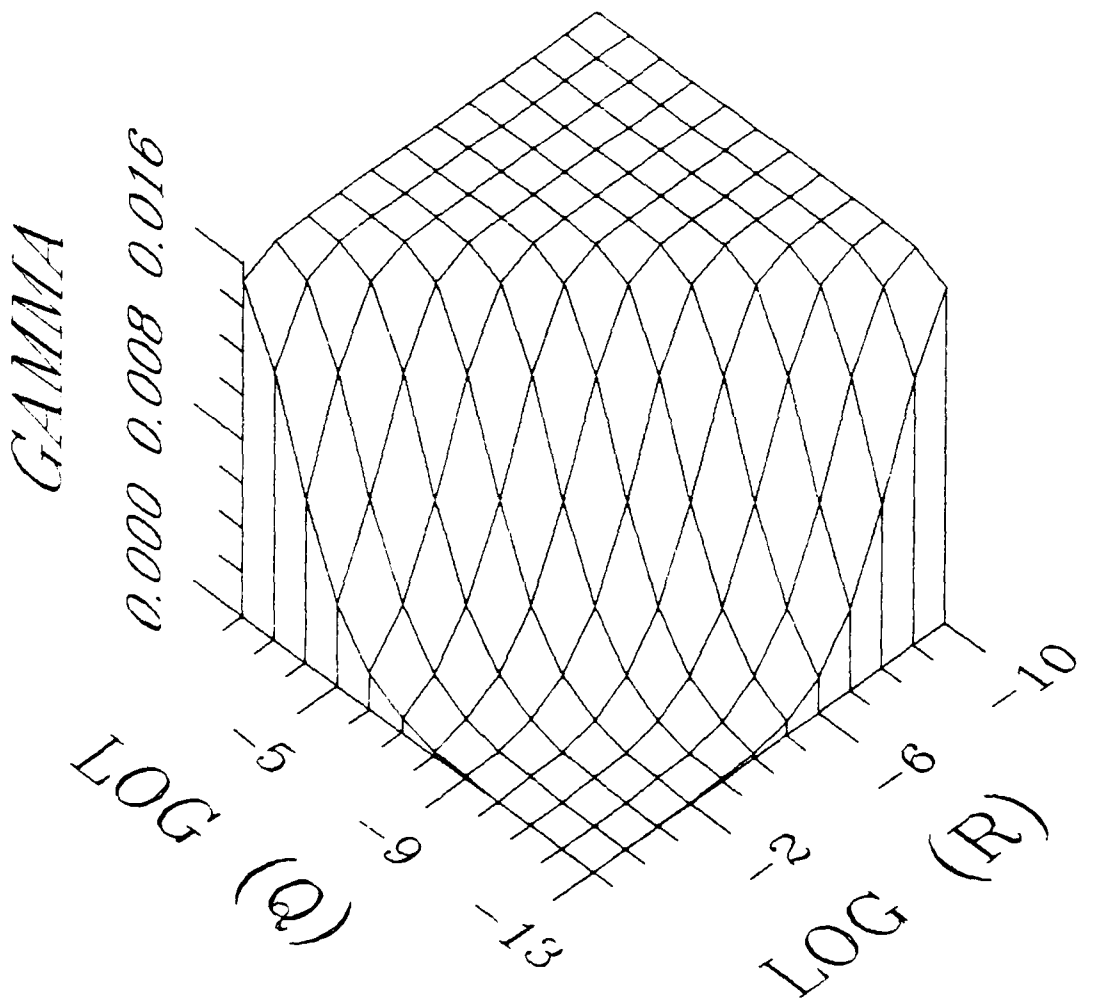

Figure 7-6 Acceleration Gain (γ) Surface (T = 10s)

7.3 Limit Analysis

By examining the equation governing m_{13} in the limit as $r \rightarrow 0$, provides the limiting or maximum values for the gains α, β, and γ. For the limiting case $r \rightarrow 0$, the following relationships hold.

$$b = \frac{qT^4}{2} \quad c = 0 \quad d = \frac{1}{24b^2}$$

$$z = b^4 \quad y = 24b^{10/3}$$

$$m_{13} = \frac{2+\sqrt{3}}{6} qT^4$$

$$m_{11} = \frac{7+4\sqrt{3}}{36} qT^6$$

$$m_{12} = \frac{12+7\sqrt{3}}{36} qT^5$$

$$\lim_{r \rightarrow 0} \alpha = 1$$

$$\lim_{r \rightarrow 0} \beta = \frac{\sqrt{3}}{T}$$

$$\lim_{r \rightarrow 0} \gamma = \frac{6(2-\sqrt{3})}{T^2}$$

For T = 10 which is the time period used in Figures 7-4 through 7-6

$$\lim_{r \rightarrow 0} \alpha = 1$$

$$\lim_{r \rightarrow 0} \beta = 0.173$$

$$\lim_{r \rightarrow 0} \gamma = 0.016$$

As can be seen in Figures 7-1 through 7-3, these are also the limiting values as r approaches zero or the tracking index approaches $+\infty$.

7.4 Summary

This chapter details a means for calculating steady state gains and error covariances for an $\alpha - \beta - \gamma$ tracking filter. The results are given as a function of the measurement and process noise covariances and the sampling period. Similar results were obtained by Ramachandra [1987]. The results contained here in have been extended with 3-dimensional surface graphs to depict gain behavior as a function of the process and measurement noise levels. In addition the analysis is extended by performing a limit analysis to determine the maximum gain values. This limit analysis proves to be pertinent to the observer design methodology outlined in Chapter 5. solution allow

CHAPTER 8
CONCLUSIONS, MAJOR CONTRIBUTIONS, AND RECOMMENDATIONS

8.1 Conclusions

This work investigates a number of techniques and methodologies for improving and analyzing tracking filters. These techniques range from complex three dimensional, six degree of freedom tracking filters that incorporate orientation measurements to one dimensional, single degree of freedom tracking filters with position only measurements. This wide range of techniques provides varying levels of insight into the complex problem of tracking maneuvering aircraft.

The nonlinear analysis most closely represents potential tracking filter capabilities. This analysis clearly shows the deficiencies of tracking filters implemented with radar only measurements. A substantial improvement in tracking abilities is achieved when orientation information is incorporated into the system dynamics and measurement set. In addition, the necessity of tuning the process noise statistics is less sensitive to the particular aircraft trajectory that is being followed. Also, the negative impact of not having radar rates for measurements is offset by the inclusion of orientation measurements.

The linear analysis addresses a key problem in tracking filter design. For any estimator to achieve good estimation and prediction performance requires that the estimator have access to the system's input. Without these inputs, estimation accuracy is degraded. The problem of unknown inputs is fundamental to the tracking filter problem. The linear analysis investigates four methods to analyze this problem. First, a

linear model that includes orientation information is presented. This filter, referred to as an $\alpha - \delta$ tracking filter, shows that its performance in tracking an unknown step input is clearly superior to the tracking performance of the $\alpha - \beta - \gamma$ tracking filter. In addition, the $\alpha - \delta$ tracking is more robust in terms of process noise selection. These conclusions are consistent with those found using the nonlinear tracking filter analysis. The linear formulation of the orientation information also has the added benefit that additional linear techniques such as Bode frequency domain analysis is possible.

Next, a combined frequency/time domain technique is used to analyze a generic system with unknown inputs. The technique is developed for both continuous and discrete cases. Both cases lead to the conclusion that the estimator states should be augmented with input states and exercised as a Kalman filter with infinite process noise levels. This leads to a unity transfer function matrix between estimated and actual inputs for the continuous case. The discrete case yields a one period time delay unity transfer function matrix for estimated and actual inputs.

An error covariance analysis technique addresses error covariance behavior between higher order and reduced order models. It is shown for both the continuous and discrete cases, that the judicious selection of process noise results in error covariance equivalent models. Specifically, this analysis technique provides a means for studying the effects of structural deficiencies for estimator models.

Finally, a linear analysis determines the steady state filter gains for a three state tracking filter. The results lead to simplified equations for determining filter gains and error covariances as a function of sampling time, process noise and measurement noise levels. This is useful in determining asymptotic behavior of the gains as process noise approaches infinity. This is important when implementing Fisher filters for systems with unknown exogenous inputs.

8.2 Summary of Major Contributions

The nonlinear analysis examines a sophisticated six degree of freedom aircraft model. This analysis extends previous research by estimating both the direction and magnitude of the force system acting on the aircraft. The results demonstrate the significant improvement that occurs when orientation information is used to supplement standard trackers with radar only measurements. Additionally, an extensive sensitivity study is performed to determine prediction accuracy robustness to modeling complexity, process noise levels, effects of radar rate availability, and aircraft stability derivative assumptions.

The linear analysis addresses a number of topics that result in new (to this author's knowledge) methodologies and extensions or improvements to previous research results.

The linear models that incorporate orientation information were formulated and developed by Andrisani [1985a, 1987]. These models were examined in terms of their ability to track unknown inputs. The time domain analysis shown in Chapter 4 demonstrates the tracking improvement that is attained when orientation information is used. The analysis also shows that the tracking filter with orientation information is far less sensitive to the selection of process noise levels. These conclusions are consistent with the results found using the nonlinear tracking filters. Given that these results are consistent with the more extensive nonlinear models gives credence to their validity.

The design of observers with unknown exogenous inputs combines both frequency domain and time domain techniques to improve the methodology for selecting the observer gains and determining observer performance. The frequency domain analysis provides the overall transfer function matrix (TFM) between observer estimates of the inputs and the true values of the inputs. The TFM is based on a specific observer implementation and the assumption of constant input dynamics, and is

applicable for any arbitrary set of observer gains. Once the observer gains have been selected, inverse transform methods can be used to determine observer input estimate response. Whereas the general rule of thumb for observer gain selection is to ensure that the observer poles are somewhat "faster" than the system poles [Luenberger; 1971], there is little guidance as to what the affect of a particular pole placement will be on the observer performance. The development of the observer input estimate to true input TFM provides a means for determining these effects. More importantly, it is demonstrated that if the observer is implemented as a Kalman filter with infinite process noise levels, the TFM simplifies to a unity matrix (with a time delay in the discrete case). This implementation unfortunately yields a high bandwidth observer which is susceptible to noise corruption. Therefore, it is suggested that the process noise level be selected to achieve the proper balance between response time and noise corruption.

The error covariance analysis provides a methodology for determining the impact of variable model structures on Kalman filter performance. The continuous and discrete analysis addresses dynamic models with upper triangular form for the dynamics matrix. The continuous case yields a single matrix differential equation that describes the error covariance difference that occurs between a higher order model (HOM) and a reduced order model (ROM). The discrete case yields a single matrix difference equation for both the filtered and predicted error covariances. The equations may used in the performance of a sensitivity analysis or as shown herein, they provide a means for achieving error covariance equivalent models.

The constant gain analysis for the three state α–β–γ tracking filter yields closed form solutions for gain and error covariance determination as a function of process and measurement noise levels and sampling period time. The determination of these closed form solutions allows for analytical techniques to be applied for

sensitivity analyses or as demonstrated herein, a limit analysis. The limit analysis reveals that the particular selection of the input dynamics in the observer design with unknown exogenous inputs is critical.

8.3 Recommendations

The linear methods were developed with generic system models to allow for a wide range of applications. The application of these techniques should be explored using other aerospace systems.

The system observer implemented as a Fischer filter could serve as an analytic redundancy module in the fault detection and isolation procedures for aircraft control inputs. The necessity of fast and accurate fault detection/isolation systems is imperative for aircraft flight control systems being designed with the ability to reconfigure control laws after the onset of a control failure.

The error covariance analysis procedure can also be used in observer/estimator based flight control systems. Often these systems are modeled without the inclusion of certain sensor and servo-actuator dynamics. The decision to include or remove these dynamics can be made based on results of an error covariance analysis. If the decision is made not to include these dynamics, appropriate modifications to the process noise levels can be made.

An additional research topic, would be to explore a modified input matrix for the three state discrete steady state gain analysis. Since using the input matrix of chapter 7 does not yield a dead-beat response for system input estimation, performing a similar analysis with an input matrix corresponding to an acceleration input would be useful.

BIBLIOGRAPHY

BIBLIOGRAPHY

Andrisani, D., Schierman, J. D., "Tracking Maneuvering Helicopters using Attitude and Rotor Angle Measurements," in Proceedings of the Twenty-first Asilomar Conference on Signals, Systems, & Computers, pp. 328-333, November 1987.

Andrisani, D., Kuhl, F.P., and Gleason, D., "A Nonlinear Tracker Using Attitude Measurements," IEEE Transactions on Aerospace and Electronic Systems, Vol. AES-22, No. 5, pp. 533-539, September 1986.

Andrisani, D., Gleason, D., and Kuhl, F.P., "A Tracker for Maneuvering Vehicles," in Proceedings of WESCON/85, September 1985a.

Andrisani, Dominick, "New Linear Tracking Filters," in Proceedings of the American Control Conference, June 1985b.

Andrisani, D., Kuhl, F. P., and Gleason, D. "A Nonlinear Tracking Filter," in Proceedings of the Fourth Army Symposium on Gun Dynamics, May 1985c.

Andrisani, D., Gleason, D., and Mavromatis, T., "Target Trackers For Maneuvering Aircraft," Report No. 0896, Batelle Columbus Laboratories, May 1985d.

Baheti, R. S., "A Suboptimal Kalman Filter Design for Target Tracking Applications" in Proceedings of the 1983 IEEE Decision and Control Conference, December 1983.

Bar-Shalom, Y., and Birmiwal, K., "Variable Dimension Filter for Maneuvering Target Tracking," IEEE Transactions on Aerospace and Electronic Systems, Vol AES-18, No. 5, pp. 621-629, Sept 1982.

Benedict, T. R. and Bordner, G. W., "Synthesis of an Optimal Set of Radar Track-While-Scan Smoothing Equations," IRE Transactions On Automatic Control, Vol. AC-7, No. 4, pp. 27-32, July 1962.

Berg, Russel F., "Estimation and Prediction for Maneuvering Target Trajectories," IEEE Transactions On Automatic Control, Vol. AC-28, No. 3, pp. 294-304, March 1983.

Blackman, Samuel S. Multiple-Target Tracking with Radar Applications, Artech House, Inc., Dedham, MA, 1986.

Bogler, P. L., "Tracking a Maneuvering Target Using Input Estimation" IEEE Transactions on Aerospace and Electronic Systems, Vol AES-23, No. 3, pp. 298-310, May 1987.

Brammer, Karl G., "Stochastic Filtering Problems in Multiradar Tracking," In Nonlinear Stochastic Problems, pp. 533-552. Edited by R. S. Bucy and J. M. F. Moura, D. Reidel Publishing Co., Dordecht, Holland 1983.

Bryson, Arthur E., and Ho, Y.C., Applied Optimal Control, Hemisphere Publishing Corp., Washington, 1975.

Bullock, T. E., and Sangsuk-Iam, "Maneuver Detection and Tracking with Nonlinear Target Model," in Proceedings of 1984 IEEE Decision and Control Conference, December 1984.

Chang, Chaw-Bing, and Tabaczynski, John A., "Application of State Estimation to Target Tracking," IEEE Transactions On Automatic Control, Vol. AC-29, No. 2, pp. 98-109, February 1984.

Chan, Y. T., Plant, J. B., and Bottomley, J. R. T., "A Kalman Tracker with a Simple Input Estimator," IEEE Transactions on Aerospace and Electronic Systems, Vol AES-18, No. 2, pp. 235-241, March 1982.

Chan, Y.T., Hu, A. G. C., and Plant, J. B., "A Kalman Filter Based Tracking Scheme with Input Estimation," IEEE Transactions on Aerospace and Electronic Systems, Vol AES-15, No. 2, pp. 237-244, March 1979.

Clark, B. L., Development of an Adaptive Kalman Target Tracking Filter and Predictor for Fire Control Applications, Naval Surface Weapons Center, Dahlgren, VA., March 1977, AD-A039907.

Clark, B. L., "The Development of an Adaptive Kalman Target Tracking Filter," in Proceedings of AIAA Guidance and Control Conference, pp. 365-382, August 1976.

Doyle, J. C., and Stein, G., "Robustness with Observers," IEEE Transactions On Automatic Control, Vol. AC-24, No. 4, pp. 607-611, August 1979.

Dziwak, Walter, J., Investigation of Kalman Filter Designs for Air Defense Based on Attack Aircraft Data, U.S. Army Armament Command, Philadelphia, PA., September 1976, AD-A036440.

Ekstrand, Bertil, "Analytical Steady State Solutions for Continuous Time Kalman Filter," IEEE Transactions on Aerospace and Electronic Systems, Vol AES-21, No. 6, pp. 746-750, November 1985.

Ekstrand, Bertil, "Analytical Steady State Solutions a Kalman Tracking Filter," IEEE Transactions on Aerospace and Electronic Systems, Vol AES-19, No. 6, pp. 815-819, November 1983.

Fitzgerald, Robert J., "Simple Tracking Filters: Steady State Filtering and Smoothing Performance," IEEE Transactions on Aerospace and Electronic Systems, Vol AES-16, No. 6, pp. 860-864, November 1980.

Fitzgerald, Robert J., "Simple Tracking Filters: Closed Form Solutions," IEEE Transactions on Aerospace and Electronic Systems, Vol AES-17, No. 6, pp. 781-784, November 1981.

Franklin, G. F., and Powell, J. D., Digital Control of Dynamic Systems, Addison-Wesley Publishing Company, Reading, MA, 1980.

Friedland, Bernard, "On the Effect of Incorrect Gain in Kalman Filters," IEEE Transactions on Automatic Control, Vol AC-12, No. 5, p. 610, October 1967.

Friedland, Bernard, "Optimum Steady-State Position and Velocity Estimation Using Noisy Sampled Position Data," IEEE Transactions on Aerospace and Electronic Systems, Vol AES-9, No. 6, pp. 906-911, November 1973.

Friedland, Bernard, "Corrections to Optimum Steady-State Position and Velocity Estimation Using Noisy Sampled Position Data," IEEE Transactions on Aerospace and Electronic Systems, Vol AES-11, No. 4, p. 675, July 1975.

Gelb, Arthur, ed. Applied Optimal Estimation, M.I.T. Press, Cambridge, 1974.

Gholson, Norman H., and Moose, Richard L., "Maneuvering Target Tracking Using Adaptive State Estimation," IEEE Transactions on Aerospace and Electronic Systems, Vol AES-13, No. 3, pp. 310-317, May 1977.

Gleason, D., and Andrisani, D., "Constant Gain Analysis for Discrete Tacking Filters," in Proceedings of NAECON '88, pp. 287-291, May 1988.

Gleason, D. and Andrisani, D., "Discrete Error Covariance Analysis for Tracking Filters," in Proceedings of the 21st Asilomar Conference on Systems, Signals, and Computers, pp. 344-350, November 1987.

Gleason, D. and Andrisani, D., "Fault Detection for Aircraft Control Inputs," in Proceedings of the Sixth DOD Conference on DEW Vulnerability, Survivability, and Effects, May 1987.

Gleason, D., and Andrisani, D., "Error Covariance Analysis for Tracking Filters," in Proceedings of NAECON '86, pp. 299-301, May 1986.

Heffes, H., "The Effect of Erroneous models on the Kalman Filter Response," IEEE Transactions on Automatic Control, Vol AC-11, No. 3, p. 541-543, July 1966.

Huddle, James R. and Wismer, David A., "Degradation of Linear Filter Performance Due to Modeling Error," IEEE Transactions on Automatic Control, Vol AC-13, No. 4, pp. 421-423 August 1968.

Hutchinson, C. E., D'Appolito, J. A., and Roy, K. J., "Applications of Minimum Variance Reduced State Estimators," IEEE Transactions on Aerospace and Electronic Systems, Vol AES-11, No. 5, pp. 785-794, September 1985.

Jones, B. W. and Schmidt, D. K., FLTSIM: Flight Simulator; A&AE Computer System, A&AE Departmental Document 78-53, School of Aeronautics and Astronautics, Purdue University, West Lafayette, IN, August 1978.

Kailath, Thomas, and Ljung, L., "The Asymptotic Behavior of Constant-Coefficient Ricatti Defferential Equations" IEEE Transactions on Automatic Control, Vol AC-21, No. 3, pp. 385-388 June 1976.

Kailath, Thomas, "An Innovations Approach to Least-Squares Estimation Part I: Linear Filtering in Additive White Noise," IEEE Transactions on Automatic Control, Vol AC-13, No. 6, pp. 646-655 December 1968.

Kalata, Paul R., "The Tracking Index: A Generalized Parameter for $\alpha-\beta$ and $\alpha-\beta-\gamma$ Target Trackers," IEEE Transactions on Aerospace and Electronic Systems, Vol AES-20, No. 2, pp. 174-182, March 1984.

Kalman, R. E., "A New Approach to Linear Filtering and Prediction Problems," ASME Journal of Basic Engineering, Vol 82, pp. 35-45, March 1960.

Kendrick, J. D., Maybeck, P.S., and Reid, J. G., "Estimation of Target Motion Using Orientation Measurements," IEEE Transactions on Aerospace and Electronic Systems, Vol AES-17, No. 2, pp. 254-259, March 1981.

Kwakernaak, H., and Sivan, R., Linear Optimal Control Systems, Wiley-Interscience, 1972.

Lefas, S. S., "Using Roll Angle Measurements to Track Aircraft Maneuvers," IEEE Transactions on Aerospace and Electronic Systems, Vol AES-20, No. 6, pp. 672-681, November 1984.

Lefferts, Robert E., "Adaptive Correlation Regions for $\alpha-\beta$ Tracking Filters," IEEE Transactions on Aerospace and Electronic Systems, Vol AES-17, No. 6, pp. 738-747, November 1984.

Lin, Ching-Fang, and Shafroth, Marc W., "A Comparative Evaluation of Some Maneuvering Target Tracking Algorithms," in Proceedings of the AIAA Guidance, Control, and Flight Mechanics Conference, pp. 39-49, August 1983.

Luenberger, David G., "An Introduction to Observers," IEEE Transactions on Automatic Control, Vol AC-16, No. 6, pp. 596-602, December 1971.

Mavromatis, T., Andrisani, D., and Kuhl, F. P., "Tracker Optimization," in Proceedings of the 21st Asilomar Conference on Systems, Signals, and Computers, pp. 339-343, November 1987.

Mayhew, Ellen and Gleason Daniel, "Fault Detection and Isolation For Reconfigurable Flight Control Systems," in Proceedings of the 8th Digital Avionics Systems Conference, October 1988.

Maybeck, Peter S., Stochastic Models, Estimation, and Control, Volumes 1-3, Academic Press, 1982.

McAulay, R. J., and Denlinger, E., "A Decision-Directed Adaptive Tracker," IEEE Transactions on Aerospace and Electronic Systems, Vol AES-9, No. 2, pp. 229-236, March 1973.

Moose, R. L., Vanlandingham, H. F., and McCabe, D. H., "Modeling and Estimation for Tracking Maneuvering Targets," IEEE Transactions on Aerospace and Electronic Systems, Vol AES-15, No. 3, pp. 448-455, May 1979.

Neal, S. R., "Linear Estimation in the Presence of Errors in Assumed Plant Dynamics," IEEE Transactions on Automatic Control, Vol AC-12, No. 5, pp. 592-594, October 1967.

Neal, S. R., "Discussion on Parametric Relationships for the $\alpha-\beta-\nu$ Filter Predictor," IEEE Transactions on Automatic Control, Vol AC-12, No. 3, pp. 315-317, June 1967.

Ramachandra, K. V., "Optimum Steady State Position, Velocity, and Acceleration Using Noisy Sampled Data," IEEE Transactions on Aerospace and Electronic Systems, Vol AES-23, No. 5, pp. 705-708, September 1987.

Rickers, George C. and Williams, Jack R., "Adaptive Tracking Filter for Maneuvering Targets," IEEE Transactions on Aerospace and Electronic Systems, Vol AES-14, No. 1, pp. 185-193, January 1978.

Roskam, J., Airplane Flight Dynamics and Automatic Control, Part 1, Roskam Aviation and Engineering Corporation, 1979.

Schwartz, Mischa, and Shaw, Leonard, Signal Processing: Discrete Spectral Analysis, Detection and Estimation, McGraw-Hill, New York, 1975.

Schweppe, Fred C., Uncertain Dynamic Systems, Prentice Hall, Inc, Englewood Cliffs, New Jersey, 1983. and Estimation, McGraw-Hill, New York, 1975.

Singer, Robert A., and Behnke, Kenneth W., "Real Time Tracking Filter Evaluation and Selection for Tactical Applications," IEEE Transactions on Aerospace and Electronic Systems, Vol AES-7, No. 1, pp. 100-110, January 1971.

Singer, Robert A., "Estimating Optimal Tracking Filter Performance for Manned Maneuvering Targets," IEEE Transactions on Aerospace and Electronic Systems, Vol AES-6, No. 4, pp. 473-483, July 1970.

Spingarn, K. and Weidmann, H. L., "Linear Regression Filtering and Prediction for Tracking Maneuvering Targets," IEEE Transactions on Aerospace and Electronic Systems, Vol AES-8, No. 6, pp. 800-810, November 1972.

Tang, Y. M., and Borrie, J. A., "Missile Guidance Based on Kalman Filter Estimation of Target Maneuver," IEEE Transactions on Aerospace and Electronic Systems, Vol AES-20, No. 6, pp. 736-741, November 1972.

Wolovich, W. A., Linear Multivariable Systems, Springer-Verlag, Heidelberg, 1974.

Yu, M. H., and Meyer, M. P., "Closed Form Solution of a Recursive Tracking Filter with A-Priori Velocity Initialization," IEEE Transactions on Aerospace and Electronic Systems, Vol AES-21, No. 2, pp. 262-264, March 1985.

-------- MACSYMA Reference Manual, Symbolics, Inc., October 1985.

VITA

VITA

Daniel Gleason [redacted]

He completed his Bachelor of Science degree in Aerospace Engineering from the University of Colorado in May 1976. During August 1976, he entered active duty in the United States Air Force, and was assigned to the Air Force Institute of Technology (AFIT). He graduated from AFIT in March 1978 with a Master of Science Degree in Systems Engineering. He was then assigned to the Rome Air Development Center as a project engineer from March 1977 through December 1981. In January 1982, he started his Ph.D. program at Purdue University. From February 1985 through December 1988, he served as a faculty member with the Department of Aeronautics and Astronautics, Air Force Institute of Technology.